공학박사학위논문

펨토셀 네트워크에서 자원 관리에 관한 연구

Study on Resource Management in Two-Tier Femtocell Networks

2014년 8월

서울대학교 대학원

전기·컴퓨터 공학부

김 주 희

펨토셀 네트워크에서
자원 관리에 관한 연구

Study on Resource Management in Two-Tier Femtocell Networks

지도 교수 전 화 숙

이 논문을 공학박사 학위논문으로 제출함

2014년 **6**월

서울대학교 대학원

전기, 컴퓨터 공학부

김 주 희

김주희의 박사 학위논문을 인준함

2014년 **6**월

위 원 장 김 종 권

부위원장 전 화 숙

위 원 권 태 경

위 원 정 동 근

위 원 박 세 웅

Abstract

Study on Resource Management in Two-Tier Femtocell Networks

Juhee Kim

The School of Electrical Engineering and Computer Science

The Graduate School

Seoul National University

Femtocell has received wide attention as a promising solution to meet explosively increasing traffic demand in cellular networks, since it can provide high quality data services to indoor users at low cost. In this thesis, we study resource management in two-tier femtocell networks where the femtocells are underlaid by macrocells, from two different aspects: spectral efficiency and energy efficiency. First, we design a downlink radio resource partitioning scheme between femtocells and their overlaid macrocell to enhance the spectral efficiency. We consider that the overlaid macrocell network adopts the fractional frequency reuse (FFR) techniques, which is also one of solutions to the mobile data surge problem. With FFR, the frequency band of a macrocell is divided into several frequency partitions (FPs) and the transmission power levels assigned to FPs differ from each other. With the proposed scheme, every FP is divided into the macro-dedicated, the shared, and the femto-dedicated portions. The ratio of these three portions is different for each FP. We suggest a method to determine a proper ratio of portions in each FP, by using optimization approach. Next, we propose a scheme to enhance the energy

efficiency in open access femtocell networks where many femto base stations (BSs) are deployed in a large public area such as office building, shopping mall, etc. In those areas, the femtocells are overlapped and underutilized during most of the operation time because femto BSs are densely deployed to support the peak traffic load. So, if we properly coordinate the user association with cells and put the femto BSs having no associated users to sleep, the network energy efficiency in the femtocell deployment area can be greatly enhanced. Therefore, we propose a femto BS sleep decision and user association (SDUA) scheme that jointly determines the operation modes (i.e., active or sleep) of femto BSs and the association between users and the active BSs. The SDUA problem is formulated as an optimization problem that aims at minimizing the total energy consumption while providing the satisfied service to users. Since the SDUA problem is too complicated to be solved, we first solve the optimal user association (UA) problem for given set of active femto BSs and then design a heuristic algorithm that finds the best set of active femto BSs by iteratively performing the optimal UA with each different set. By simulation, it is shown that the proposed schemes achieve their design goals properly and outperform existing schemes.

Keywords: Femtocell, heterogeneous cellular network, resource management, spectral efficiency, energy efficiency

Student Number: 2009-30913

Contents

1 Introduction **1**

1.1 Background and Motivation 1

1.2 Proposed Resource Management Schemes 6

1.2.1 Radio Resource Partitioning Scheme for Spectral Efficiency Enhancement 6

1.2.2 Base Station Sleep Management Scheme for Energy Efficiency Enhancement 7

1.3 Organization 9

2 Radio Resource Partitioning Scheme for Spectral Efficiency Enhancement **10**

2.1 System Model 10

2.1.1 Heterogeneous Network 10

2.1.2 Capacity Model 13

2.2 Proposed Downlink Radio Resource Partitioning Scheme 15

2.2.1 Macrocell Protection Mechanism 16

2.2.2 Determination of Dedicated Portion for Macrocell/Femtocell Users 17

2.3 Capacity Estimation 22

2.3.1 Achievable Macrosector Capacity 22

2.3.2 Achievable Femtocell Capacities 26

2.3.3 SHG Availability of Femtocell 32

3 Base Station Sleep Management Scheme for Energy Efficiency Enhancement **37**

3.1 System Model 38

3.1.1 Open Access Femtocell Network 38

3.1.2 Operation Modes and Power Consumption of a BS 40

3.1.3 Energy Efficiency 40

3.2 Analysis on Energy Efficiency 41

3.2.1 Mathematical Model 42

3.2.2 Derivation of Energy Efficiency 43

3.2.3 Numerical Results and Discussion 47

3.3 Proposed Femto BS Sleep Decision and User Association (SDUA) Scheme 50

3.3.1 Problem Formulation 50

3.3.2 Solution Approach 52

3.3.3 Implementation Example of SIR Estimation 57

4 Performance Evaluation **58**

4.1 Radio Resource Partitioning Scheme 58

4.1.1 Simulation Model 58

4.1.2 Simulation Results 61

4.2 Base Station Sleep Management Scheme 73

4.2.1 Simulation Model 73

4.2.2 Simulation Results 75

5 Conclusion **80**

Bibliography **82**

Abstract **89**

List of Figures

2.1 FFR operation in the macrocell tier. 11

2.2 q_k according to the distance between the macro BS and the macrocell user. 34

2.3 SHG availability of femtocell i, $\tilde{h}_{i,k}$. 35

3.1 System model. 38

3.2 Resource utilizations and energy efficiencies for varying scenarios: a) $\lambda_{\mathrm{u}} = 2 \times 10^{-3}$, $D_{\mathcal{A}} = 200$ m, b) $\lambda_{\mathrm{u}} = 8 \times 10^{-3}$, $D_{\mathcal{A}} = 200$ m, c) $\lambda_{\mathrm{u}} = 8 \times 10^{-3}$, $D_{\mathcal{A}} = 600$ m 48

3.3 Submodularity test of $-\Phi$. 56

4.1 Heterogeneous network model in simulation. 59

4.2 Contour of the average femtocell user throughput in the dense femtocell area. 64

4.3 Cumulative distributed function of femtocell user throughput. 65

4.4 Average femtocell user throughput. 67

4.5 Average and 5th percentile macrocell user throughput. 68

4.6 Total throughput in a macrosector coverage. 70

4.7 Effects of femtocell deployment scenarios on the total throughput. . 71

4.8 Performance difference between the optimal and heuristic algorithms. 72

4.9 Power consumptions of macro BS and femto BSs according to the location of the designated zone. 74

4.10 Energy saving according to $P_{\mathrm{f,\ sleep}}/P_{\mathrm{f,\ const}}$. 76

4.11 Performance of the proposed scheme according to reporting overhead. 77

4.12 Performance comparison in the total power consumption and the number of active femto BSs. 78

List of Tables

4.1 Channel model parameters 60

4.2 Average macrocell/femtocell user throughputs 62

4.3 Average user satisfaction ratios and proportional fairness indexes . . 63

Chapter 1. Introduction

1.1 Background and Motivation

According to the wide spread of smart portable devices (such as smart phones and tablet PCs) and the rapid diversification in wireless services, the data traffic in mobile communications systems is increasing explosively. As a promising solution to tackle this data surge, femtocells have received wide attention. Femtocells are small, inexpensive, and low-power base stations (BSs) that use the wired connections for backhaul. The femtocells can provide high quality data services to indoor cellular users. In addition, since the femtocells are deployed under the conventional macrocellular network, they can offload data traffic from the macrocell network [1]. With these advantages, the femtocells are expected to be massively deployed in a few years [2].

In a two-tier (heterogeneous) network where the femtocells are underlaid by the macrocells, the femtocells and the macrocells can operate at the different frequency bands (orthogonal-channel deployment) or at the same frequency band (co-channel deployment) [3]. In the former case, since the available bandwidth is divided and dedicated to both tiers respectively, the resource management in each dedicated portion is easy, whereas the resource efficiency can be degraded under time-varying traffic condition. In the latter case, since the users suffer from the cross-tier interferences such as macro-to-femto interference (MFI) and femto-to-macro interference (FMI), an accurate management of shared resource is needed to accomplish high spectral efficiency. On the other hand, as the energy costs are rapidly rising and the concern about carbon footprint caused by the energy consumption is growing [4], energy efficiency has also become one of essential considerations in designing the

femtocell networks [5]. The resource management for the energy-efficient femtocell networks is challenging, since it should consider various factors such as random deployment of femtocells, different access modes in femtocells (i.e., closed and open), and load balancing among femtocells and between the macrocell and femtocells. In this thesis, we study the resource management in the two-tier femtocell networks, from two different aspects: the spectral efficiency and energy efficiency.

To improve the spectral efficiency in the femtocell networks, many resource allocation schemes that consider the trade-offs between orthogonal and co-channel deployments have been proposed. In [6], the overall bandwidth is divided into two portions, the macro-dedicated portion and the shared portion that can be used by both macrocell and femtocells. In [7], the bandwidth is divided into three parts: the macro-dedicated, the shared, and the femto-dedicated portions. With these schemes, the main technical issues are to determine the ratio of each portion and to choose the sharing policy for shared portion. Refs. [6] and [7] address these problems under their own system models, respectively. Meanwhile, the FFR scheme has been adopted in order to mitigate inter-cell interference in the next generation cellular systems such as the IEEE 802.16m [8] and the 3GPP Long Term Evolution (LTE) [9]. With FFR, the frequency band of a macrocell is divided into several frequency partitions (FPs) and the transmission power levels assigned to FPs differ from each other. Moreover, the power assignment pattern of a cell is different from that of an adjacent cell. There are a lot of studies on the FFR design and performance, focusing on the effect between macrocells (e.g., [10]–[13]). Although femtocell and FFR technology respectively have been investigated extensively, only a few results are reported in the literatures on applying femtocells in the FFR framework (e.g., [14]–[16]). In [14], the femtocell uses different FPs

from those used in its overlaid macrocell, considering the strict FFR where FPs are orthogonally assigned among adjacent macrocells. In [15], the macrocell utilizes each FP without consideration of femtocell, while the femtocell can access spectrum when its disturbance to macrocell is under a certain level. Ref. [16] shows that adopting femtocells can increase system performance in FFR-based cellular system, if power control and interference cancelation are conducted properly. However, with this policy, the femtocells close to the macrocell base station (macro BS) cannot get the transmission opportunity under heavy load condition. To overcome this difficulty while heightening the spectral efficiency, in this thesis, we propose a downlink resource allocation scheme for the two-tier femtocell networks.

On the other hand, there have been also many research works to enhance the energy efficiency in the two-tier femtocell networks. The authors in [17] and [18] have investigated the resource partitioning between the macrocells and femtocells that maximizes the energy efficiency. Refs. [19] and [20] tried to enhance the energy efficiency by adjusting the transmission power of femtocell base station (femto BS). However, the energy-saving effect by transmission power control may be very limited in the femtocells, since the power consumed for data transmission at a femto BS is much smaller than the power consumed for operating the femto BS equipment itself [21]. The authors in [22] have introduced the sleep-mode operation of femto BS where the transceivers and other hardware components required for transmission are turned off. They showed that the network energy can be saved significantly, merely by putting femto BSs with low load to sleep. Ref. [22] also presents three sleep decision mechanisms: the sleep/wakeup decision of a femto BS is made either by the nearby user, the femto BS itself, or the network controller. In [23], the user wakes up nearby femto BS(s) by broadcasting wake-up signals

periodically. In [24] and [25], the femto BS can change its operation mode directly by detecting the user proximity. The authors in [26] have proposed a network-controlled scheme that determines the operation modes of femto BSs (i.e., sleep or active) of each femto BS, considering user locations. Note that the former two mechanisms have taken on a reactive operation where the operation mode of femto BS is decided according to the user proximity, whereas the network-controlled one can put the femto BSs to sleep in a proactive manner, i.e., the user association with cells is coordinated by the network controller so that more femto BSs can sleep. In this thesis, we propose a network-controlled scheme that decides jointly the operation modes of femto BSs and the association between users and the active BSs so as to enhance the energy efficiency in the network.

Meanwhile, motivated by that BSs are largely underutilized according to the real cellular traffic trace [27], the BS sleep decision and user association has been researched for single-tier (homogeneous) cellular networks (e.g., [28]–[30]). The authors in [28] have suggested a cell association policy of user, which drives the users to as few BSs as possible so that as many BSs as possible can go to sleep. In [29], the authors have contemplated the optimization problem that determines the optimal set of active BSs and user association for minimizing the network cost function, which consists of the delay performance and power consumption. Ref. [30] presents a simple algorithm to minimize the number of active BSs by sleeping BSs one by one that will increase the neighboring cell loads the least. It is noted that most of these schemes cannot be applied to the heterogeneous networks with femtocells, except a few (e.g., [30]). Even though this kind of scheme can be used in femtocell networks, the performance is not good usually since it cannot exploit the inherent merits of two-tier femtocell fully. Recently, a few literatures such as

[31]–[33] have considered the BS sleeping in the heterogeneous networks. However, they only provide guidelines of the BS sleeping ratio by using statistic geometry models and do not provide a sleep decision scheme for each specific BS.

1.2 Proposed Resource Management Schemes

1.2.1 Radio Resource Partitioning Scheme for Spectral Efficiency Enhancement

To enhance the spectral efficiency in the two-tier femtocell networks, we propose a downlink resource allocation scheme [34]. The most common radio resource management scheme for cellular systems is the data transmission scheduling: the scheduler at macro BS allocates radio resource to users, taking account of the channel status information fed back by the users. To cope with the channel variation, the BS carries out the scheduling and allocation with a short period (e.g., frame which is usually shorter than the coherent time of the channel and of which the length is on the order of milliseconds.). However, in the heterogeneous networks, a femto BS is usually installed by a private user and connected to the cellular system through a general purpose broadband network or Internet. In this environment, it is not easy for the macro BS to exchange promptly a lot of control messages with femto BSs and the radio resource management with a short-term control period is not appropriate.

Instead, we consider resource allocation based on a relatively long-term. We suggest a new resource sharing scheme, where an FP is divided into the macro-dedicated, the shared, and the femto-dedicated portions, and the ratio of these three portions is different for each FP. Once the ratio for every FP is determined, a femto BS utilizes the allocated radio resource under its own control (for example, if needed, a femto or macro BS may carry out the transmission scheduling to heighten the efficiency of the allocated radio resource). The ratio of three portions should be readjusted if the traffic pattern is largely changed, for example, by the strong

change in load, the deployments of femto BSs, and so on. Since this situation occurs on a relatively long-term basis (e.g., several tens of minutes) and the delay in readjustment is not crucial, the control messages between macro BS and femto BSs cannot be burden. In this thesis, we focus on this long-term based radio resource partitioning.

Now, the problem is to determine a proper ratio of portions in each FP, in the sense of maximizing the whole system capacity while satisfying the constraints on the minimum throughput requirements for both macrocell and femtocell users. The proposed scheme to tackle this problem is based on an optimization approach, where the estimates of achievable cell capacities for macrocell and femtocell are used as parameters. In our preliminary work [35], we designed an FFR-based resource sharing scheme that determines only the femto-dedicated portion based on computer simulation, without consideration of minimum user throughput requirements.

1.2.2 Base Station Sleep Management Scheme for Energy Efficiency Enhancement

When the femtocell is deployed by an individual user at private premises, the energy efficiency is confined to the problem of individual femtocell. On the other hand, when the femtocells are deployed in a public area (e.g., airport, shopping mall, etc.) and provide open access to users, the energy efficiency should be treated in a network-wide scale over the entire deployment area. In this case, an appropriate network management for enhancing the energy efficiency is strongly needed.

In this thesis, we focus on enhancing the energy efficiency in open access femtocell networks where many femto BSs are deployed in a public area. In such

area, the femtocells are overlapped and underutilized during most of the operation time because femto BSs are densely deployed to support the peak traffic load. So, if we properly coordinate the user association with BSs and put suitable femto BSs to sleep, the energy efficiency in the femtocell deployment area can be greatly enhanced. With this motivation, we propose a scheme that jointly decides the operation modes of femto BSs and the association between users and active BSs, aiming at maximizing energy efficiency in the area under consideration [36]. We will call the proposed scheme the "SDUA (stands for, the femto BS sleep decision and user association)."

The energy efficiency in the femtocell deployment area can be defined as the ratio of total user throughput to totally consumed power for the area (bits/s/W). The problem to maximize the energy efficiency is too complicated to solve due to its fractional form. So, based on the statistical analysis on the energy efficiency, we suggest a tractable problem that can have the same solution as the original problem. The suggested SDUA problem aims at minimizing the total power consumption in the area while all active cells are not overloaded. Unfortunately, this problem is still too complicated to be solved, because the sleep decision of femto BSs and the user association are tightly coupled with each other. To overcome this difficulty, we first solve the user association (UA) problem which minimizes the total energy consumption for given set of active femto BSs. Then, we design a heuristic algorithm that finds the best set of active femto BSs by repeatedly solving the UA problem with an iteratively updated set.

1.3 Organization

The remainder of the thesis is organized as follows. Chapter 2 describes the downlink radio resource partitioning to enhance the spectral efficiency in the two-tier femtocell network. Section 2.1 presents the system model under consideration. In Section 2.2, we propose an FFR-based radio resource partitioning scheme. The proposed scheme needs the estimate of achievable cell capacity, which is computed in Section 2.3.

In Chapter 3, we design an SDUA scheme to enhance the energy efficiency in the open access femtocell network. Section 3.1 describes the system model. The energy efficiency is formulated and analyzed in Section 3.2. Then, we suggest an SDUA scheme and discuss its implementation in Section 3.3.

In Chapter 4, we present the simulation results of two schemes. In Section 4.1, we show the performance of the proposed radio resource partitioning scheme with numerical results. Section 4.2 presents the simulation results of the proposed SDUA scheme. Finally, the thesis is concluded with Chapter 5.

Chapter 2. Radio Resource Partitioning Scheme for Spectral Efficiency Enhancement

In this chapter, we propose a resource management scheme to enhance the spectral efficiency in the two-tier networks where macrocells adopting FFR are overlaid with the femtocells. In the proposed scheme, every FP is divided into the macro-dedicated, the shared, and the femto-dedicated portions, based on the FFR framework. The ratio of these three portions is different for each FP. In order to protect the macrocell users from femtocell transmission on the shared resource, we suggest an FP-based resource prohibition where if an FP is currently assigned to the nearby macrocell user, the femtocell is prohibited from using any shared resource on the FP. Then, we design a method to determine the optimal resource partitioning so that the total sum of macrosector throughput and all underlaid femtocell throughputs is maximized while satisfying the minimum throughput requirements of both macrocell and femtocell users.

2.1 System Model

2.1.1 Heterogeneous Network

We consider a heterogeneous cellular network with macrocells and femtocells, both of which use the same frequency band. Each macro BS operates three sectors with directional antennas. We will focus on a sector rather than an entire macrocell in describing the proposed scheme. As seen from Fig. 2.1, a sector of macrocell is adjacent to two sectors in the neighboring macrocells. Hereafter, we will use the term macrosector to refer to a sector of macrocell. The macro BS adopts

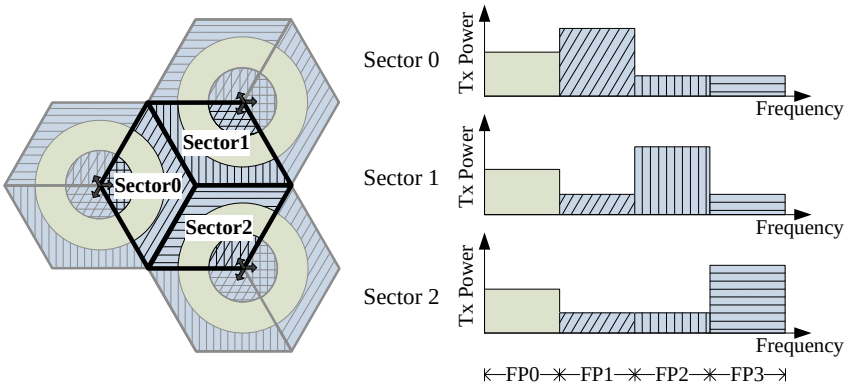

Fig. 2.1: FFR operation in the macrocell tier.

the FFR where the frequency band is divided into K FPs. Each FP consists of V subchannels, each of which has the bandwidth of W_{subch}. Fig. 2.1 shows an example of the FFR operation ($K = 4$). In the figure, three adjacent macrosectors, each of which belongs to different macro BS, are highlighted to represent the FFR operation. In all macrosectors, the transmission power for FP 0 is identical and used as the reference power. The transmission power levels for other FPs (e.g., FP 1, FP 2, and FP 3 in Fig. 2.1) are different from each other. It is noted that high transmission power is assigned to one FP, which is allocated to the users at cell edge for improving the received signal quality. Other two FPs, which are allocated to the users near the BS, are assigned with relatively low transmission power to suppress interference to neighboring macrocells, i.e., macro-to-macro interference (MMI).

On the other hand, a macrocell user is assigned to one FP in the FFR framework. The FP assignment is related to various resource management issues, for example, load balancing and scheduling. Since designing an FP assignment scheme

is beyond the scope of this thesis, we consider the following simple FP assignment, based on the average received signal-to-interference ratio (SIR) of a macrocell user on FP 0 and the predetermined thresholds, like in [37]. Let $ASIR_0$ be the average SIR on FP 0. When $\Gamma_1 < ASIR_0 \leq \Gamma_0$, the corresponding macrocell user is assigned the FPs with low power; if $\Gamma_2 < ASIR_0 \leq \Gamma_1$, the reference FP 0 is assigned to the macrocell user; when $ASIR_0 \leq \Gamma_2$, the FP with high power is assigned to the user.

We assume that a femto BS is under the management of only one macro BS; the femto BS is said to be in the coverage of the corresponding macrocell (specifically, macrosector). For the sake of simplicity in description, a macrosector coverage is assumed not to overlap with any other macrosector coverage. It is assumed that femto BSs are randomly deployed in a macrosector coverage according to a nonhomogeneous spatial Poisson point process (SPPP), in order to represent that the distribution density of femtocells cannot be homogeneous within the entire macrosector coverage. The femtocells are assumed to provide the closed access only to their own members. It is also assumed that all macrosectors and femtocells are perfectly synchronized.

The partial resource sharing approach is applied to the FFR framework. That is, the subchannels in each FP are divided into three groups: a macro-dedicated group (MDG), a shared group (SHG), and a femto-dedicated group (FDG). The resources in MDG are dedicated to the macrocell users except a special case that will be described in the next section. The resources in SHG are shared by the macrosector and the femtocells. To protect the transmission to the macrocell users, i.e., to avoid FMI, the femtocell is allowed to use the SHG resources only when it does not interfere with nearby macrocell users. In other words, if there are

one or more macrocell users close to a femtocell, the femtocell cannot access the entire SHG on the FP assigned to the macrocell users. The resources in FDG are always dedicated to the femtocells. The FDG is needed for satisfying the minimum bandwidth requirements of femtocells, especially, which are deployed near the macro BS and thereby suffer from high MFI.

For each subchannel, two indicator bits are used to represent the resource group which the subchannel belongs to: $\alpha_{k,v}$ indicates whether the subchannel v ($v = 0, 1, \cdots, V-1$) of FP k ($k = 0, 1, \cdots, K-1$) belongs to MDG or not, and $\beta_{k,v}$ represents whether the subchannel v of FP k belongs to FDG or not. When the subchannel v of FP k belongs to MDG, $\alpha_{k,v} = 1$ and $\beta_{k,v} = 0$, and if it belongs to FDG, $\alpha_{k,v} = 0$ and $\beta_{k,v} = 1$. For the subchannel v of FP k belonging to SHG, $\alpha_{k,v} = 0$ and $\beta_{k,v} = 0$. Let $\boldsymbol{\alpha} := [\alpha_{k,v}]_{K \times V}$ and $\boldsymbol{\beta} := [\beta_{k,v}]_{K \times V}$.

2.1.2 Capacity Model

In this thesis, we determine the resource configuration matrixes $\boldsymbol{\alpha}$ and $\boldsymbol{\beta}$ so as to maximize the achievable sector capacity that is the total sum capacity of macro-sector and its overlaying femtocells. To do this, we need to calculate the achievable sector capacity as a function of various system parameters. For the sake of simplicity in calculation, we assume the following multiple access scheme.

The channel time is divided into slots with fixed length. Every time slot, the macro BS schedules the transmission of macrocell users. For each FP, the BS selects a user with a round-robin manner. During a time slot, the selected macrocell user utilizes all available subchannels (i.e., within MDG and SHG) in the FP. On the other hand, although FFR is applied to macrocell, a femtocell can use any available resource irrespective of FPs. Thus, a femto BS serves only one user over all FPs

for each time slot. During a time slot, the selected (by a round-robin manner) femtocell user can be assigned all available subchannels (i.e., within FDG and SHG) in all FPs. Nevertheless, to mitigate the femto-to-femto interference (FFI) between neighboring femtocells, a femto BS uses only a portion of all available resources according to an F-ALOHA fashion [38]. That is, a femto BS accesses each available subchannel with probability ϱ_{f}.

We assume that a scheduled user (either macrocell or femtocell user) feeds back its instantaneous downlink SIR and, based on this information, the serving BS determines the transmission rate by using an adaptive modulation and coding (AMC) scheme with L levels. Let c_l denote the instantaneous transmission rate (b/s/Hz) when its instantaneous SIR lies in $[\gamma_l, \gamma_{l+1}), 1 \leq l \leq L$. We have $c_l = \log_2(1 + \kappa\gamma_l)$, where κ is the SIR gap to reflect the difference between the Shannon capacity and the practical transmission rate according to AMC [39]. Then, the average instantaneous subchannel capacity can be estimated as

$$C = W_{\mathrm{subch}} \left(\sum_{l=1}^{L-1} c_l \Pr\left[\gamma_l \leq SIR < \gamma_{l+1}\right] + c_L \Pr\left[SIR \geq \gamma_L\right] \right). \tag{2.1}$$

For the downlink channel model, we take account of path loss, lognormal shadowing, and Rayleigh fading. The thermal noise is assumed to be negligible as compared with other interference since cellular networks are interference-limited rather than noise-limited. Then, the received signal power at a user is calculated as $p_{\mathrm{R}} = p_{\mathrm{T}}\phi_{\mathrm{x}}{D_{\mathrm{x}}}^{-a_{\mathrm{x}}}G_{\mathrm{x}}$, where p_{T} is the transmitted signal power, ϕ_{x} is the fixed channel gain including the penetration loss and the antenna gains, D_{x} is the distance between the transmitter (a BS) and the receiver (a designated user), a_{x} is the path loss exponent, and G_{x} is the product of the lognormal shadowing gain and the exponentially distributed unit-mean fading gain. The subscript $\mathrm{x} \in \{\mathrm{m}, \mathrm{f}, \mathrm{mm}, \mathrm{mf}, \mathrm{ff}\}$

identifies the channel type: 'm' for the channel from the serving macro BS to a designated macrocell user; 'f' for the channel from the serving femto BS to a designated femtocell user; 'mm' for the channel from a neighboring macro BS to a designated macrocell user; 'mf' for the channel from a macro BS to a designated femtocell user; and 'ff' for the channel from a neighboring femto BS to a designated femtocell user. In addition, for indicating a neighboring BS explicitly, we add the index of the BS to the subscript. For example, 'mm i' ('ff i') means the channel from neighboring macro (femto) BS i to a designated macrocell (femtocell) user.

A composite lognormal-exponetial random variable, G_{x}, can be modeled as a lognormal random variable with $LN(\breve{\mu}_{\mathrm{x}}, \breve{\sigma}_{\mathrm{x}}^2)$, where LN denotes a lognormal distribution, and $\breve{\mu}_{\mathrm{x}}$ and $\breve{\sigma}_{\mathrm{x}}$ are respectively the mean and standard deviation of the natural logarithm of G_{x}. Then, $\breve{\mu}_{\mathrm{x}}$ and $\breve{\sigma}_{\mathrm{x}}$ are calculated using the mean, $\mu_{\mathrm{x,dB}}$, and standard deviation, $\sigma_{\mathrm{x,dB}}$, of lognormal shadowing gain (in dB) of channel x as $\breve{\mu}_{\mathrm{x}} = \xi(\mu_{\mathrm{x,dB}} - 2.5)$ and $\breve{\sigma}_{\mathrm{x}}^2 = \xi^2(\sigma_{\mathrm{x,dB}}^2 + 5.57^2)$ where $\xi = \frac{\ln 10}{10}$ [40].

2.2 Proposed Downlink Radio Resource Partitioning Scheme

As mentioned before, the resources (subchannels) in each FP are divided into three groups (MDG, SHG, and FDG). In this section, we first describe how to protect macrocell users from femtocell users in using SHG. Then, we design a resource sharing scheme that determines the resource configuration matrices, $\boldsymbol{\alpha}$ and $\boldsymbol{\beta}$.

2.2.1 Macrocell Protection Mechanism

The macrocell is devoted to the public service, whereas a closed-access femtocell is likely to be installed for private use. Thus, under the proposed resource management scheme, the macrocell users have the higher priority than femtocell users in using SHG resources. All femto and macro BSs periodically transmit their unique cell-specific preamble signals. If a macrocell user receives the preamble signal from a femtocell, of which strength is over a predetermined level, it means that the femtocell may disrupt the data transmission of the macrocell user with the FMI. The macrocell user reports this harmful femtocell to its serving macro BS. Then, the macro BS requests the corresponding femto BS not to use the shared resource, on which the macrocell user is operating.

Some previous works [41], [42] focused on resource prohibition in the unit of resource block which is a basic transmission scheduling unit. However, this type of resource management is not easy to implement since the control information exchange between the macro BS and a femto BS may not be exquisite. Thus, we suggest an FP-based resource prohibition where if an FP is currently assigned to the nearby macrocell user, the femtocell is prohibited from using any SHG subchannel of the FP.

To implement the proposed mechanism, the macro BS manages an SHG availability indicator (SAI) table consisting of $h_{i,k}$, which indicates whether the femtocell i is allowed to use the SHG resource on FP k ($h_{i,k} = 1$), or not ($h_{i,k} = 0$). Based on the harmful femtocell information reported by the macrocell users and current FP assignment to the macrocell users, the macro BS updates the SAIs. The macro BS also can be requested to change $h_{i,k}$ from neighboring macro BSs that try to

protect their users on FP k which are interfered by the femtocell i. If $h_{i,k}$ is changed from 1 to 0, the macro BS orders the femto BS i not to access the SHG on FP k. On the other hand, if the macrocell user, which reported the femtocell i as being harmful, does not receive the preamble signal stronger than a predetermined level from the femtocell i during a predefined period, the macrocell user reports that the femtocell i is not harmful any more. Then, the macro BS changes $h_{i,k}$ from 0 to 1 and informs the femto BS i of the availability of SHG on FP k.

2.2.2 Determination of Dedicated Portion for Macrocell/Femtocell Users

There can be various design criteria on determining the dedicated resource portions for macrocell and femtocell users, respectively. In this thesis, we consider that the dedicated macro (femto) portion should fulfil the minimum throughput requirements from the services via macrocell (femtocell). Let Ψ_{m} and Ψ_{f} be the minimum required throughputs of a macrocell user and a femtocell user, respectively.

First, the MDG configuration matrix, $\boldsymbol{\alpha}$, is based on the average minimum required throughput of macrosector on FPs. When $C_{\mathrm{m},k,v}$ is the achievable macrosector capacity on subchannel v of FP k and $\bar{n}_{\mathrm{m},k}$ is the average number of macrocell users on FP k, we determine the optimal MDG configuration, $\boldsymbol{\alpha}^*$, as

$$\boldsymbol{\alpha}^* = \underset{\boldsymbol{\alpha}}{\operatorname{argmin}} \sum_{k=0}^{K-1} \sum_{v=0}^{V-1} \alpha_{k,v} \tag{2.2}$$

$$\text{s.t.} \quad \sum_{v=0}^{V-1} \alpha_{k,v} C_{\mathrm{m},k,v} \geq \Psi_{\mathrm{m}} \bar{n}_{\mathrm{m},k} \qquad \forall\, k, \tag{2.3}$$

$$\alpha_{k,v} \in \{0,1\} \qquad \forall\, k, v. \tag{2.4}$$

After fixing $\boldsymbol{\alpha}^*$, we determine the FDG configuration matrix, $\boldsymbol{\beta}$, so that the

total sum of macrosector throughput and all underlaid femtocell throughputs is maximized while guaranteeing (i) the minimum throughput requirements for femtocell services are satisfied, and (ii) the ratio of a macrocell user throughput to a femtocell user throughput is not smaller than a predetermined value. First, let us examine the macrosector throughput. Note that since the macrocell users have a priority in using SHG, the achievable maximum macrosector throughput on FP k depends on $\boldsymbol{\beta}_k = (\beta_{k,0}, \cdots, \beta_{k,V-1})$. Let $T_{\mathrm{m},k}(\boldsymbol{\beta}_k)$ be the expected macrosector throughput on FP k for given $\boldsymbol{\beta}_k$. Then, $T_{\mathrm{m},k}(\boldsymbol{\beta}_k) = \sum_{v=0}^{V-1}(1-\beta_{k,v})C_{\mathrm{m},k,v}$, and the average throughput of a macrocell user on FP k is $T_{\mathrm{m},k}(\boldsymbol{\beta}_k)/\bar{n}_{\mathrm{m},k}$. Also, the expected macrosector throughput over all FPs for given $\boldsymbol{\beta}$ is given as $T_{\mathrm{m}}(\boldsymbol{\beta}) = \sum_{k=0}^{K-1} T_{\mathrm{m},k}(\boldsymbol{\beta}_k)$.

On the other hand, the expected throughput of femtocell i for given $\boldsymbol{\beta}$, denoted by $T_{\mathrm{f}i}(\boldsymbol{\beta})$, can be calculated as follows. Let $C^{(\mathrm{d})}_{\mathrm{f}i,k,v}$ and $C^{(\mathrm{s})}_{\mathrm{f}i,k,v}$ denote the capacities of femtocell i on FP k when all subchannels of FP k are dedicated to the femtocell and when all subchannels of FP k belong to SHG, respectively. Let $\widetilde{h}_{i,k}$ be the availability of FP k at femtocell i in steady-state. That is, $\widetilde{h}_{i,k}$ is equal to the probability that there exists no macrocell user using FP k in the interference range (with radius r_{FMI}) of femtocell i. Then,

$$T_{\mathrm{f}i}(\boldsymbol{\beta}) = \varrho_{\mathrm{f}} \sum_{k=0}^{K-1}\sum_{v=0}^{V-1} \Big\{ \beta_{k,v} C^{(\mathrm{d})}_{\mathrm{f}i,k,v} + (1-{\alpha^*}_{k,v})(1-\beta_{k,v})\widetilde{h}_{i,k}\ C^{(\mathrm{s})}_{\mathrm{f}i,k,v} + {\alpha^*}_{k,v}\ \mathrm{J}(\widetilde{h}_{i,k})\ C^{(\mathrm{s})}_{\mathrm{f}i,k,v} \Big\}, \tag{2.5}$$

where $\mathrm{J}(x)$ is the indicator variable: if $1-x < \epsilon$, it is 1; otherwise, 0. The first term on the right-hand side in (2.5) is the expected throughput of femtocell i by using the resource in the FDG of FP k. The second term is the expected throughput by using the resource in SHG of FP k, considering the macrocell protection against the FMI.

A femtocell utilizes the resource in FDG firstly, and then that in SHG. However, in a special case, a femtocell can use the resource in MDG, where an inherent feature of FFR is exploited. Under FFR, the macrocell users at a certain location rarely use some FPs (see Fig. 2.2 that will be explained later). For example, in Fig. 2.1, the macrocell users around the edge of Sector 0 are less likely to use the FP 0. In this case, the femtocells located in the edge of Sector 0 may utilize the MDG in FP 0, by treating the MDG of FP k like SHG. In the last term in (2.5), the indication that $\mathrm{J}(\widetilde{h}_{i,k}) = 1$ (i.e., $1 - \widetilde{h}_{i,k} < \epsilon$) with ϵ being much smaller than one, means that the macrocell users around the femtocell i are not likely to use the FP k. If it is the case, the MDG can be exploited. Thus, the last term in (2.5) is the expected throughput of femtocell i by using the resource in MDG of FP k.

When the average number of users served by the femto BS i is $\bar{n}_{\mathrm{f}i}$, the expected throughput of a user in femtocell i is $T_{\mathrm{f}i}(\boldsymbol{\beta})/\bar{n}_{\mathrm{f}i}$ and it should be larger than a minimum throughput requirement of a femtocell user, Ψ_{f}. In addition, the sum of all femtocell throughputs within the macrosector is given as $T_{\mathrm{f}}(\boldsymbol{\beta}) = \sum_{i \in \mathcal{N}_{\mathrm{f}}} T_{\mathrm{f}i}(\boldsymbol{\beta})$, where $\mathcal{N}_{\mathrm{f}}$ is the set of femto BSs deployed within the macrosector coverage.

To maximize the spectral efficiency, we determine the optimal FDG configuration $\boldsymbol{\beta}^*$ as

$$\boldsymbol{\beta}^* = \underset{\boldsymbol{\beta}}{\operatorname{argmax}} \left(T_{\mathrm{m}}(\boldsymbol{\beta}) + T_{\mathrm{f}}(\boldsymbol{\beta}) \right) \tag{2.6}$$

$$\text{s.t.} \quad \beta_{k,v} \in \{0, 1\} \qquad \forall\ k, v, \tag{2.7}$$

$$\alpha^*{}_{k,v}\ \beta_{k,v} = 0 \qquad \forall\ k, v, \tag{2.8}$$

$$T_{\mathrm{f}i}(\boldsymbol{\beta}) \geq \Psi_{\mathrm{f}}\ \bar{n}_{\mathrm{f}i} \qquad \forall\ i \in \mathcal{N}_{\mathrm{f}}, \tag{2.9}$$

$$\frac{T_{\mathrm{m},k}(\boldsymbol{\beta}_k)}{\bar{n}_{\mathrm{m},k}} \geq \min\left\{ \eta \times \min_{i \in \mathcal{N}_{\mathrm{f}}} \left(\frac{T_{\mathrm{f}i}(\boldsymbol{\beta})}{\bar{n}_{\mathrm{f}i}} \right), \frac{\sum_{v=0}^{V-1} C_{\mathrm{m},k,v}}{\bar{n}_{\mathrm{m},k}} \right\} \quad \forall\ k, \tag{2.10}$$

where η is the inter-tier fairness parameter to balance the macrocell user throughput and the femtocell user throughput.

As mentioned in the Introduction section, the proposed resource (re)partitioning scheme can be invoked periodically to adapt to the *considerable* change in traffic pattern, caused by the strong change in load, the deployments of femto BSs, and so on, which is on a long-term basis in usual. Since the invocation interval is relatively long,[1] the macro BS (or the BS controller) can use various methods to obtain the solution to this partitioning problem (2.2)–(2.10) without tight constraint on the computational time. The computational complexity of the entire partitioning problem is governed by the problem (2.6)–(2.10). When an exhaustive search is used for determining the binary indicators ($\beta_{k,v}$), its complexity is $\mathcal{O}\left(2^{KV}\right)$. To reduce the computational complexity, some simpler heuristic search algorithms can be used at the cost of performance degradation. In this thesis, we exemplify such a heuristic search algorithm as follows. Since $\alpha^*_{k,v}\beta_{k,v} = 0$, the total throughput in (2.6) can be reexpressed as.

$$T_{\mathrm{m}}(\boldsymbol{\beta}) + T_{\mathrm{f}}(\boldsymbol{\beta}) = \sum_{k=0}^{K-1}\Bigg[\sum_{v\in\mathcal{V}_k}\Theta_{k,v}\beta_{k,v} + \sum_{v=0}^{V-1}\Bigg\{C_{\mathrm{m},k,v} + \rho_{\mathrm{f}}\sum_{i\in\mathcal{N}_{\mathrm{f}}}\Big[(1-\alpha^*_{k,v})\widetilde{h}_{i,k}\ C^{(\mathrm{s})}_{\mathrm{f}\,i,k,v} + \alpha^*_{k,v}\ \mathrm{J}(\widetilde{h}_{i,k})\ C^{(\mathrm{s})}_{\mathrm{f}\,i,k,v}\Big]\Bigg\}\Bigg], \tag{2.11}$$

where $\mathcal{V}_k = \{v|\alpha^*_{k,v} = 0, 0 \le v \le V-1\}$ and $\Theta_{k,v} = -C_{\mathrm{m},k,v} + \rho_{\mathrm{f}}\sum_{i\in\mathcal{N}_{\mathrm{f}}}\left(C^{(\mathrm{d})}_{\mathrm{f}\,i,k,v} - \widetilde{h}_{i,k}\ C^{(\mathrm{s})}_{\mathrm{f}\,i,k,v}\right)$. As we can know from (2.11), only $\Theta_{k,v}$ is relevant to $\beta_{k,v}$. Thus, in getting $\boldsymbol{\beta}$ to maximize the total throughput of (2.11) for given $\boldsymbol{\alpha}^*$, it is better to assign the subchannels with higher $\Theta_{k,v}$ to FDG on FP k. Keeping this in mind, we design a heuristic algorithm to solve the problem (2.6)–(2.10). In Algorithm 1

[1] It is, for example, from several minutes to several hours.

Algorithm 1: Heuristic algorithm to solve (2.6)–(2.10)

for each FP k **do**

let $\imath(v)$ be the index of subchannel v that is renumbered in a descending order of $\Theta_{k,v}$;

$n_k = V - \sum_{v=0}^{V-1} \alpha^*_{k,v}$;

end

$\mathcal{S} = \{(b_0, b_1, \cdots, b_{K-1}) | b_k = 0, 1, \cdots, n_k \quad \forall\ k\}$;

$maxThruput \leftarrow 0$;

for all $(b_0, b_1, \cdots, b_{K-1}) \in \mathcal{S}$ **do**

fix $\boldsymbol{\beta}$ so that for all (k, v), if $\imath(v) < b_k$, $\beta_{k,v} = 1$; otherwise, $\beta_{k,v} = 0$;

if *all the constraints of the problem* (2.6)–(2.10) *are satisfied* **then**

calculate $T_{\mathrm{m}}(\boldsymbol{\beta}) + T_{\mathrm{f}}(\boldsymbol{\beta})$ for given $\boldsymbol{\beta}$;

if $maxThruput < T_{\mathrm{m}}(\boldsymbol{\beta}) + T_{\mathrm{f}}(\boldsymbol{\beta})$ **then**

$maxThruput \leftarrow T_{\mathrm{m}}(\boldsymbol{\beta}) + T_{\mathrm{f}}(\boldsymbol{\beta})$;

$\boldsymbol{\beta}^* \leftarrow \boldsymbol{\beta}$;

end

end

end

on the next page, the variable b_k denotes the number of subchannels belonging to FDG on FP k, and $\mathcal{S}$ is a set of all feasible combinations for the number of FDG subchannels on each FP. The computational complexity of Algorithm 1 depends on the number of elements in the set $\mathcal{S}$. Accordingly, Algorithm 1 has the worst case computational complexity of $\mathcal{O}(V^K)$.

After a macro BS determines appropriate $\boldsymbol{\alpha}$ and $\boldsymbol{\beta}$, it notifies all the femto BSs within its coverage. Now, to implement the proposed scheme, we need to estimate $C_{\mathrm{m},k,v}$, $C^{(\mathrm{d})}_{\mathrm{f}\,i,k,v}$, $C^{(\mathrm{s})}_{\mathrm{f}\,i,k,v}$, and $\widetilde{h}_{i,k}$. In the next section, we compute these estimates with a simplified analytic model.

2.3 Capacity Estimation

2.3.1 Achievable Macrosector Capacity

The macrosectors (and the corresponding macro BSs) are indexed by i ($i = 0, 1, \cdots$). The location of a macrocell user in a two-dimensional Cartesian coordinate system is denoted by $\mathbf{r} := (r_1, r_2)$. Let us focus on a macro BS of which index is 0 and location is $(0, 0)$, and a macrocell user at location $\mathbf{r}$ served by the macro BS 0. Hereafter, we will omit the index 0 of the macro BS to avoid overcrowding in expressions, if there is no confusion.

We first examine the received SIR of this designated macrocell user on a subchannel v of FP k. Assume that a macro BS assigns the same transmission power to all subchannels in an FP. Let $p_{\mathrm{m}\,i,k}$ be the transmission power of macro BS i on a subchannel of FP k. When $S_{\mathrm{m},k}(\mathbf{r})$ denotes the received signal power of the

designated user on a subchannel of FP k,

$$S_{\mathrm{m},k}(\mathbf{r}) = p_{\mathrm{m}\,0,k}\phi_{\mathrm{m}}\|\mathbf{r}\|^{-a_{\mathrm{m}}}G_{\mathrm{m}}, \tag{2.12}$$

where $\|\cdot\|$ denotes the Euclidean norm. Let us investigate the total interference power from neighboring macro BSs on the subchannel v of FP k, denoted by $I_{\mathrm{mm},k,v}(\mathbf{r})$. Note that a neighboring macro BS j can be an interferer only when the subchannel v of FP k does not belong to FDG in the macrosector j. When $\mathcal{B}_{k,v}(\mathbf{r})$ is the set of interfering macro BSs for the designated macrocell user on subchannel v of FP k,

$$I_{\mathrm{mm},k,v}(\mathbf{r}) = \sum_{j\in\mathcal{B}_{k,v}(\mathbf{r})} p_{\mathrm{m}\,j,k}\phi_{\mathrm{m}}\,\|\mathbf{r}-\mathbf{b}_{\mathrm{m}\,j}\|^{-a_{\mathrm{m}}}G_{\mathrm{mm}\,j}, \tag{2.13}$$

where $\mathbf{b}_{\mathrm{m}\,j}$ is the location of the macro BS j. G_{m} and $G_{\mathrm{mm}\,j}$ are independent and identically distributed as $LN(\breve{\mu}_{\mathrm{m}}, \breve{\sigma}^2_{\mathrm{m}})$. Assuming that the FMI is negligible by the low transmission power of femto BS and the proposed macrocell protection mechanism, the received SIR of the designated macrocell user is

$$SIR_{\mathrm{m},k,v}(\mathbf{r}) = S_{\mathrm{m},k}(\mathbf{r})/I_{\mathrm{mm},k,v}(\mathbf{r}). \tag{2.14}$$

In (2.12), $S_{\mathrm{m},k}(\mathbf{r})$ is distributed as $LN(\mu_{S_{\mathrm{m},k}(\mathbf{r})}, \sigma^2_{S_{\mathrm{m},k}(\mathbf{r})})$, where $\mu_{S_{\mathrm{m},k}(\mathbf{r})} = \breve{\mu}_{\mathrm{m}} + \ln(p_{\mathrm{m}\,0,k}\phi_{\mathrm{m}}\|\mathbf{r}\|^{-a_{\mathrm{m}}})$ and $\sigma_{S_{\mathrm{m},k}(\mathbf{r})} = \breve{\sigma}_{\mathrm{m}}$. On the other hand, since the sum of independent lognormal random variables can be approximated as a single lognormal random variable [43], [44], we model $I_{\mathrm{mm},k,v}(\mathbf{r})$ as a lognormal random variable with $LN(\mu_{I_{\mathrm{mm},k,v}(\mathbf{r})}, \sigma^2_{I_{\mathrm{mm},k,v}(\mathbf{r})})$, where $\mu_{I_{\mathrm{mm},k,v}(\mathbf{r})}$ and $\sigma_{I_{\mathrm{mm},k,v}(\mathbf{r})}$ can be calculated numerically according to the approximation method in [44]. Then, the

SIR distribution of the designated macrocell user can be obtained as

$$\begin{aligned}\mathcal{F}_{\mathrm{m},k,v}(\mathbf{r},\gamma) &:= \Pr\left[SIR_{\mathrm{m},k,v}(\mathbf{r}) \le \gamma\right] \\ &= \mathrm{Q}\left(\frac{\mu_{S_{\mathrm{m},k}(\mathbf{r})} - \mu_{I_{\mathrm{mm},k,v}(\mathbf{r})} - \ln\,\gamma}{\sqrt{\sigma^2_{S_{\mathrm{m},k}(\mathbf{r})} + \sigma^2_{I_{\mathrm{mm},k,v}(\mathbf{r})}}}\right),\end{aligned} \tag{2.15}$$

where $\mathrm{Q}(\cdot)$ is the Q-function.

The macrosector capacity depends on the FP assignment policy of FFR. Now, we calculate the probability that the designated macrocell user is assigned to FP k, denoted by $q_k(\mathbf{r})$. As mentioned in the system model of Section 2.1, the macro BS determines the FP of the designated user by comparing its average SIR on FP 0 with the predetermined SIR thresholds, $\mathbf{\Gamma}_{\mathrm{th}} = (\Gamma_0, \cdots, \Gamma_K)$ where $\Gamma_0 = \infty > \Gamma_1 \ge \cdots \ge \Gamma_{K-1} > \Gamma_K = 0$. Let $ASIR_0(\mathbf{r})$ denote the average received SIR of the designated user on FP 0. That is, $ASIR_0(\mathbf{r}) = \left(\sum_{v=0}^{V-1} SIR_{\mathrm{m},0,v}(\mathbf{r})\right)/V$. Then,

$$q_k(\mathbf{r}) = \Pr\left[\Gamma_{k'+1} < ASIR_0(\mathbf{r}) \le \Gamma_{k'}\right], \tag{2.16}$$

where k' is the index of the FP k which is re-numbered in ascending order of the transmission power. For example, in Sector 0 of Fig. 2.1, $k' = 0,\ 0,\ 2,$ and 3 correspond to $k = 2,\ 3,\ 0,$ and 1, respectively.[2]

Note that $SIR_{\mathrm{m},0,v}(\mathbf{r})$ is a lognomal random variable with $LN(\mu_{SIR_{\mathrm{m},0,v}(\mathbf{r})}, \sigma^2_{SIR_{\mathrm{m},0,v}(\mathbf{r})})$, where $\mu_{SIR_{\mathrm{m},0,v}(\mathbf{r})} = \mu_{S_{\mathrm{m},0}(\mathbf{r})} - \mu_{I_{\mathrm{mm},0,v}(\mathbf{r})}$ and $\sigma_{SIR_{\mathrm{m},0,v}(\mathbf{r})} = \sqrt{\sigma^2_{S_{\mathrm{m},0}(\mathbf{r})} + \sigma^2_{I_{\mathrm{mm},0,v}(\mathbf{r})}}$. Since the sum of independent lognormal variables can be approximated as another lognormal random variable [43], [44], we model $ASIR_0(\mathbf{r})$ as a lognormal random variable with $LN(\mu_{ASIR_0(\mathbf{r})}, \sigma^2_{ASIR_0(\mathbf{r})})$. We can easily get $\mu_{ASIR_0(\mathbf{r})}$ and $\sigma_{ASIR_0(\mathbf{r})}$

[2]Since FP 2 and FP 3 use the same subchannel transmission power, if $\Gamma_1 < ASIR_0(\mathbf{r}) \le \Gamma_0$, the macro BS may randomly assign FP 2 or FP 3 to the user at location $\mathbf{r}$.

by using various numerical calculation tools. Then,

$$q_k(\mathbf{r}) = \mathrm{Q}\left(\frac{\mu_{ASIR_0(\mathbf{r})} - \ln \Gamma_{k'}}{\sigma_{ASIR_0(\mathbf{r})}}\right) - \mathrm{Q}\left(\frac{\mu_{ASIR_0(\mathbf{r})} - \ln \Gamma_{k'+1}}{\sigma_{ASIR_0(\mathbf{r})}}\right). \tag{2.17}$$

We calculate $C_{\mathrm{m},k,v}$ by using the SIR distribution spatially averaged over the macrosector coverage. For tractability, a circular macrocell of which radius is $\hat{R}_{\mathrm{m}} = \sqrt{\frac{3\sqrt{3}r_{\mathrm{m}}^2}{2\pi}}$ is considered instead of a hexagonal cell with side length of r_{m}. Let $\mho_{\mathrm{m}} := \{\mathbf{r} | \mathbf{r} = (r\cos\theta, r\sin\theta) \text{ for } r \leq \hat{R}_{\mathrm{m}}, -\frac{\pi}{3} \leq \theta \leq \frac{\pi}{3}\}$. Considering that any macrocell user is served only through its assigned FP, the cumulative distribution function (CDF) of $SIR_{\mathrm{m},k,v}$ can be spatially averaged as

$$\mathcal{Z}_{\mathrm{m},k,v}(\gamma) = \mathrm{E}_{\mathbf{r}\in\mho_{\mathrm{m}}}[\mathcal{F}_{\mathrm{m},k,v}(\mathbf{r},\gamma) | \text{FP } k \text{ is assigned to the user at } \mathbf{r}], \tag{2.18}$$

where $\mathrm{E}[\cdot]$ means the statistical expectation. Let $f_{\mathbf{R}_{\mathrm{m}}}(\mathbf{r})$ be the probability density function (PDF) of a random variable $\mathbf{R}_{\mathrm{m}}$ representing a macrocell user location. Since a macrocell user at location $\mathbf{r}$ can be assigned to FP k with the probability of $q_k(\mathbf{r})$, the conditional PDF of $\mathbf{R}_{\mathrm{m}}$ is $f_{\mathbf{R}_{\mathrm{m}}}(\mathbf{r}|\text{FP } k \text{ is assigned}) = \frac{q_k(\mathbf{r}) f_{\mathbf{R}_{\mathrm{m}}}(\mathbf{r})}{\int_{\mathbf{r}\in\mho_{\mathrm{m}}} q_k(\mathbf{r}) f_{\mathbf{R}_{\mathrm{m}}}(\mathbf{r})\, d\mathbf{r}}$. Considering $\mathbf{r} = (r\cos\theta, r\sin\theta)$, we re-denote $\mathcal{F}_{\mathrm{m},k,v}(\mathbf{r},\gamma)$, $q_k(\mathbf{r})$, and $f_{\mathbf{R}_{\mathrm{m}}}(\mathbf{r})$ by $\mathcal{F}_{\mathrm{m},k,v}(r,\theta,\gamma)$, $q_k(r,\theta)$, and $f_{R,\Theta}(r,\theta)$, respectively. Then, (2.18) can be expressed as

$$\mathcal{Z}_{\mathrm{m},k,v}(\gamma) = \frac{1}{g_k} \int_0^{\hat{R}_{\mathrm{m}}} \int_{-\frac{\pi}{3}}^{\frac{\pi}{3}} \mathcal{F}_{\mathrm{m},k,v}(r,\theta,\gamma) q_k(r,\theta) f_{R,\Theta}(r,\theta) d\theta dr, \tag{2.19}$$

where $g_k = \int_{\mathbf{r}\in\mho_{\mathrm{m}}} q_k(\mathbf{r}) f_{\mathbf{R}_{\mathrm{m}}}(\mathbf{r})\, d\mathbf{r}$. A closed form expression of (2.19) can be hardly derived.

In this thesis, we obtain an approximate value of $\mathcal{Z}_{\mathrm{m},k,v}(\gamma)$ with following assumptions. First, we assume that the macrocell users are uniformly distributed in the macrosector coverage. Second, let us divide the sector coverage into A non-overlapping annuli and then divide each annulus into B slabs by angle. The mth

annulus has inner radius $\mathcal{R}_{m-1}$ and outer radius $\mathcal{R}_m$ ($1 \leq m \leq A$, $\mathcal{R}_0 = 0$, and $\mathcal{R}_A = \hat{R}_{\mathrm{m}}$) and the nth slab in an annulus has lower angle Θ_{n-1} and upper angle Θ_n ($1 \leq n \leq B$, $\Theta_0 = -\frac{\pi}{3}$, and $\Theta_B = \frac{\pi}{3}$). When A and B are sufficiently large, we can suppose that the SIR on a subchannel is identically distributed for the macrocell users inside the same slab. That is, $\mu_{SIR_{\mathrm{m},k,v}(r,\theta)} \approx \mu_{SIR_{\mathrm{m},k,v}(\mathcal{R}_m,\Theta_n)}$ and $\sigma_{SIR_{\mathrm{m},k,v}(r,\theta)} \approx \sigma_{SIR_{\mathrm{m},k,v}(\mathcal{R}_m,\Theta_n)}$, when $\mathcal{R}_{m-1} \leq r \leq \mathcal{R}_m$ and $\Theta_{n-1} \leq \theta \leq \Theta_n$. We also suppose that the FP assignment probability is the same for any macrocell users within the same slab. That is, $q_k(r,\theta) \approx q_k(\mathcal{R}_m, \Theta_n)$, for $\mathcal{R}_{m-1} \leq r \leq \mathcal{R}_m$ and $\Theta_{n-1} \leq \theta \leq \Theta_n$. Then,

$$\mathcal{Z}_{\mathrm{m},k,v}(\gamma) \approx \frac{1}{\hat{g}_k} \sum_{m=1}^{A} \sum_{n=1}^{B} \left\{ \left(\frac{\mathcal{R}_m^2 - \mathcal{R}_{m-1}^2}{\hat{R}_{\mathrm{m}}^2 B} \right) \cdot \mathcal{F}_{\mathrm{m},k,v}(\mathcal{R}_m, \Theta_n, \gamma)\, q_k(\mathcal{R}_m, \Theta_n) \right\}, \quad (2.20)$$

where $\hat{g}_k = \sum_{m=1}^{A} \sum_{n=1}^{B} \left\{ \left(\frac{\mathcal{R}_m^2 - \mathcal{R}_{m-1}^2}{\hat{R}_{\mathrm{m}}^2 B} \right) q_k(\mathcal{R}_m, \Theta_n) \right\}$. From (2.1) and (2.20), we can obtain the achievable macrocell capacity on subchannel v of FP k as

$$C_{\mathrm{m},k,v} = W_{\mathrm{subch}} \left[\sum_{l=1}^{L-1} c_l \left\{ \mathcal{Z}_{\mathrm{m},k,v}(\gamma_{l+1}) - \mathcal{Z}_{\mathrm{m},k,v}(\gamma_l) \right\} + c_L \left\{ 1 - \mathcal{Z}_{\mathrm{m},k,v}(\gamma_L) \right\} \right]. \quad (2.21)$$

2.3.2 Achievable Femtocell Capacities

Since the location of a femtocell user is not likely to change during service time, the throughputs of the users at femtocell boundary can be lower than those of other users. In determining the resource configuration, we need to pay careful attention to these users at cell edge (shortly, the edge users). Thus, we will estimate the achievable femtocell capacity in a conservative manner by assuming that all femtocell users are located at the edge of the femtocell. It is noted that the resulting capacity corresponds to the minimum achievable femtocell capacity. Let us calculate $C_{\mathrm{f}i,k,v}^{(\mathrm{d})}$, the minimum achievable capacity of femtocell i on subchannel v of

FP k when the subchannel belongs to FDG, and $C^{(\mathrm{s})}_{\mathrm{f}\,i,k,v}$, the minimum achievable capacity of femtocell i on the subchannel v of FP k when the subchannel belongs to SHG.

To calculate the achievable femtocell capacity, we need to know the SIR distributions of a femtocell edge user on FDG and SHG. We assume that a femto BS assigns the same transmission power to all subchannels regardless of FPs. It is noted that the FFR configuration is applied only to macrocells and a femto BS can utilize any subchannel if it is available to the femtocell. In addition, the subchannel transmission power of all femto BSs is assumed to be the same.

First, let us calculate the SIR distribution when using SHG of FP k. We focus on a femtocell edge user at location $\mathbf{r}$, which we will call the designated femtocell user. Let p_{f} be the transmission power of a femto BS on a subchannel and r_{f} be the service radius of a femto BS. When S_{f} denotes the received signal power on a subchannel at the femtocell edge user,

$$S_{\mathrm{f}} = p_{\mathrm{f}}\phi_{\mathrm{f}} r_{\mathrm{f}}^{-a_{\mathrm{f}}} G_{\mathrm{f}}. \tag{2.22}$$

Since G_{f} is distributed as $LN(\breve{\mu}_{\mathrm{f}}, \breve{\sigma}^2_{\mathrm{f}})$, S_{f} also has a lognormal distribution $LN(\mu_{S_{\mathrm{f}}}, \sigma^2_{S_{\mathrm{f}}})$ where $\mu_{S_{\mathrm{f}}} = \breve{\mu}_{\mathrm{f}} + \ln(p_{\mathrm{f}}\phi_{\mathrm{f}} r_{\mathrm{f}}^{-a_{\mathrm{f}}})$ and $\sigma_{S_{\mathrm{f}}} = \breve{\sigma}_{\mathrm{f}}$.

On an SHG subchannel, a femtocell user receives interference from neighboring femto BSs (i.e., FFI) and from its overlaid macro BS and other neighboring macro BSs (MFI). Since the femto BSs are assumed to be spatially distributed according to a nonhomogeneous SPPP, FFI of the designated femtocell user depends on the density of other femto BSs within its interference area. Let r_{FFI} denote the radius of femtocell interference to the neighboring femtocell users and $N_{\mathrm{f}}(\mathbf{r})$ be the number of femto BSs in this interference area. For analytical tractability, we assume

that the femto BSs are distributed in the interference area of the designated femtocell user according to homogeneous SPPP with intensity of $\zeta_{\mathrm{f}}(\mathbf{r}) = N_{\mathrm{f}}(\mathbf{r})/(\pi r_{\mathrm{FFI}}^2)$. Furthermore, each femto BS merely uses a portion ϱ_{f} of the available resource for femtocells according to F-ALOHA in order to decrease FFI. Thus, the designated femtocell user has interfering femto BSs distributed according to SPPP with intensity of $\varrho_{\mathrm{f}}\ \zeta_{\mathrm{f}}(\mathbf{r})$. When $I_{\mathrm{ff}}(\mathbf{r})$ denotes the interference power that the designated femtocell user receives from other femtocells,

$$I_{\mathrm{ff}}(\mathbf{r}) = \sum_{j \in \Lambda_{\mathrm{f}}(\mathbf{r})} p_{\mathrm{f}} \phi_{\mathrm{ff}} \|\mathbf{r} - \mathbf{b}_{\mathrm{f}\,j}\|^{-a_{\mathrm{ff}}} G_{\mathrm{ff}\,j}, \tag{2.23}$$

where $\Lambda_{\mathrm{f}}(\mathbf{r})$ is the set of interfering femto BSs, $\mathbf{b}_{\mathrm{f}\,j}$ is the location of the femto BS j, and $G_{\mathrm{ff}\,j}$ is distributed as $LN(\breve{\mu}_{\mathrm{ff}}, \breve{\sigma}_{\mathrm{ff}}^2)$. On the other hand, the interference power from neighboring macro BSs is different for each subchannel since the resource configurations of macrocells may differ from each other. When $I_{\mathrm{mf},k,v}(\mathbf{r})$ denotes the total power that the designated femtocell user receives from interfering macro BSs on subchannel v belonging to SHG of FP k,

$$I_{\mathrm{mf},k,v}(\mathbf{r}) = \sum_{j \in \Omega_{\mathrm{m},k,v}(\mathbf{r})} p_{\mathrm{m}\,j,k} \phi_{\mathrm{mf}} \|\mathbf{r} - \mathbf{b}_{\mathrm{m}\,j}\|^{-a_{\mathrm{mf}}} G_{\mathrm{mf}\,j}, \tag{2.24}$$

where $\Lambda_{\mathrm{m},k,v}(\mathbf{r})$ is the set of interfering macro BSs, including the overlaid macro BS, on the subchannel v of FP k. $I_{\mathrm{mf},k,v}(\mathbf{r})$ also can be modeled as a single log-normal random variable with $LN(\mu_{I_{\mathrm{mf}}(\mathbf{r})}, \sigma_{I_{\mathrm{mf}}(\mathbf{r})}^2)$, where $\mu_{I_{\mathrm{mf}}(\mathbf{r})}$ and $\sigma_{I_{\mathrm{mf}}(\mathbf{r})}$ can be obtained by using the approximation method in [44]. Then, the received SIR of the designated femtocell user on the subchannel v belonging to the SHG of FP k is expressed as $SIR_{\mathrm{f},k,v}^{(\mathrm{s})}(\mathbf{r}) = \frac{S_{\mathrm{f}}}{I_{\mathrm{mf},k,v}(\mathbf{r}) + I_{\mathrm{ff}}(\mathbf{r})}$.

Let us derive $\mathcal{F}_{\mathrm{f},k,v}^{(\mathrm{s})}(\mathbf{r}, \gamma) := \Pr[SIR_{\mathrm{f},k,v}^{(\mathrm{s})}(\mathbf{r}) \leq \gamma]$. Like in [45], we decompose $\mathcal{F}_{\mathrm{f},k,v}^{(\mathrm{s})}(\mathbf{r}, \gamma)$ into two parts as follows: $\mathcal{F}_{\mathrm{f},k,v}^{(\mathrm{s})}(\mathbf{r}, \gamma) = \Pr[\frac{S_{\mathrm{f}}}{I_{\mathrm{mf},k,v}(\mathbf{r})} \leq \gamma] + \Pr[SIR_{\mathrm{f},k,v}^{(\mathrm{s})}(\mathbf{r}) \leq$

$\gamma, \frac{S_{\rm f}}{I_{{\rm mf},k,v}(\mathbf{r})} > \gamma]$. Note that $S_{\rm f}$ and $I_{{\rm mf},k,v}(\mathbf{r})$ are independent lognormal random variables. Since dividing a lognormal random variable by an independent lognormal random variable results in another lognormal random variable, the distribution of $SIR^{(\rm s)}_{{\rm f},k,v}(\mathbf{r})$ without the FFI term can be easily obtained as

$$\Pr\left[\frac{S_{\rm f}}{I_{{\rm mf},k,v}(\mathbf{r})} \le \gamma\right] = {\rm Q}\left(\frac{\mu_{S_{\rm f}} - \mu_{I_{\rm mf}(\mathbf{r})} - \ln\gamma}{\sqrt{\sigma^2_{S_{\rm f}} + \sigma^2_{I_{\rm mf}(\mathbf{r})}}}\right). \tag{2.25}$$

On the other hand, $\Pr[SIR^{(\rm s)}_{{\rm f},k,v}(\mathbf{r}) \le \gamma, \frac{S_{\rm f}}{I_{{\rm mf},k,v}(\mathbf{r})} > \gamma]$ does not have a closed form expression. However, by using Gauss-Hermite integration [46], we can obtain its approximate lower bound as

$$\begin{aligned}
&\Pr\left[SIR^{(\rm s)}_{{\rm f},k,v}(\mathbf{r}) \le \gamma,\ \frac{S_{\rm f}}{I_{{\rm mf},k,v}(\mathbf{r})} > \gamma\right] \\
&\quad\ge \sum_{n=1}^{N}\sum_{m=1}^{M} \frac{t_m \nu_n \breve{u}_{m,n}}{\pi} \cdot \Bigg\{1 - \exp\Bigg[- \varkappa_{\rm f}\gamma^{\frac{2}{a_{\rm ff}}} \Big(\exp[\mu_{S_{\rm f}} + \sqrt{2}\sigma_{S_{\rm f}} X_m] \\
&\qquad\qquad - \gamma \exp[\mu_{I_{\rm mf}(\mathbf{r})} + \sqrt{2}\sigma_{I_{\rm mf}(\mathbf{r})} Y_n]\Big)^{-\frac{2}{a_{\rm ff}}}\Bigg]\Bigg\},
\end{aligned} \tag{2.26}$$

where $\varkappa_{\rm f} = \pi\varsigma_{\rm f}(\mathbf{r})\varrho_{\rm f}\left(p_{\rm f}\phi_{\rm ff}\right)^{\frac{2}{a_{\rm ff}}} \exp\left[2\breve{\mu}_{\rm ff}/a_{\rm ff} + 2\breve{\sigma}^2_{\rm ff}/a^2_{\rm ff}\right]$. And, M and N, t_m and ν_n, and X_m $(m = 1, \cdots, M)$ and Y_n $(n = 1, \cdots, N)$ are the orders, weight factors, and abscissas of Gauss-Hermite integration, respectively [46, Table 25.10]. $\breve{u}_{m,n}$ is the conditional weight factor, which gives one if $\left(\sigma_{S_{\rm f}} X_m - \sigma_{I_{\rm mf}(\mathbf{r})} Y_n\right) \ge (\ln\gamma - \mu_{S_{\rm f}} + \mu_{I_{\rm mf}(\mathbf{r})})/\sqrt{2}$ and zero otherwise. The derivation of (2.26) is as follows. $\Pr[SIR^{(\rm s)}_{{\rm f},k,v}(\mathbf{r}) \le \gamma, \frac{S_{\rm f}}{I_{{\rm mf},k,v}(\mathbf{r})} > \gamma]$ can be obtained as

$$\begin{aligned}
&\Pr\left[SIR^{(\rm s)}_{{\rm f},k,v}(\mathbf{r}) \le \gamma, \frac{S_{\rm f}}{I_{{\rm mf},k,v}(\mathbf{r})} > \gamma\right] \\
&= \int_0^\infty \int_{\gamma z}^\infty \Pr\left[\frac{y}{z + I_{\rm ff}(\mathbf{r})} \le \gamma | S_{\rm f} = y, I_{{\rm mf},k,v}(\mathbf{r}) = z\right] d\mathcal{F}_{S_{\rm f}}(y)\ d\mathcal{F}_{I_{\rm mf}}(z),
\end{aligned} \tag{2.27}$$

where $\mathcal{F}_{S_{\rm f}}(y)$ and $\mathcal{F}_{I_{\rm mf}}(z)$ are the CDF of $S_{\rm f}$ and $I_{{\rm mf},k,v}(\mathbf{r})$, respectively. In the

following derivation, $\mathbf{r}$, k, and v will be omitted to avoid overcrowding in expressions. According to [38, Lemma 2], the distribution of I_{ff} has the lower bound as $\Pr\left[I_{\mathrm{ff}} \geq x\right] \geq 1 - \exp\left[-\pi\varrho_{\mathrm{f}}\zeta_{\mathrm{f}}\left(x^{-1}p_{\mathrm{f}}\phi_{\mathrm{ff}}\right)^{\frac{2}{a_{\mathrm{ff}}}} \mathrm{E}\left[G_{\mathrm{ff}}^{\frac{2}{a_{\mathrm{ff}}}}\right]\right]$. Then, an approximate lower bound of (2.27) can be expressed as

$$
\begin{aligned}
&\Pr\left[SIR_{\mathrm{f}}^{(\mathrm{s})} \leq \gamma, \frac{S_{\mathrm{f}}}{I_{\mathrm{mf}}} > \gamma\right] \\
&\geq \int_0^\infty \int_{\gamma z}^\infty 1 - \exp\left[-\varkappa_{\mathrm{f}}\gamma^{\frac{2}{a_{\mathrm{ff}}}}\left(y-\gamma z\right)^{-\frac{2}{a_{\mathrm{ff}}}}\right] d\mathcal{F}_{S_{\mathrm{f}}}(y)\; d\mathcal{F}_{I_{\mathrm{mf}}}(z) \\
&= \int_0^\infty \int_{\gamma z}^\infty \left\{1 - \exp\left[-\varkappa_{\mathrm{f}}\gamma^{\frac{2}{a_{\mathrm{ff}}}}\left(y-\gamma z\right)^{-\frac{2}{a_{\mathrm{ff}}}}\right]\right\} \frac{\exp\left[-\frac{\left(\ln y - \mu_{S_{\mathrm{f}}}\right)^2}{2\sigma_{S_{\mathrm{f}}}^2}\right]}{y\sigma_{S_{\mathrm{f}}}\sqrt{2\pi}} dy\; d\mathcal{F}_{I_{\mathrm{mf}}}(z) \\
&= \int_0^\infty \int_{\frac{\ln\gamma z - \mu_{S_{\mathrm{f}}}}{\sqrt{2}\sigma_{S_{\mathrm{f}}}}}^\infty \left\{1 - \exp\left[-\varkappa_{\mathrm{f}}\gamma^{\frac{2}{a_{\mathrm{ff}}}}\left(\mathrm{e}^{\sqrt{2}\sigma_{S_{\mathrm{f}}}x + \mu_{S_{\mathrm{f}}}} - \gamma z\right)^{-\frac{2}{a_{\mathrm{ff}}}}\right]\right\} \frac{1}{\sqrt{\pi}}\mathrm{e}^{-x^2} dx\; d\mathcal{F}_{I_{\mathrm{mf}}}(z)
\end{aligned}
\tag{2.28}
$$

$$
\approx \int_0^\infty \sum_{m=1}^{M} \frac{t_m u_m(z)}{\sqrt{\pi}} \left\{1 - \exp\left[-\varkappa_{\mathrm{f}}\gamma^{\frac{2}{a_{\mathrm{ff}}}}\left(\mathrm{e}^{\sqrt{2}\sigma_{S_{\mathrm{f}}}X_m + \mu_{S_{\mathrm{f}}}} - \gamma z\right)^{-\frac{2}{a_{\mathrm{ff}}}}\right]\right\} d\mathcal{F}_{I_{\mathrm{mf}}}(z), \tag{2.29}
$$

where $\varkappa_{\mathrm{f}} = \pi\varrho_{\mathrm{f}}\zeta_{\mathrm{f}}\left(p_{\mathrm{f}}\phi_{\mathrm{ff}}\right)^{\frac{2}{a_{\mathrm{ff}}}} \exp\left[2\breve{\mu}_{\mathrm{ff}}/a_{\mathrm{ff}} + 2\breve{\sigma}_{\mathrm{ff}}^2/a_{\mathrm{ff}}^2\right]$. By using Gauss-Hermite integration [46], the integral in (2.28) is approximated with a weighted sum of function values at some specified points as in (2.29). Note that since the integration range in (2.28) is from $\frac{\ln\gamma z - \mu_{S_{\mathrm{f}}}}{\sqrt{2}\sigma_{S_{\mathrm{f}}}}$ to ∞, we add a weight function $u_m(z)$, which gives one if $X_m \geq \frac{\ln\gamma z - \mu_{S_{\mathrm{f}}}}{\sqrt{2}\sigma_{S_{\mathrm{f}}}}$ and zero otherwise. Let $\Xi_m := \sqrt{2}\sigma_{S_{\mathrm{f}}}X_m + \mu_{S_{\mathrm{f}}}$ for simplified expression. Using Gauss-Hermite integration again, (2.29) can be modified as

$$
\begin{aligned}
&\Pr\left[SIR_{\mathrm{f}}^{(\mathrm{s})} \le \gamma, \frac{S_{\mathrm{f}}}{I_{\mathrm{mf}}} > \gamma\right] \\
&\geq \int_0^{\infty} \sum_{m=1}^{M} \frac{t_m u_m(z)}{\sqrt{\pi}} \left\{1 - \exp\left[-\varkappa_{\mathrm{f}} \gamma^{\frac{2}{a_{\mathrm{ff}}}} \left(\mathrm{e}^{\Xi_m} - \gamma z\right)^{-\frac{2}{a_{\mathrm{ff}}}}\right]\right\} \frac{\exp\left[-\frac{\left(\ln z - \mu_{I_{\mathrm{mf}}}\right)^2}{2\sigma_{I_{\mathrm{mf}}}^2}\right]}{z\sigma_{I_{\mathrm{mf}}}\sqrt{2\pi}} dz \\
&\approx \sum_{n=1}^{N} \sum_{m=1}^{M} \frac{t_m v_n \breve{u}_{m,n}}{\pi} \left\{1 - \exp\left[-\varkappa_{\mathrm{f}} \gamma^{\frac{2}{a_{\mathrm{ff}}}} \left(\mathrm{e}^{\Xi_m} - \gamma \mathrm{e}^{\sqrt{2}\sigma_{I_{\mathrm{mf}}} Y_n + \mu_{I_{\mathrm{mf}}}}\right)^{-\frac{2}{a_{\mathrm{ff}}}}\right]\right\}, \qquad (2.30)
\end{aligned}
$$

where $u_m(z)$ is modified to the conditional weight factor, $\breve{u}_{m,n}$, which gives one if $\sigma_{S_{\mathrm{f}}} X_m - \sigma_{I_{\mathrm{mf}}} Y_n \geq \frac{\ln\gamma + \mu_{I_{\mathrm{mf}}} - \mu_{S_{\mathrm{f}}}}{\sqrt{2}}$ and zero otherwise.

When $\Phi_{\mathrm{F}i}$ is a set of edge positions of femtocell i, i.e., $\Phi_{\mathrm{f}i} := \{\mathbf{r} | \|\mathbf{r} - \mathbf{b}_{\mathrm{f}i}\| = r_{\mathrm{f}}\}$ and $f_{\mathbf{R}_{\mathrm{f}}}(\mathbf{r})$ is the probability density function of random variable $\mathbf{R}_{\mathrm{f}}$ representing an edge position of femtocell i, we can have the spatially averaged CDF of $SIR_{\mathrm{f},k,v}^{(\mathrm{s})}$ as

$$
\mathcal{Z}_{\mathrm{f}i,k,v}^{(\mathrm{s})}(\gamma) = \int_{\mathbf{r} \in \Phi_{\mathrm{f}i}} \mathcal{F}_{\mathrm{f},k,v}^{(\mathrm{s})}(\mathbf{r}, \gamma) f_{\mathbf{R}_{\mathrm{m}}}(\mathbf{r}) d\mathbf{r}. \qquad (2.31)
$$

An edge position of femtocell i can be expressed with respect to the location of femto BS i, $\mathbf{b}_{\mathrm{f}i}$, and the angle from the femto BS i, θ. That is, $\mathbf{r} = \mathbf{b}_{\mathrm{f}i} + (r_{\mathrm{f}} \cos\theta, r_{\mathrm{f}} \sin\theta)$. When $I_{\mathrm{mf},k,v}(\mathbf{r})$ is re-denoted by $I_{\mathrm{mf},k,v}(i,\theta)$ with $LN(\mu_{I_{\mathrm{mf}}(i,\theta)}, \sigma_{I_{\mathrm{mf}}(i,\theta)}^2)$, (2.31) is as

$$
\begin{aligned}
\mathcal{Z}_{\mathrm{f}i,k,v}^{(\mathrm{s})}(\gamma) \approx \int_{-\pi}^{\pi} \frac{1}{2\pi} \Bigg[& \mathrm{Q}\left(\frac{\mu_{S_{\mathrm{f}}} - \mu_{I_{\mathrm{mf}}(i,\theta)} - \ln\gamma}{\sqrt{\sigma_{S_{\mathrm{f}}}^2 + \sigma_{I_{\mathrm{mf}}(i,\theta)}^2}}\right) \\
& + \sum_{n=1}^{N} \sum_{m=1}^{M} \frac{t_m \nu_n \breve{u}_{m,n}}{\pi} \\
& \cdot \Bigg\{1 - \exp\Big[-\varkappa_{\mathrm{f}} \gamma^{\frac{2}{a_{\mathrm{ff}}}} \big(\exp[\sqrt{2}\sigma_{S_{\mathrm{f}}} X_m + \mu_{S_{\mathrm{f}}}] \\
& \quad - \gamma \exp[\sqrt{2}\sigma_{I_{\mathrm{mf}}(i,\theta)} Y_n + \mu_{I_{\mathrm{mf}}(i,\theta)}]\big)^{-\frac{2}{a_{\mathrm{ff}}}}\Big]\Bigg\}\Bigg] d\theta.
\end{aligned} \qquad (2.32)
$$

We can calculate (2.32) numerically using Simpson's rule. By applying $\mathcal{Z}_{\mathrm{f}i,k,v}^{(\mathrm{s})}(\gamma)$

to (2.1),

$$C_{\mathrm{f}i,k,v}^{(\mathrm{s})} = W_{\mathrm{subch}} \left[\sum_{l=1}^{L-1} c_l \left\{ \mathcal{Z}_{\mathrm{f}i,k,v}^{(\mathrm{s})}(\gamma_{l+1}) - \mathcal{Z}_{\mathrm{f}i,k,v}^{(\mathrm{s})}(\gamma_l) \right\} + c_L \left\{ 1 - \mathcal{Z}_{\mathrm{f}i,k,v}^{(\mathrm{s})}(\gamma_L) \right\} \right]. \tag{2.33}$$

Next, we calculate $C_{\mathrm{f}i,k,v}^{(\mathrm{d})}$ on the subchannal v belonging to FDG of FP k. Since the overlaid macro BS does not use FDG subchannels, the femtocell user does not receive the interference from its overlaid macro BS, i.e., the macro BS 0. Thus, when calculating MFI in (2.24), the macro BS 0 should be excluded from $\Lambda_{\mathrm{m},k,v}(\mathbf{r})$. Then, we can get $C_{\mathrm{f}i,k,v}^{(\mathrm{d})}$ by applying (2.22)–(2.33).

2.3.3 SHG Availability of Femtocell

The SAI, $h_{i,k}$, is set to 0 if any macrocell user assigned to FP k is staying in the interference range (with radius r_{FMI}) of femtocell i and 1 otherwise. We do modeling the SHG availability by using the queueing technique. Let λ be the arrival rate of macrocell users to the femtocell interference area, $1/\delta$ be the average femtocell sojourn time of a macrocell user, m_k be the maximum allowable number of macrocell users assigned to FP k in a macrosector, and $\hat{q}_{c,i,k}$ be the probability that a macrocell user, who is staying within the interference range of femtocell i while being served by a macro BS c, is assigned to FP k. Then, the availability for the SHG of FP k at the femtocell i in macrosector c can be modeled by an M/M/m_k/m_k queue with the arrival rate $\lambda\hat{q}_{c,i,k}$ and the service rate δ. If the femtocell i is near the boundary of its overlaid macrosector, the femtocell interference area may span two or more macrosectors. The SHG availability in a steady state, $\widetilde{h}_{i,k}$, is equal to the probability that there exists no macrocell user assigned to FP k in the interference range of femtocell i, irrespective of the serving BS of the macrocell

user. Let $\aleph_i$ be a set of macrosectors within the interference range of femtocell i. From an M/M/m_k/m_k queue,

$$\widetilde{h}_{i,k} = \prod_{c \in \aleph_i} \left(\sum_{j=0}^{m_k} \frac{(\hat{q}_{c,i,k} \bar{n}_{\mathrm{I},c,i})^j}{j!} \right)^{-1}, \tag{2.34}$$

where $\bar{n}_{\mathrm{I},c,i}$ $(= \lambda/\delta)$ is the average number of the macrocell users which are staying in the interference area of femtocell i while being served by the macro BS c. Since $\bar{n}_{\mathrm{I},c,i}$ can be used as a single parameter instead of λ and δ in calculating $\widetilde{h}_{i,k}$, we do not need to estimate λ and δ separately if we can guess $\bar{n}_{\mathrm{I},0,i}$ directly. For example, when the macrocell users are assumed to be uniformly distributed within the sector, $\bar{n}_{\mathrm{I},0,i}$ can be estimated as $\bar{n}_{\mathrm{m}} \mathcal{A}_{c,i} / (\sqrt{3} r_{\mathrm{m}}^2 / 2)$, where $\mathcal{A}_{c,i}$ is the interference area size of femtocell i within the macrosector c. We approximate the location of any macrocell user inside the femtocell as the location of the femto BS, by considering the small coverage of femtocell. Thus, we can easily get $\hat{q}_{c,i,k}$ by applying (2.16) for a user at location $\mathbf{b}_{\mathrm{f}\,i}$ served by the macro BS c. Furthermore, m_k can be estimated as the total number of macrocell users in the sector, since it is possible for all macrocell users to be assigned to FP k.

It is obvious that $\widetilde{h}_{i,k}$ is influenced by the number of macrocell users assigned to FP k, which depends on the total number of macrocell users in the overlaid sector, $\bar{n}_{\mathrm{m}}$, and the FP k assignment probability of a macrocell user, q_k. Fig. 2.2 and Fig. 2.3 respectively illustrate q_k and $\widetilde{h}_{i,k}$, under the FFR configuration of Sector 0 in Fig. 2.1 where the subchannel transmission power of each FP relative to FP 0, is set to 4 dB, -6 dB, and -6 dB for FP 1, 2, and 3, respectively. In addition, $r_{\mathrm{FMI}} = 40$ m, $\mathbf{\Gamma}_{\mathrm{th}} = (\infty, 14, 14, 9, -\infty)$ in dB, and the side length of a hexagonal macrocell $r_{\mathrm{m}} = 800$ m. The channel model parameter values are given in Table I.

We can observe from Fig. 2.2 that FP 2 and FP 3 are mainly assigned to the

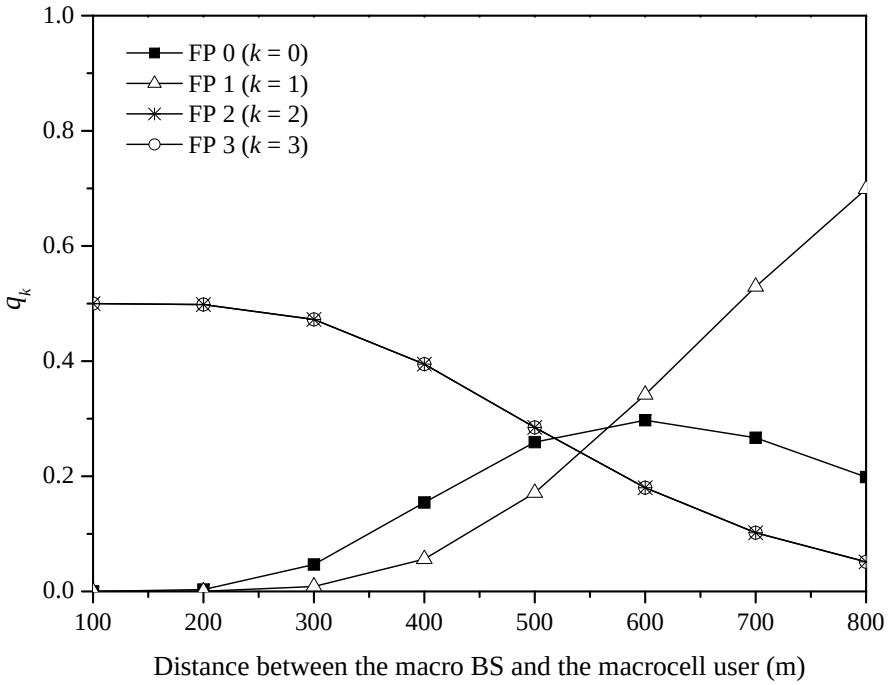

Fig. 2.2: q_k according to the distance between the macro BS and the macrocell user.

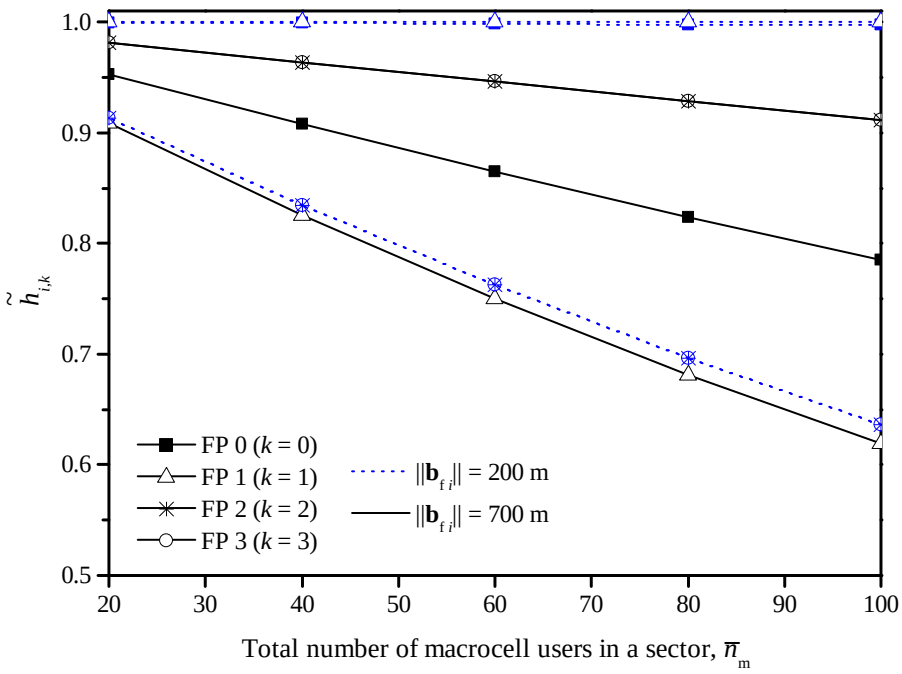

Fig. 2.3: SHG availability of femtocell i, $\tilde{h}_{i,k}$.

users in the innermost region of the sector. Furthermore, FP 1 is highly probable to be assigned to the users of the outermost area. On the other hand, Fig. 2.3 shows that the SHG of each FP is less available for a femtocell when there are more macrocell users in the sector. It is also observed from Fig. 2.3 that the SHG availability on FPs is influenced by the location of the femto BS. When $\|\mathbf{b}_{\mathrm{f}i}\| = 200$ m, the femtocell i locates at the region where FP 2 and FP 3 are mainly allocated; when $\|\mathbf{b}_{\mathrm{f}i}\| = 700$ m, the macrocell users around the femtocell i are likely to be allocated to FP 1 (see Fig. 2.2). Thus, the femto BS close to the macro BS has more access opportunities for SHGs of FP 0 and FP 1, whereas the SHGs of FP 2 and FP 3 are the most available to the femto BS far from the macro BS.

Now, we can get the proposed resource sharing in Section 2.2, by using $C_{\mathrm{m},k,v}$, $C^{(\mathrm{d})}_{\mathrm{f}i,k,v}$, $C^{(\mathrm{s})}_{\mathrm{f}i,k,v}$, and $\widetilde{h}_{i,k}$ calculated in this section.

Chapter 3. Base Station Sleep Management Scheme for Energy Efficiency Enhancement

In this chapter, we propose a BS sleep management scheme to enhance the energy efficiency in the open access femtocell networks. The proposed scheme determines the operation modes (i.e., active or sleep) of femto BSs and the association between user and the active BSs. The energy efficiency in the femtocell deployment area is defined as the ratio of total user throughput to totally consumed power for the area. Since the problem to maximize the energy efficiency is too complicated to be solved due to its fractional form, we try to find a tractable problem that can have the same solution as the original problem. Let us consider that the cellular network provide the data services only as requested by users for energy saving. Then, if all cells are not overloaded, the total throughput in the network is constant as the sum of required data rates of users and, as a result, the energy efficiency depends only on the total power consumption. However, if some of cells are overloaded, the total throughput will relatively decrease much more compared to the power consumption, since the users struggle with limited resource. So, we presume that the energy efficiency in this case will be much lower than when all the cells are underloaded. Under this presumption, the energy efficiency is maximized when the total power consumption is minimized while all cells are not overloaded. Accordingly, we suggest a femto BS sleep decision and user association (SDUA) problem that aims at minimizing the total power consumption in the network while all active cells are not overloaded. We first analyze the energy efficiency by using a mathematical model and empirically verify the presumption through numerical results. Next, we design the proposed SDUA scheme based on an optimization

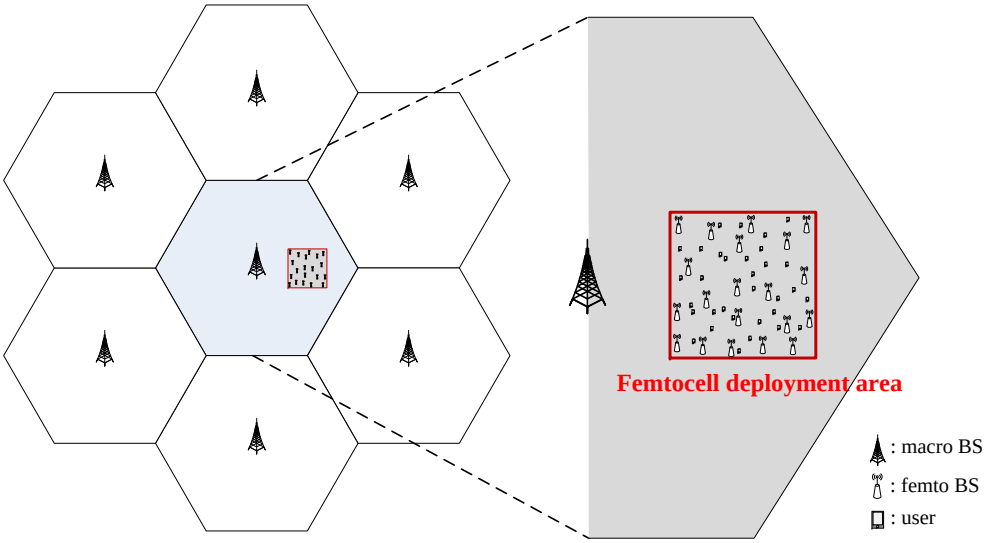

Fig. 3.1: System model.

approach and discuss the implementation of the proposed scheme.

3.1 System Model

3.1.1 Open Access Femtocell Network

We consider a two-tier femtocell network consisting of a macrocell overlaid with a lot of femtocells. Specifically, we focus on a specific zone covering a part of the macrocell, where N_{f} open-access femto BSs are deployed densely, as exemplified in Fig. 3.1. In this thesis, this zone is called the designated zone and denoted by $\mathcal{A}$. The femto BSs are controlled by a femtocell management system (FMS)[1] via wired broadband connections. The index set of the femto BSs in $\mathcal{A}$ is denoted by $\mathcal{B}_{\mathrm{f}} = \{1, 2, \cdots, N_{\mathrm{f}}\}$. We use the BS index of zero to represent the BS of macrocell

[1]The FMS can be located separately in the designated zone or be implemented inside the macro BS.

(macro BS). The cells have the same indices as those of their own BSs. Let $\mathcal{U}$ denote the set of the users who are staying in $\mathcal{A}$. Since the femtocells provide open access to users, a user in $\mathcal{A}$ is associated with the macro BS or one of N_{f} femto BSs.

Since the downlink traffic is much higher than the uplink one in usual multimedia communications, in designing the SDUA scheme, we focus on downlink transmission. The macro BS uses the whole downlink bandwidth of B, while the femto BSs reuse a part of the band, $\upsilon_{\mathrm{f}}B$ $(0 < \upsilon_{\mathrm{f}} \leq 1)$. Especially, the macro BS allocates non-shared resource to its associated users in $\mathcal{A}$, since they can suffer from high interference from adjacent femto BS(s) on the shared resource. We assume that the frequency resource of $\upsilon_{\mathrm{m}}^{(\mathcal{A})}B$ is available for the macrocell users in $\mathcal{A}$, where $0 < \upsilon_{\mathrm{m}}^{(\mathcal{A})} \leq 1 - \upsilon_{\mathrm{f}}$.

An arbitrary user j is characterized by its data rate requirement, denoted by R_j. Even for the same data rate requirement, the impact of the requirement on the serving cell may differ according to the cell capacity. Thus, we define the "relative resource requirement" of user j as the fraction of R_j to the cell capacity. That is, when $\psi_{i,j}$ denotes the relative resource requirement of user j at the cell i, $\psi_{i,j}$ can be estimated as

$$\psi_{i,j} = \frac{R_j}{W_i \log_2(1 + \kappa \breve{\gamma}_{i,j})}, \tag{3.1}$$

where $\breve{\gamma}_{i,j}$ is the SIR from cell i that the user j experiences; κ is the SIR gap between the Shannon capacity and the practical transmission rate; and W_i is the total bandwidth available for the cell i, i.e., $W_0 = B$ and $W_i = \upsilon_{\mathrm{f}}B$ for $i \in \mathcal{B}_{\mathrm{f}}$.

3.1.2 Operation Modes and Power Consumption of a BS

We assume that the macro BS is always active[2] whereas a femto BS is either active or sleeping. The femto BS in active mode serves users associated with itself. However, in sleep mode, the femto BS turns off its radio transceivers and other hardware components not in use, except when it occasionally transmits cell-specific preambles so that adjacent users can detect the BS.

The power consumption in an active BS is modeled as the sum of two portions, P_{const} and P_{tx}: P_{const} is constant power consumption for operating the BS equipment; P_{tx} is power consumption for signal transmission, which is proportional to the radio frequency (RF) output power. Let us assume that fixed transmission power is equally allocated to resource units. Then, when a BS uses more radio resource in the cell, P_{tx} gets higher usually. In detail, when Δ denotes the power consumption for transmission at full utilization of the cell resource, we have $P_{\text{tx}} = \Delta \cdot \rho$ where ρ is the resource utilization at the operating cell. On the other hand, a BS in sleep mode consumes a constant power of P_{sleep}.

3.1.3 Energy Efficiency

Since the users can be served by the femtocells and the overlaid macrocell, the total power consumption in the designated zone is expressed as

$$P_{\text{total}} = P_{\text{m}}^{(\mathcal{A})} + \textstyle\sum_{i \in \mathcal{B}_{\text{f}}} P_{\text{f}i}, \tag{3.2}$$

[2]This assumption is reasonable in that the macro BS usually has more than one users due to its large cell coverage and it should be always ready for the potential access of user(s) in order to provide the network connectivity without latency to the cellular users at any time.

where $P_{\mathrm{m}}^{(\mathcal{A})}$ is the power consumed by the macro BS for serving its associated users in $\mathcal{A}$ and $P_{\mathrm{f}\,i}$ is the power consumption at femto BS i. When the femto BS i is active and has the cell resource utilization of $\rho_{\mathrm{f}\,i}$, we have $P_{\mathrm{f}\,i} = \Delta_{\mathrm{f}}\rho_{\mathrm{f}\,i} + P_{\mathrm{f,\,const}}$, where Δ_{f} is the power that a femto BS consumes for data transmission when the cell resource is fully utilized, and $P_{\mathrm{f,\,const}}$ is the constantly consumed power at a femto BS. On the other hand, when the femto BS i is in sleep mode, we have $P_{\mathrm{f}\,i} = P_{\mathrm{f,\,sleep}}$. The power consumed by the macro BS for serving its associated users in $\mathcal{A}$ is obtained as $P_{\mathrm{m}}^{(\mathcal{A})} = \Delta_{\mathrm{m}}\rho_{\mathrm{m}}^{(\mathcal{A})}$, where Δ_{m} is the power consumption for data transmission when the whole resource is utilized at the macrocell and $\rho_{\mathrm{m}}^{(\mathcal{A})}$ is the resource utilization for serving the macrocell users in $\mathcal{A}$. Note that unlike $P_{\mathrm{f}\,i}$, the constant power consumption of macro BS is not considered in assessing $P_{\mathrm{m}}^{(\mathcal{A})}$. This is because the macro BS serves not only the users in $\mathcal{A}$ but also other users outside of $\mathcal{A}$ within its cell coverage.

The total throughput in $\mathcal{A}$ is expressed as $T_{\mathrm{total}} = T_{\mathrm{m}}^{(\mathcal{A})} + \sum_{i\in\mathcal{B}_{\mathrm{f}}} T_{\mathrm{f}\,i}$, where $T_{\mathrm{m}}^{(\mathcal{A})}$ is the sum throughtput of macrocell users[3] within $\mathcal{A}$ and $T_{\mathrm{f}\,i}$ is the cell throughput at femto BS i. Accordingly, the energy efficiency in the designated zone can be expressed as

$$EE \text{ (bits/Joule)} := \frac{T_{\mathrm{total}}}{P_{\mathrm{total}}} = \frac{T_{\mathrm{m}}^{(\mathcal{A})} + \sum_{i\in\mathcal{B}_{\mathrm{f}}} T_{\mathrm{f}\,i}}{P_{\mathrm{m}}^{(\mathcal{A})} + \sum_{i\in\mathcal{B}_{\mathrm{f}}} P_{\mathrm{f}\,i}}. \tag{3.3}$$

3.2 Analysis on Energy Efficiency

When the number of active femto BSs is sufficiently high and thereby the active femtocells and overlaid macrocell serve all the users with satisfied data rate, the

[3]In this thesis, we refer to a user who is served by macro BS as *a macrocell user* and a user who is served by femto BS as *a femtocell user*.

energy efficiency in the designated zone depends only on the total power consumption since the sum throughput of users is constant. In this case, maximizing the energy efficiency is equivalent to minimizing the total power consumption. On the contrary, when too few cells are active and the active cells are overloaded, the total throughput decreases as the number of active cells decreases. Since the total power consumption also decreases as more femto BSs go to sleep, we do not know how the energy efficiency is exactly influenced by the number of active cells in the case. Nevertheless, we presume that the energy efficiency gets lower with decreasing number of active cells, since the decrease of total throughput due to the cell overload has more impact on the energy efficiency than the decrease of total power consumption. To verify this, we analyze the energy efficiency by using a mathematical model and show some numerical results [47].

3.2.1 Mathematical Model

For the analysis, we use a statistical model where the femto BSs and users are spatially distributed in the designated zone, $\mathcal{A}$, according to homogeneous SPPP with intensity of λ_{f} and λ_{u}, respectively. Even though the femto BS distribution cannot follow homogeneous SPPP around the area edge, we assume that the homogeneity is maintained even at the edge, for analytical tractability. Like when we estimate the transmission capacity in 2.1.2, we model the channel gain as $\phi_{\mathrm{x}} D_{\mathrm{x}}^{-a_{\mathrm{x}}} G_{\mathrm{x}}$, where x represents the channel type, ϕ_{x} is the fixed channel gain, D_{x} is the distance between the transmitter (a BS) and the receiver (a designated user), a_{x} is the path loss exponent, and G_{x} is the product of the lognormal shadowing gain and the exponentially distributed unit-mean fading gain.

Assume that an adaptive modulation and coding scheme with L levels is applied.

Then, when the instantaneous SIR of a user lies in $[\gamma_l, \gamma_{l+1}), 1 \leq l \leq L$, the instantaneous transmission rate (b/s/Hz) is given as $c_l = \log_2(1 + \kappa\gamma_l)$. When a user at location $\mathbf{r}$ has its required data rate of R_{req}, the expected average relative resource requirement of the user at a cell can be computed as

$$\psi_{\text{x}}(\mathbf{r}) := \frac{R_{\text{req}}}{W_{\text{x}}} \left[\sum_{l=1}^{L-1} \frac{1}{c_l} \Pr\left\{\gamma_l \leq SIR_{\text{x}}(\mathbf{r}) < \gamma_{l+1}\right\} + \frac{1}{c_L} \Pr\left\{SIR_{\text{x}}(\mathbf{r}) \geq \gamma_L\right\} \right], \quad (3.4)$$

where W_{x} is the total bandwidth available for the cell, i.e., $W_{\text{f}} = \upsilon_{\text{f}} B$ and $W_{\text{m}} = B$.

With the analytical model, we first derive the energy efficiency according to the femto BS-sleeping ratio θ, which is the ratio of sleeping femto BSs to the total number of femto BSs in the designated zone. After that, we investigate the region of the optimal value θ^* for maximizing the energy efficiency through the numerical results.

3.2.2 Derivation of Energy Efficiency

According to the SPPP, the average number of active femto BSs is $(1-\theta)\lambda_{\text{f}}|\mathcal{A}|$, where $|\mathcal{A}|$ is the size of the area $\mathcal{A}$. Assume that all the users in $\mathcal{A}$ have the same data rate requirement of R_{req}. When each active femtocell serves $\bar{n}_{\text{f}}$ users on average, we have the average total throughput of the femtocell users as $\mathbb{E}\left[\sum_{i\in\mathcal{B}_{\text{f}}} T_{\text{f}\,i}\right] = (1-\theta)\lambda_{\text{f}}|\mathcal{A}|\bar{n}_{\text{f}}R_{\text{req}}$, where $\mathbb{E}[\cdot]$ means the statistical expectation. The remaining users except the femtocell users are served by the macro BS. Thus, we have $\mathbb{E}\left[T_{\text{m}}^{(\mathcal{A})}\right] = \{\lambda_{\text{u}} - (1-\theta)\lambda_{\text{f}}\bar{n}_{\text{f}}\}|\mathcal{A}|R_{\text{svc}}$, where R_{svc} is the servable data rate of a macrocell user, which will be explained later. On the other hand, when the average resource utilization at an active femtocell is $\bar{\rho}_{\text{f}}$, the average power consumption of all the deployed femto BSs can be estimated as $\mathbb{E}\left[\sum_{i\in\mathcal{B}_{\text{f}}} P_{\text{f}\,i}\right] = (1-\theta)\lambda_{\text{f}}|\mathcal{A}|\left(\Delta_{\text{f}}\bar{\rho}_{\text{f}} + P_{\text{f, const}}\right) + \theta\lambda_{\text{f}}|\mathcal{A}|P_{\text{f, sleep}}$. In addition, when the average resource

utilization for the macrocell users in $\mathcal{A}$ is given as $\bar{\rho}_{\mathrm{m}}^{(\mathcal{A})}$, we have $\mathbb{E}\left[P_{\mathrm{m}}^{(\mathcal{A})}\right] = \Delta_{\mathrm{m}}\bar{\rho}_{\mathrm{m}}^{(\mathcal{A})}$. Accordingly, (3.3) can be re-expressed with respect to θ as

$$EE(\theta) = \frac{(1-\theta)\lambda_{\mathrm{f}}\bar{n}_{\mathrm{f}}R_{\mathrm{req}} + \{\lambda_{\mathrm{u}} - (1-\theta)\lambda_{\mathrm{f}}\bar{n}_{\mathrm{f}}\}R_{\mathrm{svc}}}{(1-\theta)\lambda_{\mathrm{f}}\left(\Delta_{\mathrm{f}}\bar{\rho}_{\mathrm{f}} + P_{\mathrm{f,const}}\right) + \theta\lambda_{\mathrm{f}}P_{\mathrm{f,sleep}} + \Delta_{\mathrm{m}}\bar{\rho}_{\mathrm{m}}^{(\mathcal{A})}/|\mathcal{A}|}. \tag{3.5}$$

To calculate (3.5) for given θ, we need to estimate $\bar{n}_{\mathrm{f}}$, $\bar{\rho}_{\mathrm{f}}$, $\bar{\rho}_{\mathrm{m}}^{(\mathcal{A})}$, and R_{svc}. These estimates are computed in the following.

Let us consider that a user is positioned at location $\mathbf{r}$ within $\mathcal{A}$. Since the femto BSs are distributed according to the SPPP, the distance between the user and its closest active femto BS, which is denoted by D_{f}, is distributed as

$$\Pr\{D_{\mathrm{f}} > x\} = \exp[-\pi(1-\theta)\lambda_{\mathrm{f}}x^2]. \tag{3.6}$$

Thus, assuming that a user selects its serving cell according to the received signal strength, the femtocell selection probability that the user selects one of femtocells as its serving cell is

$$q_{\mathrm{f}}(\mathbf{r}) := \Pr\left\{p_{\mathrm{f}}\phi_{\mathrm{f}}G_{\mathrm{f}}D_{\mathrm{f}}^{-a_{\mathrm{f}}} > p_{\mathrm{m}}\phi_{\mathrm{m}}G_{\mathrm{m}}\|\mathbf{r}\|^{-a_{\mathrm{m}}}\right\}, \tag{3.7}$$

where p_{m} and p_{f} are the transmission powers on a resource unit of macrocell and femtocell, respectively, and $\|\cdot\|$ denotes the Euclidean norm. It is assumed that the macro BS is located at origin. Let $b_{\mathrm{f}} := 2/a_{\mathrm{f}}$ and $\hat{G} := (G_{\mathrm{f}}/G_{\mathrm{m}})^{b_{\mathrm{f}}}$. The random variable $\hat{G}$ has a lognormal distribution with $\mu_{\hat{G}} = b_{\mathrm{f}}\left(\breve{\mu}_{\mathrm{f}} - \breve{\mu}_{\mathrm{m}}\right)$ and $\sigma_{\hat{G}}^2 =$

$b_{\mathrm{f}}^2\left(\breve{\sigma}_{\mathrm{f}}^2+\breve{\sigma}_{\mathrm{m}}^2\right)$. Then, from (3.6), we have $q_{\mathrm{f}}(\mathbf{r})$ in (3.7) as

$$\begin{aligned}
q_{\mathrm{f}}(\mathbf{r}) =& 1-\mathbb{E}\big[e^{-\zeta\|\mathbf{r}\|^{a_{\mathrm{m}}b_{\mathrm{f}}}\hat{G}}\big], \\
=& 1-\int_0^{\infty}\frac{e^{-\zeta\|\mathbf{r}\|^{a_{\mathrm{m}}b_{\mathrm{f}}}x}}{x\sigma_{\hat{G}}\sqrt{2\pi}}\exp\big[-\frac{\left(\ln x-\mu_{\hat{G}}\right)^2}{2\sigma_{\hat{G}}^2}\big]\mathrm{d}x \\
=& 1-\int_{-\infty}^{\infty}\frac{1}{\sqrt{\pi}}\exp[-\zeta\|\mathbf{r}\|^{a_{\mathrm{m}}b_{\mathrm{f}}}e^{(\sqrt{2}\sigma_{\hat{G}}z+\mu_{\hat{G}})}]e^{-z^2}\mathrm{d}z \\
\approx& 1-\sum_{n=1}^{N}\frac{v_n}{\sqrt{\pi}}\exp\big[-\zeta\|\mathbf{r}\|^{a_{\mathrm{m}}b_{\mathrm{f}}}e^{(\sqrt{2}\sigma_{\hat{G}}X_n+\mu_{\hat{G}})}\big], \qquad (3.8)
\end{aligned}$$

where $\zeta=\pi(1-\theta)\lambda_{\mathrm{f}}\left(\frac{p_{\mathrm{f}}\phi_{\mathrm{f}}}{p_{\mathrm{m}}\phi_{\mathrm{m}}}\right)^{b_{\mathrm{f}}}$. The moment generating function of $\hat{G}$, i.e., $\mathbb{E}\big[e^{-\zeta\|\mathbf{r}\|^{a_{\mathrm{m}}b_{\mathrm{f}}}\hat{G}}\big]$ is approximately calculated by using Gauss-Hermite integration [46]. N, v_n, and X_n in the last line of (3.8) are the orders, weight factors, and abscissas of Gauss-Hermite integration, respectively [46, Table 25.10].

While computing $\bar{n}_{\mathrm{f}}$, $\bar{\rho}_{\mathrm{f}}$, and $\bar{\rho}_{\mathrm{m}}^{(\mathcal{A})}$, we consider the following approach for easy computation. We divide the designated zone into K non-overlapping subregions with the same area size. The kth subregion has the center point of $\mathbf{r}_{\mathrm{c}}^{(k)}(k=1,2,\cdots,K)$. When K is sufficiently large, we can suppose that the femtocell selection probability is the same for users within the same subregion. That is, $q_{\mathrm{f}}(\mathbf{r})\approx q_{\mathrm{f}}(\mathbf{r}_{\mathrm{c}}^{(k)})$ for any location $\mathbf{r}$ within the kth subregion. We denote $q_{\mathrm{f}}^{(k)}:=q_{\mathrm{f}}(\mathbf{r}_{\mathrm{c}}^{(k)})$.

Now, let us estimate $\bar{\rho}_{\mathrm{f}}$ and $\bar{n}_{\mathrm{f}}$. Consider that a user at $\mathbf{r}$ is associated with its closest femto BS. When the distance between the user and the femto BS, D_{f}, is given as x, the SIR distribution of the femtocelll user can be obtained from (24)–(25) in [34]. Let the conditional SIR distribution denote $\Psi_l(\mathbf{r},x):=\Pr\{SIR_{\mathrm{f}}(\mathbf{r})\le\gamma_l|\ D_{\mathrm{f}}=x\}$. The detailed derivation of $\Psi_l(\mathbf{r},x)$ is omitted due to the lack of space. Instead, the readers can refer to [34] for the details. The average SIR distribution is obtained as $\mathcal{F}_{\mathrm{f},l}(\mathbf{r}):=\Pr\{SIR_{\mathrm{f}}(\mathbf{r})\le\gamma_l\}=\int_0^{\infty}\Psi_l(\mathbf{r},x)f_{D_{\mathrm{f}}}(x)\mathrm{d}x$, where $f_{D_{\mathrm{f}}}(x)$ is the probability density function of D_{f}, which is given as $f_{D_{\mathrm{f}}}(x)=$

$2\pi(1-\theta)\lambda_{\mathrm{f}} x e^{-\pi(1-\theta)\lambda_{\mathrm{f}} x^2}$ from (3.6). We can approximately calculate the SIR distribution as $\mathcal{F}_{\mathrm{f},l}(\mathbf{r}) \approx \sum_{v=1}^{V} \chi_v \Psi\left(\mathbf{r}, \sqrt{\frac{Z_v}{\pi(1-\theta)\lambda_{\mathrm{f}}}}\right)$, by using the Gauss-Laguerre integration [46, Table 25.9]. V, χ_v, and Z_v are the parameters used for the Gauss-Laguerre integration. Applying $\mathcal{F}_{\mathrm{f},l}(\mathbf{r})$ to (3.4), the relative resource requirement at $\mathbf{r}$ can be obtained as $\psi_{\mathrm{f}}(\mathbf{r}) = \frac{R_{\mathrm{req}}}{v_{\mathrm{f}} W}\left[\sum_{l=1}^{L-1} \frac{\mathcal{F}_{\mathrm{f},l+1}(\mathbf{r}) - \mathcal{F}_{\mathrm{f},l}(\mathbf{r})}{c_l} + \frac{1-\mathcal{F}_{\mathrm{f},L}(\mathbf{r})}{c_L}\right]$. Since we can suppose that the femtocell users within a subregion have identical SIR distribution, the load of $\tilde{\rho}_{\mathrm{f}}^{(k)} = \lambda_{\mathrm{u}} q_{\mathrm{f}}^{(k)} \psi_{\mathrm{f}}(\mathbf{r}_{\mathrm{c}}^{(k)}) / \left((1-\theta)\lambda_{\mathrm{f}}\right)$ is imposed on an active femtocell in subregion k. Thus, we have the average resource utilization in subregion k as $\hat{\rho}_{\mathrm{f}}^{(k)} = \min\left(1, \tilde{\rho}_{\mathrm{f}}^{(k)}\right)$ and the average femtocell resource utilization over the entire zone area as

$$\bar{\rho}_{\mathrm{f}} = \frac{1}{K} \sum_{k=1}^{K} \hat{\rho}_{\mathrm{f}}^{(k)}. \tag{3.9}$$

On the other hand, the users, who select femtocells as their serving cell, can be blocked to access the femtocells with the probability of $\Upsilon_{\mathrm{f}}^{(k)} = \frac{\tilde{\rho}_{\mathrm{f}}^{(k)} - \hat{\rho}_{\mathrm{f}}^{(k)}}{\tilde{\rho}_{\mathrm{f}}^{(k)}}$ due to the cell overload. Accordingly, the average number of users associated with a femtocell can be estimated as

$$\bar{n}_{\mathrm{f}} = \frac{\lambda_u}{K(1-\theta)\lambda_f} \sum_{k=1}^{K} q_{\mathrm{f}}^{(k)} (1 - \Upsilon_{\mathrm{f}}^{(k)}). \tag{3.10}$$

Finally, $\bar{\rho}_{\mathrm{m}}^{(\mathcal{A})}$ and R_{svc} can be computed as follows. Consider that a user at $\mathbf{r}$ is associated with the overlaid macrocell. The received signal power of the user, i.e., $S_{\mathrm{m}}(\mathbf{r}) = P_{\mathrm{m}} \phi_{\mathrm{m}} G_{\mathrm{m}} \|\mathbf{r}\|^{-a_{\mathrm{m}}}$ is distributed as $LN(\mu_{S_{\mathrm{m}}(\mathbf{r})}, \sigma^2_{S_{\mathrm{m}}(\mathbf{r})})$, where $\mu_{S_{\mathrm{m}}(\mathbf{r})} = \breve{\mu}_{\mathrm{m}} + \ln(p_{\mathrm{m}} \phi_{\mathrm{m}} \|\mathbf{r}\|^{-a_{\mathrm{m}}})$ and $\sigma_{S_{\mathrm{m}}(\mathbf{r})} = \breve{\sigma}_{\mathrm{m}}$, respectively. The sum of interference powers from neighboring macro BSs, which is denoted by $I_{\mathrm{m}}(\mathbf{r})$, also can be modeled as a lognormal random variable with $LN(\mu_{I_{\mathrm{m}}(\mathbf{r})}, \sigma^2_{I_{\mathrm{m}}(\mathbf{r})})$ [44]. Thus, the SIR distribution of the macrocell user is obtained as $\mathcal{F}_{\mathrm{m},l}(\mathbf{r}) := \Pr\left[SIR_{\mathrm{m}}(\mathbf{r}) = \frac{S_{\mathrm{m}}(\mathbf{r})}{I_{\mathrm{m}}(\mathbf{r})} \leq \gamma_l\right] = \mathrm{Q}\left(\frac{\mu_{S_{\mathrm{m}}(\mathbf{r})} - \mu_{I_{\mathrm{m}}(\mathbf{r})} - \ln \gamma_l}{\sqrt{\sigma^2_{S_{\mathrm{m}}(\mathbf{r})} + \sigma^2_{I_{\mathrm{m}}(\mathbf{r})}}}\right)$. Applying $\mathcal{F}_{\mathrm{m},l}(\mathbf{r})$ to (3.4), we can have the relative resource

requirement of the macrocell user, $\psi_{\mathrm{m}}(\mathbf{r})$. A user in the subregion k is connected to the macrocell with the probability of $1-q_{\mathrm{f}}^{(k)}+\Upsilon_{\mathrm{f}}^{(k)}q_{\mathrm{f}}^{(k)}$. Then, the resource requirement for the macrocell users in $\mathcal{A}$ is obtained as $\tilde{\rho}_{\mathrm{m}}^{(\mathcal{A})} \approx \frac{|\mathcal{A}|\lambda_{\mathrm{u}}}{K}\sum_{k=1}^{K}\left(1-q_{\mathrm{f}}^{(k)}+\Upsilon_{\mathrm{f}}^{(k)}q_{\mathrm{f}}^{(k)}\right)\cdot \psi_{\mathrm{m}}(\mathbf{r}_{\mathrm{c}}^{(k)})$, supposing that the macrocell users within a subregion experience the same SIR distribution. Since the resource utilization for the macrocell users in $\mathcal{A}$ cannot exceed $\upsilon_{\mathrm{m}}^{(\mathcal{A})}$, the average resource utilization is as

$$\bar{\rho}_{\mathrm{m}}^{(\mathcal{A})} = \min(\upsilon_{\mathrm{m}}^{(\mathcal{A})}, \tilde{\rho}_{\mathrm{m}}^{(\mathcal{A})}). \tag{3.11}$$

In addition, assuming that the macrocell provides limited service to its associated users in an overload state, the servable data rate of the macro BS is $R_{\mathrm{svc}} = (\bar{\rho}_{\mathrm{m}}^{(\mathcal{A})}/\tilde{\rho}_{\mathrm{m}}^{(\mathcal{A})})R_{\mathrm{req}}$.

By using the above-calculated $\bar{n}_{\mathrm{f}}$, $\bar{\rho}_{\mathrm{f}}$, $\bar{\rho}_{\mathrm{m}}^{(\mathcal{A})}$, and R_{svc}, we can get the energy efficiency in (3.5) for given femto BS-sleeping ratio.

3.2.3 Numerical Results and Discussion

Let us consider a two-tier femtocell network, which is composed of seven hexagonal macrocells and a square-shaped femtocell deployment area within the central macrocell, as seen in Fig. 3.1. The distance between the central macro BS to the center point of the designated area is $D_{\mathcal{A}}$. We set $\lambda_{\mathrm{f}} = 8\times10^{-4}$ and $R_{\mathrm{req}} = 300$ kb/s. Other parameters are set as presented in 4.2.1.

We first examine the effect of the femto BS-sleeping ratio, θ on the energy efficiency for different network traffic loads (see Figs. 3.2(a) and 3.2(b)). As θ increases, the resource utilizations, $\bar{\rho}_{\mathrm{f}}$ and $\bar{\rho}_{\mathrm{m}}^{(\mathcal{A})}$, get higher since the same number of users is served by fewer BSs. When the traffic load is low (Fig. 3.2(a), $\lambda_{\mathrm{u}} = 2\times10^{-3}$), both $\bar{\rho}_{\mathrm{f}}$ and $\bar{\rho}_{\mathrm{m}}^{(\mathcal{A})}$ are less than their upper bounds, i.e., 1 and $\upsilon_{\mathrm{m}}^{(\mathcal{A})}$,

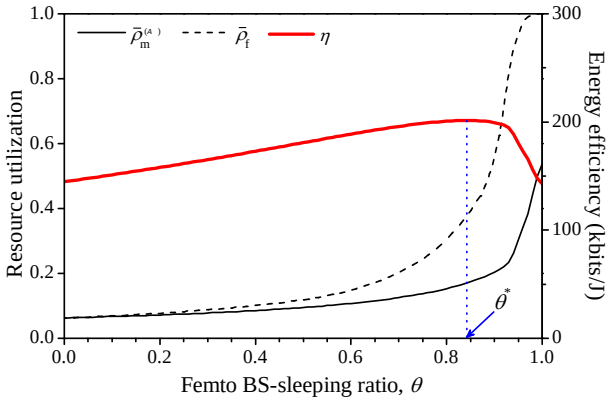

(a)

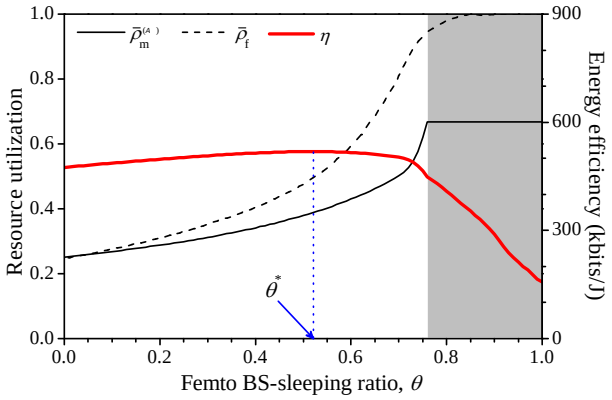

(b)

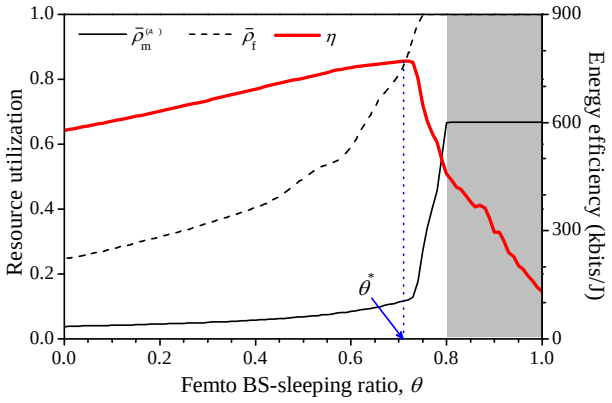

(c)

Fig. 3.2: Resource utilizations and energy efficiencies for varying scenarios: a) $\lambda_{\mathrm{u}} = 2 \times 10^{-3}$, $D_{\mathcal{A}} = 200$ m, b) $\lambda_{\mathrm{u}} = 8 \times 10^{-3}$, $D_{\mathcal{A}} = 200$ m, c) $\lambda_{\mathrm{u}} = 8 \times 10^{-3}$, $D_{\mathcal{A}} = 600$ m

respectively. In this low load condition, since the rate requirement of all users are satisfied, the total throughput of the users in $\mathcal{A}$ is constant as $\lambda_{\mathrm{u}}|\mathcal{A}|R_{\mathrm{req}}$ regardless of θ. In addition, the power consumption of femto BSs decreases with higher θ whereas that of macro BS increases since more users select the macro BS as their serving BS due to increasing sparsity of femto BSs. On the contrary, when the traffic load is high (Fig. 3.2(b), $\lambda_{\mathrm{u}} = 8 \times 10^{-3}$), both $\bar{\rho}_{\mathrm{f}}$ and $\bar{\rho}_{\mathrm{m}}^{(\mathcal{A})}$ meet their upper bounds with high θ. This is because a few active femtocells are all crowded with users and thereby the users are forced to connect to the macrocell. When the macrocell is overloaded, the total throughput is reduced since the macrocell users receive limited services. Consequently, with higher θ, the energy efficiency gets much worse, as seen from Fig. 3.2(b). It is natural that the optimal femto BS-sleeping ratio, θ^*, to maximize the energy efficiency gets lower with increasing traffic load.

Next, we assess the energy efficiency according to the location of the designated zone, by comparing Figs. 3.2(b) and 3.2(c). When the femtocell deployment area is located far from the macro BS, the users receive weaker signal power from the overlaid macro BS than when they are close to the macro BS. Then, fewer users are associated with the macro BS, which results in the decrease of $\bar{\rho}_{\mathrm{m}}^{(\mathcal{A})}$. On the contrary, the femtocell resource utilization, $\bar{\rho}_{\mathrm{f}}$, does not increase largely even though the femtocells serve more users. This is because the SIRs of the femtocell users are improved due to reduced macro-to-femto interference. As a result, the energy efficiency becomes higher than when the designated zone is close to the macro BS and the optimal θ^* also has the higher value under the same traffic load.

In all subfigures of Fig. 3.2, we observe that the optimal θ^* is determined outside of the region where the macrocell is overloaded, i.e., $\bar{\rho}_{\mathrm{m}}^{(\mathcal{A})} = \upsilon_{\mathrm{m}}^{(\mathcal{A})}$ (the macrocell

overload regions are shadowed in the subfigures, if exists). Note that the femtocell is always underloaded or fully loaded (not overloaded), since it accommodates only affordable number of users in order to provide QoS-guaranteed service to its users. Remind that when all the active cells are not overloaded, the energy efficiency depends only on the total power consumption. Thus, from the observation, we can verify the presumption that *the maximum energy efficiency can be achieved when the total power consumption is minimized while the cells are not overloaded.* We have made the same observation for many other scenarios, for which the numerical results are not shown here due to lack of space.

3.3 Proposed Femto BS Sleep Decision and User Association (SDUA) Scheme

3.3.1 Problem Formulation

Now, we formulate the proposed SDUA scheme that determines the operation modes of femto BSs and the user association with cells in the open access femtocell networks. Let $\mathcal{S}_{\text{act}}$ be the set of active femto BSs ($\mathcal{S}_{\text{act}} \subseteq \mathcal{B}_{\text{f}}$). Thus, if a femto BS does not belong to $\mathcal{S}_{\text{act}}$, this means the femto BS is in sleep mode. Let $a_{i,j}$ be the user association indicator of which value is 1 if user j is associated with BS i, and 0 otherwise. Then, the user association matrix in the open access femtocell network is represented by $\mathbf{a} = [a_{i,j}]_{|\{0\}\cup\mathcal{B}_{\text{f}}|\times|\mathcal{U}|}$. If femto BS i is in sleep mode, $a_{i,j} = 0$ for all j since it cannot accommodate any user. Thus, when $\mathbb{A}_{\mathcal{S}_{\text{act}}}$ denotes a set of feasible user association matrixes for given $\mathcal{S}_{\text{act}}$, $\mathbb{A}_{\mathcal{S}_{\text{act}}} = \big\{\mathbf{a}|\ \forall j \in \mathcal{U},\ a_{i,j} \in \{0,1\}$ if $i \in \{0\} \cup \mathcal{S}_{\text{act}},$ and $a_{i,j} = 0$ if $i \notin \{0\} \cup \mathcal{S}_{\text{act}}\big\}$.

In formulating the SDUA problem, we consider the following constraints. First, each cell should not be overloaded so that it can provide satisfied data services to its users. Therefore, we have the constraint that $\sum_{j\in\mathcal{U}} \psi_{0,j} a_{0,j} \leq \upsilon_{\mathrm{m}}^{(\mathcal{A})}$ and $\sum_{j\in\mathcal{U}} \psi_{i,j} a_{i,j} \leq 1$ for all $i \in \mathcal{S}_{\mathrm{act}}$. Second, we consider the association of each user with only one BS (a femto BS or a macro BS). This constraint is expressed as $\sum_{i\in\{0\}\cup\mathcal{S}_{\mathrm{act}}} a_{i,j} = 1$, for all $j \in \mathcal{U}$.

The objective of the SDUA problem is to minimize the total power consumption in the designated zone $\mathcal{A}$. For given $\mathbf{a}$, the active femtocell i has the resource utilization of $\sum_{j\in\mathcal{U}} \psi_{i,j} a_{i,j}$ and thus we have $P_{\mathrm{f}i} = \Delta_{\mathrm{f}} \left(\sum_{j\in\mathcal{U}} \psi_{i,j} a_{i,j} \right) + P_{\mathrm{f,\,const}}$. On the other hand, the power consumed by the macro BS for serving its associated users in $\mathcal{A}$ is obtained as $P_{\mathrm{m}}^{(\mathcal{A})} = \Delta_{\mathrm{m}} \left(\sum_{j\in\mathcal{U}} \psi_{0,j} a_{0,j} \right)$. Remind that unlike $P_{\mathrm{f}i}$, the constant power consumption of macro BS is not considered in assessing $P_{\mathrm{m}}^{(\mathcal{A})}$.

Accordingly, for given $\mathcal{S}_{\mathrm{act}}$ and $\mathbf{a}$, the total power consumption in (3.2) is as

$$P_{\mathrm{total}} = \left(\sum_{j\in\mathcal{U}} \psi_{0,j} a_{0,j} \right) \Delta_{\mathrm{m}} + \sum_{i\in\mathcal{S}_{\mathrm{act}}} \left\{ \big(\sum_{j\in\mathcal{U}} \psi_{i,j} a_{i,j} \big) \Delta_{\mathrm{f}} + P_{\mathrm{f,\,const}} \right\} + \sum_{i\in\mathcal{B}_{\mathrm{f}}\setminus\mathcal{S}_{\mathrm{act}}} P_{\mathrm{f,\,sleep}}.$$

Since $\sum_{i\in\{0\}\cup\mathcal{S}_{\mathrm{act}}} a_{i,j} = 1$, when substituting $a_{0,j}$ by $\big(1 - \sum_{i\in\mathcal{S}_{\mathrm{act}}} a_{i,j}\big)$,

$$P_{\mathrm{total}} = -\sum_{i\in\mathcal{S}_{\mathrm{act}}} \sum_{j\in\mathcal{U}} \zeta_{i,j} a_{i,j} + \big(P_{\mathrm{f,\,const}} - P_{\mathrm{f,\,sleep}} \big) |\mathcal{S}_{\mathrm{act}}| + \sum_{j\in\mathcal{U}} \Delta_{\mathrm{m}} \psi_{0,j} + N_{\mathrm{f}} P_{\mathrm{f,\,sleep}}, \tag{3.12}$$

where $\zeta_{i,j} = \Delta_{\mathrm{m}} \psi_{0,j} - \Delta_{\mathrm{f}} \psi_{i,j}$. Since the last two terms in (3.12) are constant, we will consider only the terms related to the variables $\mathcal{S}_{\mathrm{act}}$ and $\mathbf{a}$ in formulating the SDUA problem. Let $\mathcal{P}(\mathcal{S}_{\mathrm{act}}, \mathbf{a}) := -\sum_{i\in\mathcal{S}_{\mathrm{act}}} \sum_{j\in\mathcal{U}} \zeta_{i,j} a_{i,j} + \big(P_{\mathrm{f,\,const}} - P_{\mathrm{f,\,sleep}} \big) |\mathcal{S}_{\mathrm{act}}|$.

Then, the SDUA problem is defined as

$$\min_{\mathcal{S}_{\rm act}, \mathbf{a}\in\mathbb{A}_{\mathcal{S}_{\rm act}}} \quad \mathcal{P}(\mathcal{S}_{\rm act}, \mathbf{a}) \tag{3.13}$$

$$\text{s.t.} \quad \textstyle\sum_{j\in\mathcal{U}} \psi_{0,j} a_{0,j} \le v_{\rm m}^{(\mathcal{A})} \tag{3.14}$$

$$\textstyle\sum_{j\in\mathcal{U}} \psi_{i,j} a_{i,j} \le 1, \qquad \forall i \in \mathcal{S}_{\rm act} \tag{3.15}$$

$$\textstyle\sum_{i\in\{0\}\cup\mathcal{S}_{\rm act}} a_{i,j} = 1, \qquad \forall j \in \mathcal{U}. \tag{3.16}$$

3.3.2 Solution Approach

The SDUA problem (3.13)–(3.16) is hard to solve, since it has the set variables as well as binary integer variables. To overcome this difficulty, we first solve the user association (UA) problem which minimizes the total power consumption for given set of active femto BSs, $\mathcal{S}_{\rm act}$. Then, we design an iterative algorithm for heuristically solving the SDUA problem, which finds the best set of active femto BSs by solving the UA problem repeatedly with different $\mathcal{S}_{\rm act}$ at each iteration.

Solving UA problem

When $\mathcal{S}_{\rm act}$ is given, the UA problem can be formulated as

$$\Phi(\mathcal{S}_{\rm act}) = \min_{\mathbf{a}\in\mathbb{A}_{\mathcal{S}_{\rm act}}} \mathcal{P}(\mathcal{S}_{\rm act}, \mathbf{a}) \tag{3.17}$$

$$\text{s.t. (3.14)} - \text{(3.16)}.$$

The problem (3.17) is a binary integer optimization problem, which is still complicated to be solved. To reduce the complexity, we relax the binary variable $a_{i,j}$ to take on a real value between 0 and 1. Let $\widetilde{\mathbb{A}}_{\mathcal{S}_{\rm act}}$ denote the relaxed domain of $\mathbf{a}$ in $\mathbb{A}_{\mathcal{S}_{\rm act}}$, i.e., $\widetilde{\mathbb{A}}_{\mathcal{S}_{\rm act}} = \big\{\mathbf{a}|\ \forall j \in \mathcal{U}, 0 \le a_{i,j} \le 1 \text{ if } i \in \{0\}\cup\mathcal{S}_{\rm act}, \text{ and } a_{i,j} = 0 \text{ if } i \notin \{0\}\cup\mathcal{S}_{\rm act}\big\}$. Then, we solve the optimal solution of the UA problem

(3.17) by using the Lagrangian dual method [48]. The Lagrangian function of the problem (3.17) is $\mathcal{L}(\mathbf{a}, \boldsymbol{\omega}) = -\sum_{i\in\mathcal{S}_{\rm act}}\sum_{j\in\mathcal{U}}\zeta_{i,j}a_{i,j} + \omega_0\left(\sum_{j\in\mathcal{U}}\psi_{0,j}a_{0,j} - v_{\rm m}^{(\mathcal{A})}\right) + \sum_{i\in\mathcal{S}_{\rm act}}\omega_i\left(\sum_{j\in\mathcal{U}}\psi_{i,j}a_{i,j} - 1\right) + H_{\mathcal{S}_{\rm act}}$, where ω_i is a Lagrangian multiplier and $H_{\mathcal{S}_{\rm act}} = \big(P_{\rm f,\,const} - P_{\rm f,\,sleep}\big)|\mathcal{S}_{\rm act}|$. Let $\boldsymbol{\omega} := (\omega_0, \omega_1, \cdots, \omega_{N_{\rm f}})$. It is noted that $\omega_i = 0$ for $i \notin \{0\}\cup\mathcal{S}_{\rm act}$. Then, $\mathcal{L}(\mathbf{a}, \boldsymbol{\omega}) = \sum_{j\in\mathcal{U}}\sum_{i\in\{0\}\cup\mathcal{S}_{\rm act}}\Lambda_{i,j}a_{i,j} - \omega_0 v_{\rm m}^{(\mathcal{A})} - \sum_{i\in\mathcal{S}_{\rm act}}\omega_i + H_{\mathcal{S}_{\rm act}}$, where $\Lambda_{0,j} = \omega_0\psi_{0,j}$ and $\Lambda_{i,j} = \omega_i\psi_{i,j} - \zeta_{i,j}$ for $i \in \mathcal{S}_{\rm act}$.

The Lagrange dual function, $g(\boldsymbol{\omega})$, is given as

$$
\begin{aligned}
g(\boldsymbol{\omega}) = \min_{\mathbf{a}\in\widetilde{\mathbb{A}}_{\mathcal{S}_{\rm act}}} \; & \sum_{j\in\mathcal{U}}\sum_{i\in\{0\}\cup\mathcal{S}_{\rm act}}\Lambda_{i,j}a_{i,j} - \omega_0 v_{\rm m}^{(\mathcal{A})} - \sum_{i\in\mathcal{S}_{\rm act}}\omega_i + H_{\mathcal{S}_{\rm act}} \qquad (3.18)\\
\text{s.t.} \; & \sum_{i\in\{0\}\cup\mathcal{S}_{\rm act}} a_{i,j} = 1, \qquad \forall j \in \mathcal{U}.
\end{aligned}
$$

For given $\mathcal{S}_{\rm act}$ and $\boldsymbol{\omega}$, since $\mathcal{L}(\cdot)$ is an affine function of $a_{i,j}$ having a slope of $\Lambda_{i,j}$, we can easily solve (3.18) as follows. For each user j, from the constraint that $\sum_{i\in\{0\}\cup\mathcal{S}_{\rm act}} a_{i,j} = 1$, $a_{\ell,j} = 1$ such that $\ell = \text{argmin}_{i\in\{0\}\cup\mathcal{S}_{\rm act}}\Lambda_{i,j}$, and $a_{i,j} = 0$ for all $i \neq \ell$. Note that there can exist multiple ℓ's such that $\ell = \text{argmin}_i\,\Lambda_{i,j}$, even though the probability is very small. In this case, one among the multiple ℓ's is chosen and, for the chosen ℓ, $a_{\ell,j} = 1$.

The dual problem of the primal problem (3.17) is defined as

$$
\begin{aligned}
\max_{\boldsymbol{\omega}} \quad & g(\boldsymbol{\omega}) \qquad (3.19)\\
\text{s.t.} \quad & \boldsymbol{\omega} \succeq \mathbf{0},
\end{aligned}
$$

where $\succeq$ denotes the component-wise inequality. The solution of (3.17) is obtained by solving (3.19). Since the optimal Lagrangian multipliers $\boldsymbol{\omega}^*$ in (3.19) can be easily found with the subgradient method [48], we do not present the detailed procedure to find $\boldsymbol{\omega}^*$ in this thesis.

Algorithm 2: Proposed SDUA algorithm

$\mathcal{S}_{\text{act}} \leftarrow \mathcal{B}_{\text{f}}$;

$minPwC \leftarrow \Phi(\mathcal{S}_{\text{act}})$

while $\mathcal{S}_{act} \neq \emptyset$ **do**

  calculate $\psi_{i,j}$ $\forall i, j$, for given $\mathcal{S}_{\text{act}}$;

  $\mho \leftarrow \emptyset$;

  forall the $i \in \mathcal{S}_{act}$ **do**

    obtain $\Phi(\mathcal{S}_{\text{act}} \setminus \{i\})$ according to the UA problem (3.17);

    if *the solution of* (3.17) *exists* **then**

      $\mho \leftarrow \mho \cup \{i\}$;

    end

  end

  if $\mho = \emptyset$ **then**

    break;

  end

  $i^{-} \leftarrow \text{argmin}_{i \in \mho} \Phi(\mathcal{S}_{\text{act}} \setminus \{i\})$;

  if $\Phi(\mathcal{S}_{act} \setminus \{i^{-}\}) < minPwC$ **then**

    $minPwC \leftarrow \Phi(\mathcal{S}_{\text{act}} \setminus \{i^{-}\})$;

    $\mathcal{S}^{*}_{\text{act}} \leftarrow \mathcal{S}_{\text{act}} \setminus \{i^{-}\}$;

  end

  $\mathcal{S}_{\text{act}} \leftarrow \mathcal{S}_{\text{act}} \setminus \{i^{-}\}$;

end

return $\mathcal{S}^{*}_{\text{act}}$ and $\mathbf{a}^{*} = \text{argmin}_{\mathbf{a}} \mathcal{P}(\mathcal{S}^{*}_{\text{act}}, \mathbf{a})$

Finding Best $\mathcal{S}_{\mathbf{act}}$

Now, we suggest a heuristic algorithm for solving the SDUA problem (3.13)–(3.16). In Algorithm 2, all the femto BSs are initially set to be active. At each iteration, the proposed algorithm updates the relative resource requirement $\psi_{i,j}$ with given $\mathcal{S}_{\text{act}}$ because the relative resource requirement depends on the set of active femto BSs (this will be explained in detail in Section 3.3.3). Then, it selects a femto BS to be excluded from the current $\mathcal{S}_{\text{act}}$, which can reduce the total power consumption the most if going to sleep. Specifically, the algorithm obtains $\Phi(\cdot)$ in (3.17) while excluding femto BSs in the current $\mathcal{S}_{\text{act}}$ one by one. Then, it chooses one with the lowest value of Φ among the femto BSs in current $\mathcal{S}_{\text{act}}$ and excludes the selected one from the current $\mathcal{S}_{\text{act}}$ for the next iteration. The iterations stop when there exists no femto BS without which the UA solution of (3.17) can be obtained. The proposed algorithm returns the best solution having the lowest total power consumption during the iterations.

Remark 1: Since activating or deactivating one additional femto BS may have a considerable impact on the total amount of interference in a densely deployed femtocell network, $\psi_{i,j}$ in the SDUA problem (3.13)–(3.16) is not be constant, but depends on $\mathcal{S}_{\text{act}}$. As a result, $-\Phi$ may not hold submodularity. We empirically test the submodularity of $-\Phi$ as seen in Fig. 3.3. The set function $-\Phi$ is submodular if it satisfies the condition that $\Phi(\mathcal{S}_{\text{act},1}) - \Phi(\mathcal{S}_{\text{act},1} \cup \{i\}) \geq \Phi(\mathcal{S}_{\text{act},2}) - \Phi(\mathcal{S}_{\text{act},2} \cup \{i\})$, for all $\mathcal{S}_{\text{act},1} \subseteq \mathcal{S}_{\text{act},2} \subseteq \mathcal{B}_{\text{f}}$ and $i \in \mathcal{B}_{\text{f}} \setminus \mathcal{S}_{\text{act},2}$. We observe from the figure that the submodularity condition is not satisfied while most negative values of $[\Phi(\mathcal{S}_{\text{act},1}) - \Phi(\mathcal{S}_{\text{act},1} \cup \{i\})] - [\Phi(\mathcal{S}_{\text{act},2}) - \Phi(\mathcal{S}_{\text{act},2} \cup \{i\})]$ are almost zero. Accordingly, the proposed algorithm searches the best solution for the iterations.

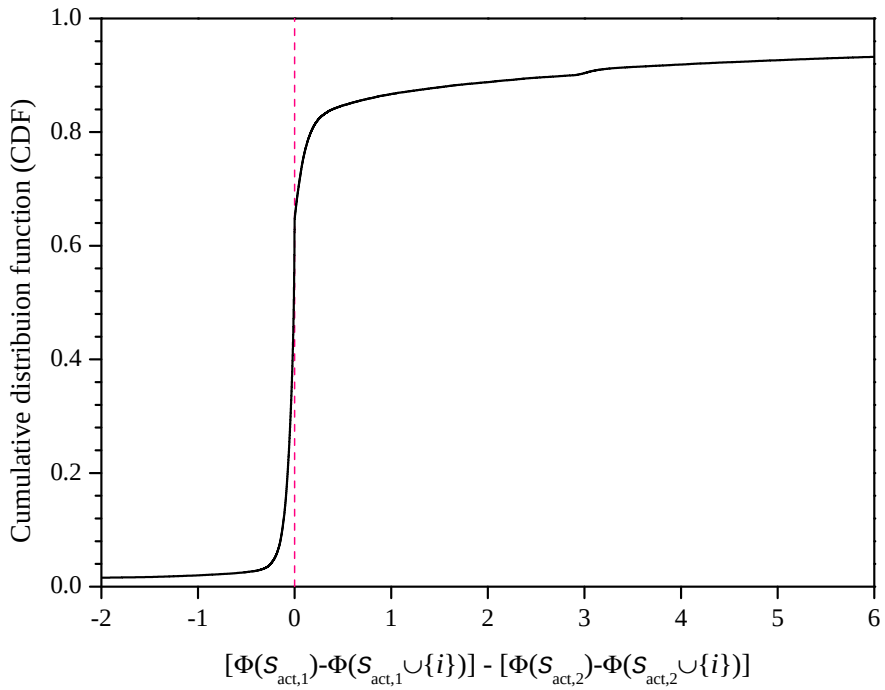

Fig. 3.3: Submodularity test of $-\Phi$.

Remark 2: Since the subgradient method has $\mathcal{O}(1/\epsilon^2)$ iterations to find an ϵ-suboptimal point, a computation time of $\mathcal{O}\left(|\mathcal{S}_{\text{act}}||\mathcal{U}|/\epsilon^2\right)$ is needed in obtaining $\Phi(\mathcal{S}_{\text{act}})$. Thus, the Algorithm 2 has the computational complexity of $\mathcal{O}\left(|\mathcal{B}_{\text{f}}|^3|\mathcal{U}|/\epsilon^2\right)$. Note that at most tens of femto BSs will be deployed in a limited area such as shopping mall and airport, and the SDUA does not have a tight constraint on computational time since it is expected to be performed on a relatively long term basis, unlike the data transmission scheduling. Therefore, the computational complexity of the Algorithm 2 seems affordable to practical implementation.

3.3.3 Implementation Example of SIR Estimation

To obtain the SDUA solution, the femtocell management system (FMS) should compute $\psi_{i,j}$, which needs $\breve{\gamma}_{i,j}$ as shown in (3.4). The SIR estimate from femto BS i to user j is calculated using the measurements reported by user j, as follows.

$$\breve{\gamma}_{i,j} = \frac{X_{\mathrm{f}i,j}}{I_{\mathrm{mf}j} + \sum_{i' \in \mathcal{S}_{\mathrm{act}} \setminus \{i\}} X_{\mathrm{f}i',j}}, \tag{3.20}$$

where $X_{\mathrm{f}i,j}$ is the received preamble signal strength (RSS) of femto BS i at the user j and $I_{\mathrm{mf}j}$ is the total sum of RSSs from macro BSs (including the overlaid macro BS as well as neighboring macro BSs). Before solving the SDUA problem, the FMS should get the measurements from any femto BS i to any user j (i.e., $I_{\mathrm{mf}j}, X_{\mathrm{f}1,j}, X_{\mathrm{f}2,j}, \cdots, X_{\mathrm{f}N_{\mathrm{f}},j}$), since it cannot know which femto BSs will belong to $\mathcal{S}_{\mathrm{act}}$. Thus, during the operation, all active femto BSs transmit cell-specific preamble periodically, and those in sleep mode also wake up a few frames before determining a new SDUA solution and transmit the preambles. After measuring the RSSs of preambles, each user reports the measurements to the FMS via its serving BS. In addition, each user j also reports the measured SIR from its overlaid macro BS, $\breve{\gamma}_{0,j}$. Note that the feedback information amount may be considerable. To reduce the reporting overhead, we suggest that each user j sorts $X_{\mathrm{f}i,j}$'s in a decreasing order and then reports only M highest $X_{\mathrm{f}i,j}$'s to its serving cell.

Chapter 4. Performance Evaluation

4.1 Radio Resource Partitioning Scheme

4.1.1 Simulation Model

System Deployment

In simulation, we consider a heterogeneous network in Fig. 4.1, where seven macro BSs are positioned over a hexagonal grid and femto BSs are randomly deployed in each macrocell coverage. Each macro BS operates three sectors with directional antennas and each femto BS uses an omni-directional antenna. We focus on a sector of the macrocell at the center of the network in evaluating the performance of the proposed scheme. In addition, we consider more practical femtocell deployment model where there exists a dense femtocell area within the target sector as seen in Fig. 4.1. The radius of the dense femtocell area is set to 150 m and the center of the dense femtocell area (denoted by $\mathbf{r}_c$ in Fig. 4.1) is located along the dashed line in the figure. Unless stated otherwise, the distance between the central macro BS and the center of the dense femtocell area is 200 m and the number of femto BSs within this dense area is 30. 10 femto BSs are randomly deployed over each sector coverage except the dense femtocell area.

Channel and Power

The total system bandwidth of 10 MHz is divided into 48 subchannels. The number of FPs for FFR operation is $K = 4$ and the FFR configuration of each sector is the same as in Fig. 2.1, where Sector 0 corresponds to the target sector in Fig. 4.1. A femto BS assigns the same transmission power of 3.2 dBm to all subchannels,

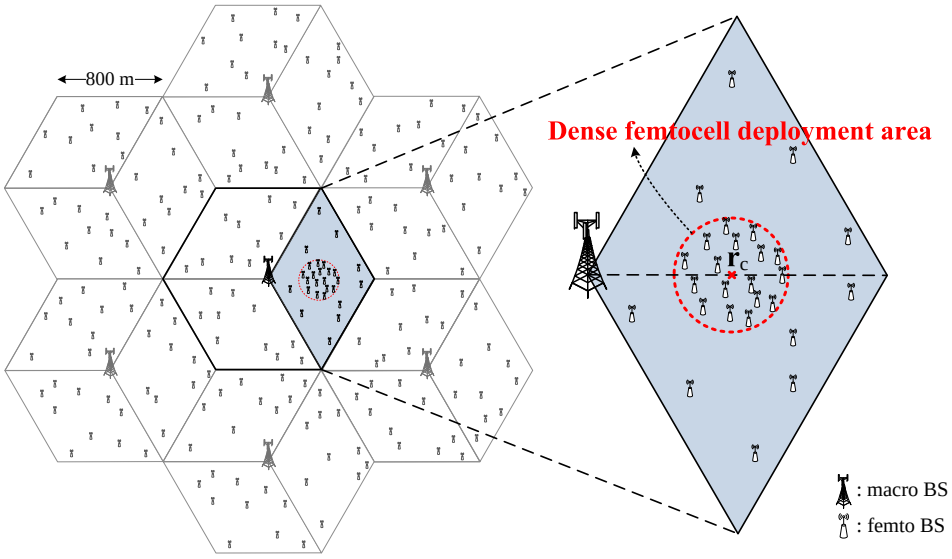

Fig. 4.1: Heterogeneous network model in simulation.

whereas a macro BS applies three transmission power levels on FPs like in Fig. 2.1. At each macro BS, the subchannel transmission power of the reference FP 0 is fixed to 29.2 dBm, and the ratios of high power level and low power level to the power of FP 0 are respectively set to 4 dB and -6 dB. In addition, $\mathbf{\Gamma}_{\text{th}} = (\infty, 14, 14, 9, -\infty)$ dB, $\Delta = 3$ dB, $L = 11$, $\gamma_1 = 0$ dB and $\gamma_l = \gamma_{l-1} + 2$ dB for $l = 2, \cdots, 11$. In modeling channel, we use the values in Table I. Also, the correlation model in [49] is used for shadowing, where the decorrelation length is 5 m. The Rayleigh fading is generated by using a Jakes spectrum model [50], with a carrier frequency of 2.5 GHz.

Macrocell/Femtocell Users

At initialization, 50 macrocell users are randomly located within each sector having $r_{\text{m}} = 800$ m. A macrocell user moves to a direction selected randomly between 0

Tab. 4.1: Channel model parameters

Parameter	Value
$(a_{\mathrm{m}}, a_{\mathrm{f}}, a_{\mathrm{mf}}, a_{\mathrm{ff}})$	(3.7, 3, 3.7, 4)
$(\mu_{\mathrm{m,\,dB}}, \mu_{\mathrm{f,\,dB}}, \mu_{\mathrm{mf,\,dB}}, \mu_{\mathrm{ff,\,dB}})$	(0, 0, 0, 0)
$(\sigma_{\mathrm{m,\,dB}}, \sigma_{\mathrm{f,\,dB}}, \sigma_{\mathrm{mf,\,dB}}, \sigma_{\mathrm{ff,\,dB}})$	(8, 4, 10, 12)
$(\phi_{\mathrm{m,\,dB}}, \phi_{\mathrm{f,\,dB}}, \phi_{\mathrm{mf,\,dB}}, \phi_{\mathrm{ff,\,dB}})$	(-16, -35, -26, -55)

and 360 degrees with a speed that is uniformly distributed between 0 and 6 km/h. After a random duration uniformly distributed between 0 and 30 seconds, the moving direction of a macrocell user is updated randomly between 90 and -90 degrees from the current direction and its new moving speed is determined with uniform distribution between 0 and 6 km/h. When a macrocell user goes out of its sector, it is again located randomly within the sector, in order to maintain the constant number of macrocell users in a sector during a simulation run. On the other hand, the service radius and interference radius of a femto BS are respectively set as $r_{\mathrm{f}} = 30$ m and $r_{\mathrm{FMI}} = r_{\mathrm{FFI}} = 40$ m. At initialization, two femtocell users are randomly located within a service area of each femto BS and their locations are not changed during simulation run. In addition, all macrosectors and femtocells are assumed to be fully loaded. Unless stated otherwise, $\Psi_{\mathrm{m}} = 100$ kb/s, $\Psi_{\mathrm{f}} = 5$ Mb/s, $\varrho_{\mathrm{f}} = 1$, $\eta = 0.04$, and $\epsilon = 0.01$.

Medium Access Control (MAC) Model

$\boldsymbol{\alpha}$ and $\boldsymbol{\beta}$ of the target sector are determined at the start of simulation and applied during a simulation run. Note that since the proposed scheme treats the resource sharing and partition between femtocell and macrocell, the design of MAC and scheduling is beyond the scope of this thesis. To evaluate the throughput performance of the proposed scheme without a specific MAC, we take the following simple method. Every time slot of 1 ms, a femto BS selects one user according to round-robin fashion and the selected user reports the received SIRs of FDG subchannels and available SHG subchannels on all FPs. The femto BS calculates the transmission rate of each subchannel based on the reported SIRs and takes the sum transmission rate of used subchannels as the instantaneous femtocell throughput at the corresponding slot. Similarly, a macro BS carries out the above work for each FP.

4.1.2 Simulation Results

The performance results of the proposed scheme in Figs. 4.2–4.7 are obtained by conducting simulation with the optimal solution of the problem (2.2)–(2.10).

We first examine that the minimum throughput requirements of both macrocell user and femtocell user are satisfied with the proposed scheme. Table 4.2 shows the average macrocell/femtocell user throughputs for given minimum throughput requirements and η. Note that Ψ_{m} is a key constraint for α^*, and Ψ_{f} and η have the great influence on determining β^*. We can see in Table 4.2 that the proposed scheme achieves good throughput performance, especially for femtocell users, while satisfying minimum throughput requirements. When the macrocell users require

Tab. 4.2: Average macrocell/femtocell user throughputs

Ψ_m (kb/s)	Ψ_f (Mb/s)	η	macrocell user throughput (kb/s)				femtocell user throughput (Mb/s)
			FP 0	FP 1	FP 2	FP 3	
100	5	0.01	134	129	159	158	17.8
		0.04	258	254	332	329	13.5
		0.1	290	333	422	422	11.6
		0.4	306	440	454	453	10.5
200	5	0.01	215	207	232	231	13.2
		0.04	261	251	344	333	11.0
		0.1	292	329	432	425	9.2
		0.4	305	440	463	458	8.0

more resource dedicated to themselves with larger Ψ_m, it is natural that the femtocell user throughput decreases since the resource that can be used by the femtocell users is reduced. With larger η, the portion of SHG on FP increases for the tighter throughput balance between macrocell user and femtocell user. Since the macrocell users have a higher priority in using SHG, with larger η, the macrocell user throughput increases whereas the femtocell user throughput gets lower.

The proposed scheme aims at maximizing the spectral efficiency while satisfying minimum throughput requirements. Nevertheless, it can also provide proportional fairness between the femtocell users and the macrocell users, since it considers the inter-tier fairness parameter, η, in determining the resource configuration. Table 4.3 shows the average user satisfaction ratios (USRs) and the proportional fairness indexes for given parameters. The USR is defined as the ratio of the user

Tab. 4.3: Average user satisfaction ratios and proportional fairness indexes

Ψ_{m} (kb/s)	Ψ_{f} (Mb/s)	η	user satisfaction ratio		proportional fairness index
			macrocell	femtocell	
100	5	0.01	1.44	3.56	2.12
		0.04	2.92	2.70	0.22
		0.1	3.59	2.32	1.27
		0.4	3.97	2.10	1.87
200	5	0.01	1.11	2.64	1.53
		0.04	1.48	2.20	0.72
		0.1	1.81	1.84	0.03
		0.4	1.99	1.60	0.39

throughput to the minimum throughput requirement and the proportional fairness index is defined as the absolute difference between the USR of macrocell user and that of femtocell user [51]. We can see from the table that proportional fairness between the femtocell users and the macrocell users can be achieved by adjusting η for given minimum throughput requirements.

Fig. 4.2 depicts the average throughput contour of a femtocell user within dense femtocell area, according to the location and femtocell density of the area. To evaluate the effect of FDG on the femtocell throughput, we also examine in Fig. 4.2(b) a special case of the proposed scheme without FDG, i.e., $\beta_{k,v} = 0$ for all k and v, which will be called the "w/o_FDG" scheme. As seen from Fig. 4.2, the average throughput of a femtocell user within dense area gets lower when the dense area is located nearer to the macro BS because of the increased MFI, and it is also decreased with more densely deployed femtocells due to the increased FFI. When

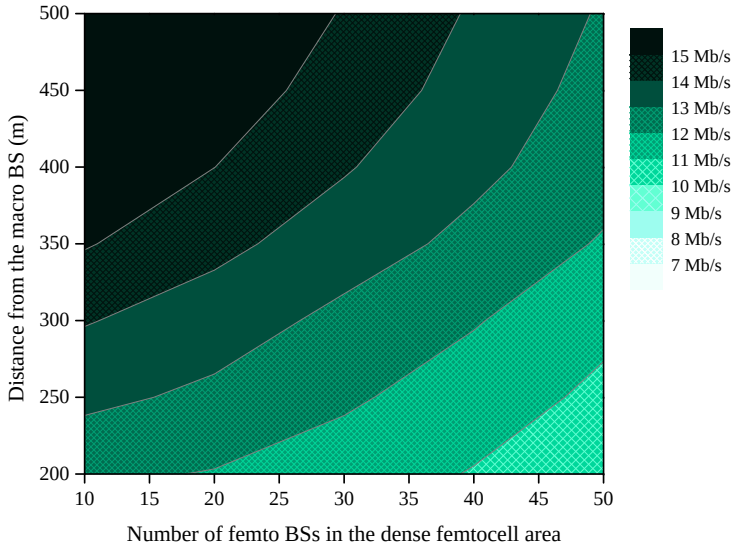

(a) Proposed scheme

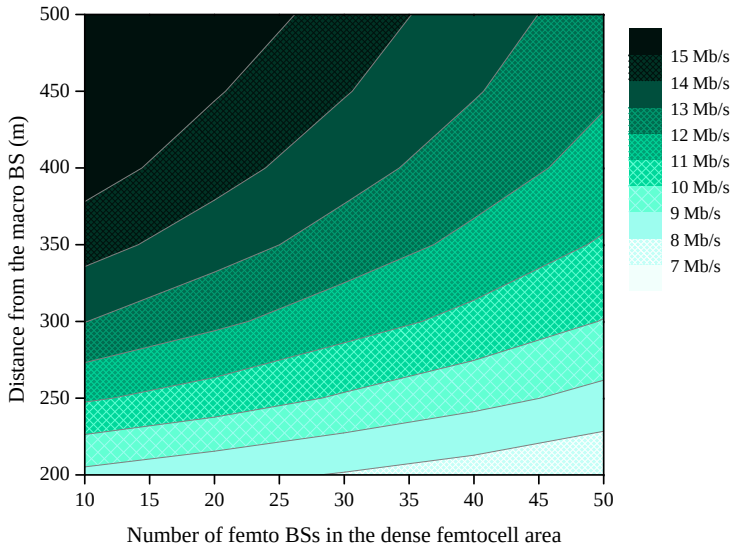

(b) w/o_FDG scheme

Fig. 4.2: Contour of the average femtocell user throughput in the dense femtocell area.

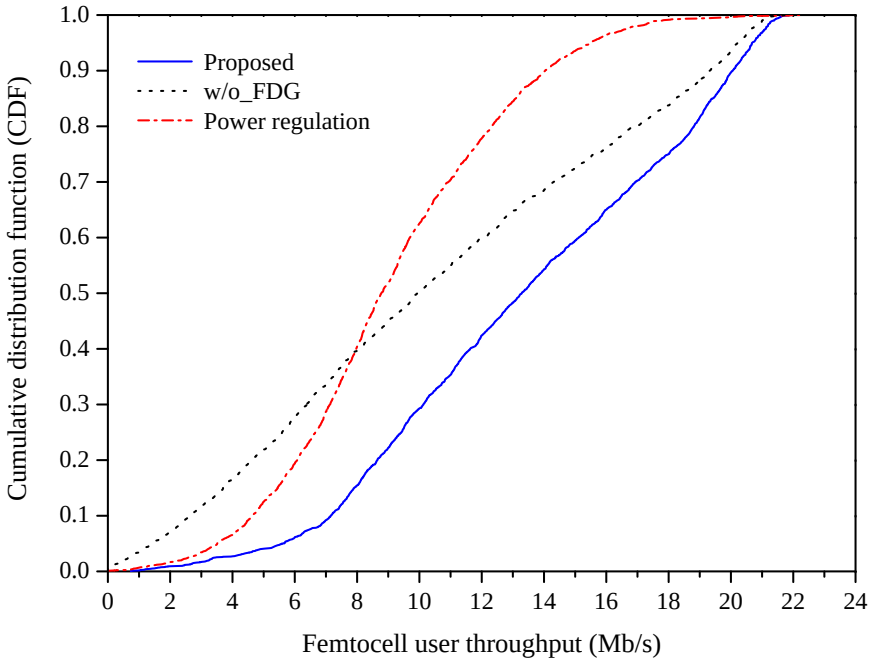

Fig. 4.3: Cumulative distributed function of femtocell user throughput.

comparing Fig. 4.2(a) with Fig. 4.2(b), we can observe that this throughput decrease phenomenon is greatly relieved with the proposed scheme. This is because the proposed scheme can diminish the MFI by allocating the dedicated resources to femtocells with FDG.

In Figs. 4.3–4.6, we compare the throughput performance of the proposed scheme with those of other two schemes, respectively called "power regulation" [45] and "FP regulation" [52]. Although the power regulation scheme does not utilize FFR, for fair comparison, all of four schemes in Figs. 4.3–4.6 perform the same operation on macro-tier. That is, the power regulation scheme is the same as the proposed scheme without FDG (i.e., w/o_FDG), except that the w/o_FDG scheme

uses the mechanism of Section 2.2.1 for protecting the macrocell users whereas, in the power regulation scheme, each femto BS determines the subchannel transmission power so that the outage probabilities of nearby macrocell users and its edge user are not larger than 0.1. In the power regulation scheme, the subchannel transmission power of femto BS is limited to -16.8 dBm at minimum and 3.19 dBm at maximum. The SIR thresholds for outage are set to 0 dB and 10 dB for a macrocell user and a femtocell user, respectively. In the FP regulation scheme, the macrosector coverage is partitioned into multiple regions: "cell-center," "cell-mid," and "cell-edge". Then, a femto BS uses only part of FPs according to its location so that it does not give FMI to any nearby macrocell user(s) on the FP which is assigned to the users. For example, in Fig. 2.1, a femto BS in the cell-center region of Sector 0 uses only FP 0 and FP 1, since the macrocell users near to the femto BS are mostly likely to be assigned with FP 2 and FP 3. Likewise, a femto BS in the cell-mid region and one in the cell-edge region use FPs except FP 0 and FP 1, respectively.

Fig. 4.3 shows the empirical CDF of femtocell user throughput. It is obvious that the femtocells located closer to the macro BS have lower throughput because of stronger MFI. Since the proposed scheme allocates more FDG subchannels on FP 2 and FP 3 for the femtocells close to the macro BS, the portion of femtocell users having low throughput is much smaller in the proposed scheme than the w/o_FDR scheme. Moreover, since the femto BSs under the power regulation scheme use low transmission power without the dedicated resource for femtocells, the received SIRs of the femtocell users close to the macro BS gets very low. Thus, as seen from Fig. 4.3, the power regulation scheme has more femtocell users with low throughput than the proposed scheme.

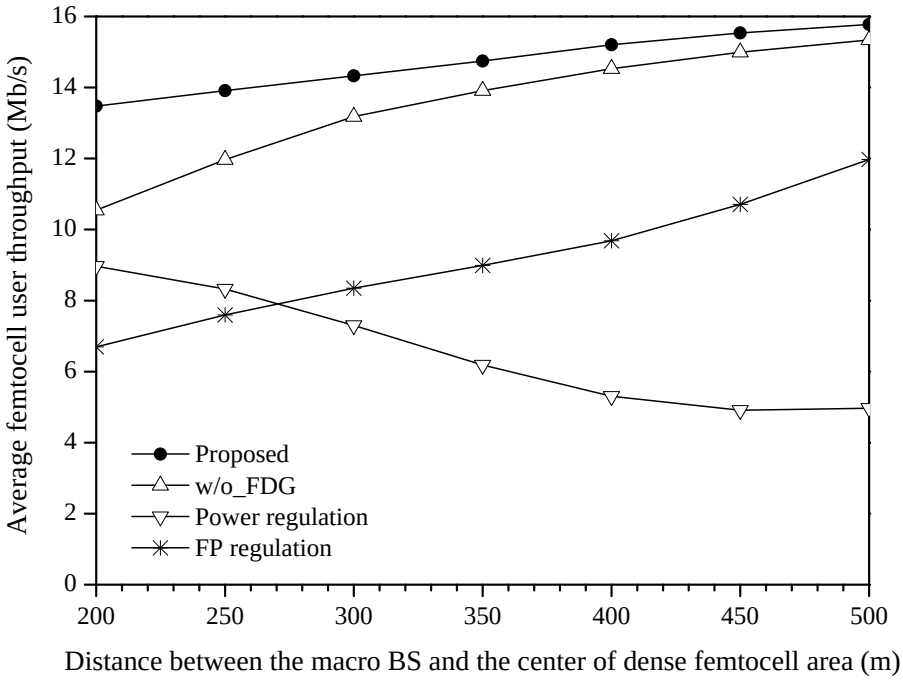

Fig. 4.4: Average femtocell user throughput.

Fig. 4.4 shows the average throughput of femtocell users in the target macrosector. As already observed in Fig. 4.2, the proposed scheme can obviously provide the higher throughput to a femtocell user than the w/o_FDG scheme, since a portion of resource is dedicated to the femto BSs under the proposed scheme. Especially, when there are more femto BSs that suffer from strong MFI by locating close to the macro BS, the FDG subchannels largely contribute on improving the femtocell throughput performance. On the other hand, in the power regulation scheme, each femto BS uses sufficiently low subchannel transmission power so as not to interfere with any potentially nearby macrocell user. The FP regulation scheme limits the

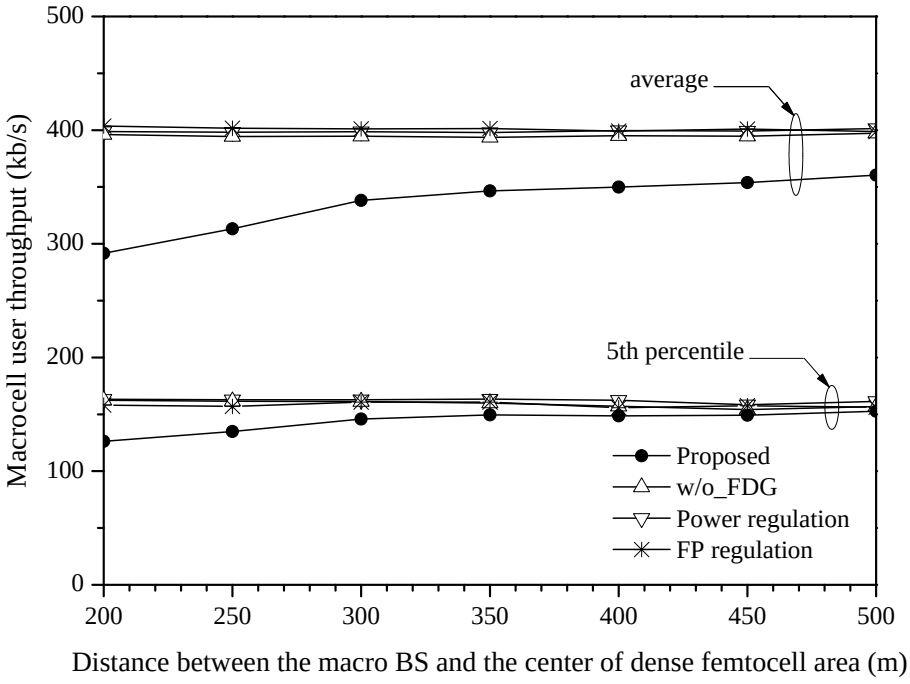

Fig. 4.5: Average and 5th percentile macrocell user throughput.

usage of FPs for protecting any potentially nearby one. However, with the proposed scheme, since a femto BS does not use the shared subchannels only when any macrocell user is near to the femto BS, the femto BSs can use the higher transmission power under the proposed scheme. As a result, the power regulation scheme and the FP regulation scheme provide much lower femtocell user throughput than the proposed scheme or the w/o_FDG scheme.

We can see from Fig. 4.5 that the macrocell user throughput of the proposed scheme is lower than those of other schemes, in both of the average throughput and the 5th percentile throughput. This is because a macro BS under the proposed

scheme serves its users with less resource due to FDG. However, as shown from the figure, the proposed scheme can guarantee the minimum throughput requirement (Ψ_{m} = 100 kb/s) even for the users having the 5th percentile throughput. On the other hand, a macrocell user in the power regulation scheme hardly receives interference from the femto BSs even when they are close to femtocells due to low femtocell power, whereas a macrocell user under the proposed macrocell protection mechanism can receive strong FMI until the neighboring femto BS stops transmission on FP assigned to the macrocell user. In the FP regulation scheme, when a macrocell user is assigned with the FP different from the expected one (e.g., a macrocell user in the cell-edge region can be assigned with FP 0 rather than FP 1 according to its channel status), it can experience FMI from nearby femto BS(s). Thus, the power regulation scheme outperforms the w/o_FDG scheme and the FP regulation scheme in macrocell throughput, but the performance difference between them is not noticeable. This means that the macrocell users are effectively protected from underlaid femtocells with the proposed macrocell protection mechanism, when considering that the power regulation scheme and the w/o_FDG scheme are different from each other only in macrocell user protection.

Fig. 4.6 shows the total throughput in a macrocell coverage, which is the sum of the throughputs of the target macrosector and its all underlaid femtocells. The proposed scheme greatly outperforms the power regulation scheme and the FP regulation scheme, because of its outstanding femtocell throughput performance.

We also examine the performance of the proposed scheme under two different femtocell deployment scenarios: the first is the scenario of Fig. 4.1, where a dense femtocell area exists; under the second scenario, femtocells are uniformly distributed over the entire macrosector. Fig. 4.7 shows the total throughput in a

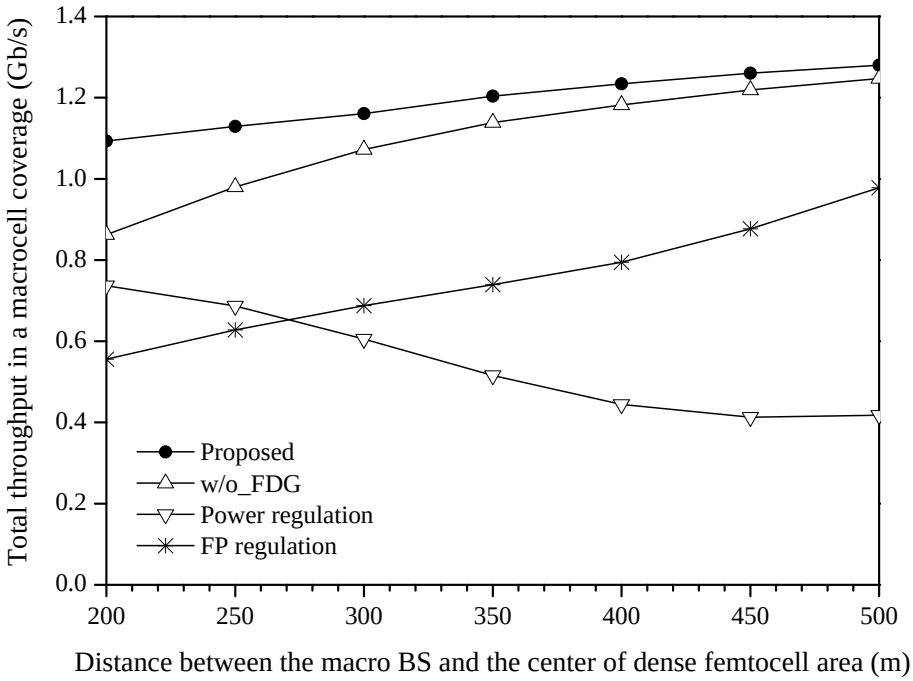

Fig. 4.6: Total throughput in a macrosector coverage.

macrocell coverage, according to the total number of femto BSs in a macrosector. Under the scenario with a dense femtocell area, as in Figs. 4.3–4.6, ten femto BSs are randomly deployed over the sector coverage excluding the dense femtocell area and the remaining femto BSs are deployed within the dense area. The simulation parameter values are the same as for Figs. 4.3–4.6, except that the distance from the macro BS to the center of the dense femtocell area is set to 200 m. From the figure, we can see that, although the proposed scheme is designed for the practical femtocell systems with dense femtocell area, it works well also in the systems without dense femtocell area. Moreover, the performance under the scenario without

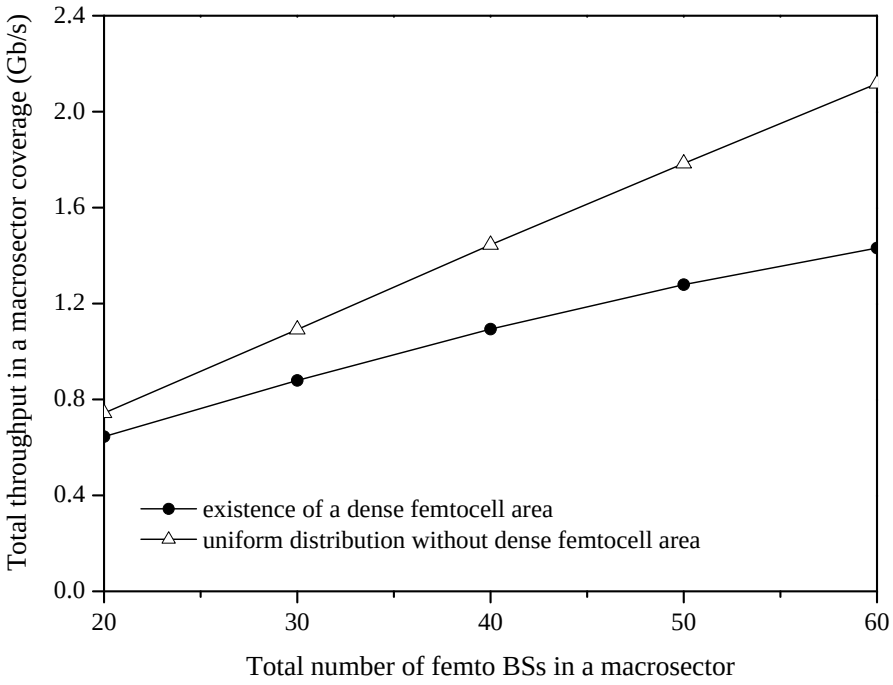

Fig. 4.7: Effects of femtocell deployment scenarios on the total throughput.

dense femtocell area is better than that with it, and the throughput gap gets larger as the number of femto BSs in a macrosector increases. This is because, under the scenario without dense femtocell area, the number of femtocell users suffering high FFI decreases.

Finally, we compare the performances of the optimal and heuristic algorithms according to the average throughputs of the femtocell and macrocell users. As seen from Fig. 4.8, the performance difference between two algorithms is little noticeable. With this heuristic algorithm, we can obtain the near-optimal solution of the problem (2.6)–(2.10).

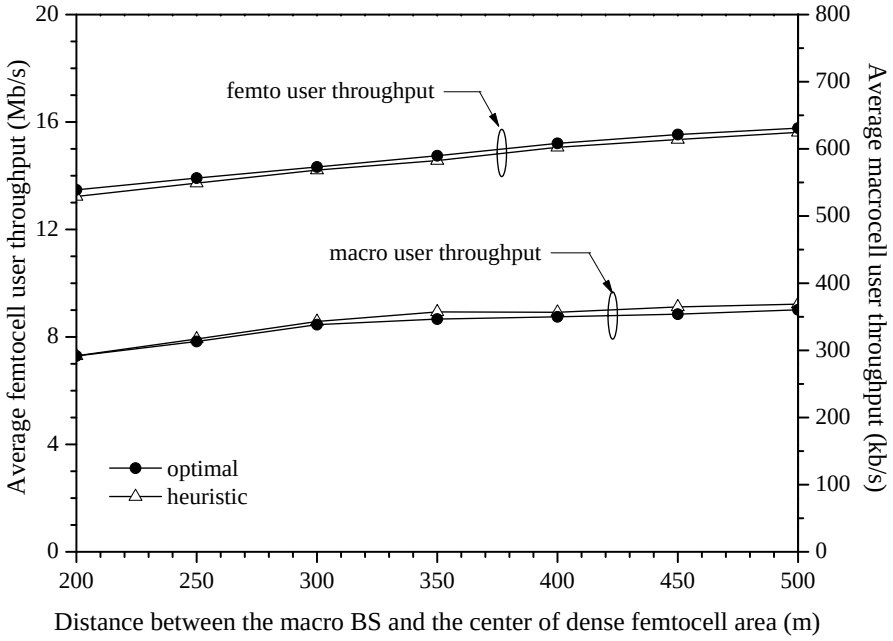

Fig. 4.8: Performance difference between the optimal and heuristic algorithms.

4.2 Base Station Sleep Management Scheme

4.2.1 Simulation Model

We evaluate the performance of the proposed SDUA scheme by using computer simulation. In simulation, we consider an open access femtocell network where 20 femto BSs ($N_{\mathrm{f}} = 20$) are uniformly installed in a designated zone with a 160 m $\times$ 160 m square-shape. As seen in Fig. 3.1, the open access femtocell network is underlaid by a macrocell network consisting of seven macrocells. A macro BS is located at the center of each hexagonal macrocell of which side length is 750 m. The designated zone is in the central macrocell. Let $D_{\mathcal{A}}$ denote the distance between the central macro BS and the center of the designated zone.

The nominal parameter values are $B = 10$ MHz, $\upsilon_{\mathrm{f}} = \frac{1}{3}$, and $\upsilon_{\mathrm{m}}^{(\mathcal{A})} = \frac{2}{3}$. Specifically, referring to [3] and [21], we set the power-related parameters as $\Delta_{\mathrm{m}} = 106.4$ W, $\Delta_{\mathrm{f}} = 0.75$ W, and $P_{\mathrm{f,\,const}} = 4.8$ W. Unless stated otherwise, $D_{\mathcal{A}} = 400$ m, $M = 20$, and $P_{\mathrm{f,\,sleep}} = 1.92$ W.

At the start of a simulation run, users are uniformly located in the designated zone. The moving direction of each user is determined according to uniform distribution between $[0, 2\pi]$. The moving speed is also uniformly determined between $[0, 4]$ km/h. A user updates its direction and speed in the same manner, after a random duration distributed uniformly between $[0, 30]$ seconds. To maintain a fixed number of users in the designated zone during a simulation run, it is assumed that, when a user reaches the zone boundary, its moving direction is reset toward the center of the zone. The number of users in the designated zone is 70, unless stated otherwise. The rate requirement of each user is 300 kb/s and all the users are assumed to be fully loaded.

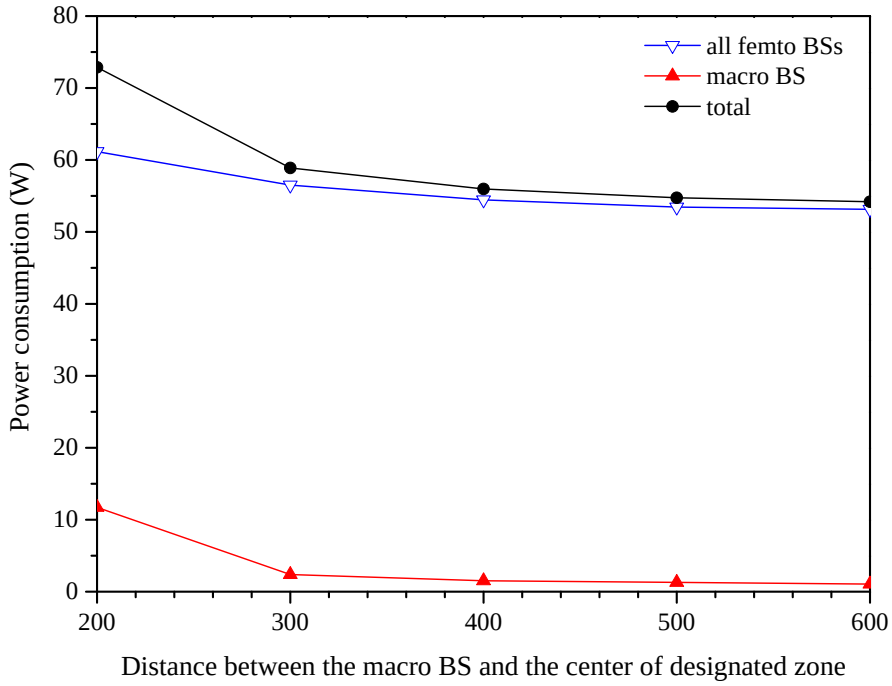

Fig. 4.9: Power consumptions of macro BS and femto BSs according to the location of the designated zone.

In modeling the channel, we consider path loss, lognormal shadowing, and Rayleigh fading. The path loss from the macro BS to a user is calculated as $10^{-3.1}d^{-4}$ and that from a femto BS to a user is $10^{-3.7}d^{-3.5}$, where d is the distance from a BS to a user. The standard deviation of shadowing gain is 10 dB for the macro BS-to-user link and 12 dB for the femto BS-to-user link. Also, the shadowing correlation model in [49] is used with the decorrelation length of 5 m.

4.2.2 Simulation Results

Fig. 4.9 shows the power consumption under the proposed scheme, according to the location of designated zone. When the designated zone is far from the macro BS, due to weaker desired signals, the users within the zone have higher relative resource requirements for the macrocell than when the area is close to the macro BS. So, the proposed scheme will assign fewer users to the macrocell in order to minimize the total power consumption. Accordingly, the power consumption of macro BS decreases with larger $D_{\mathcal{A}}$ (see Fig. 4.9). We also observe from the figure that the total power consumption of femto BSs also decreases as $D_{\mathcal{A}}$ increases. This is because the relative resource requirements of femtocell users decrease due to reduced interference from the macro BS and this makes one femto BS be able to accommodate more users and, as a result, fewer femto BSs are activated. However, as shown in Fig. 4.9, the decreasing effect of consumed power is not great, as long as the designated zone is not close to the macro BS.

Fig. 4.10 shows the energy saving performance of the proposed scheme according to the power of femto BS in sleep mode, normalized by $P_{\text{f, const}}$. The energy saving ratio is defined as the ratio of the power reduction with the proposed scheme to the total power consumption when all the femto BSs are always active and the users select their serving cells by themselves according to the RSS. As $P_{\text{f, sleep}}$ decreases relative to $P_{\text{f, const}}$, the energy can be saved more with the proposed scheme. In addition, when there are fewer users in the designated zone (i.e., the lower network traffic load), the energy saving ratio gets higher because more femto BSs enter the sleep mode.

Next, we examine in Fig. 4.11 the effect of reporting overhead on the perfor-

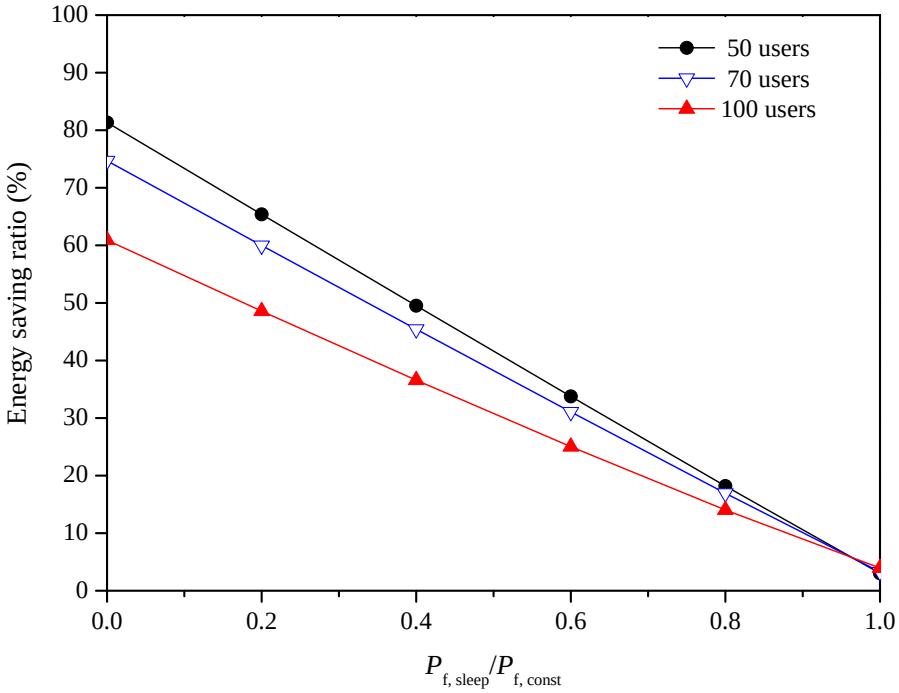

Fig. 4.10: Energy saving according to $P_{\text{f, sleep}}/P_{\text{f, const}}$.

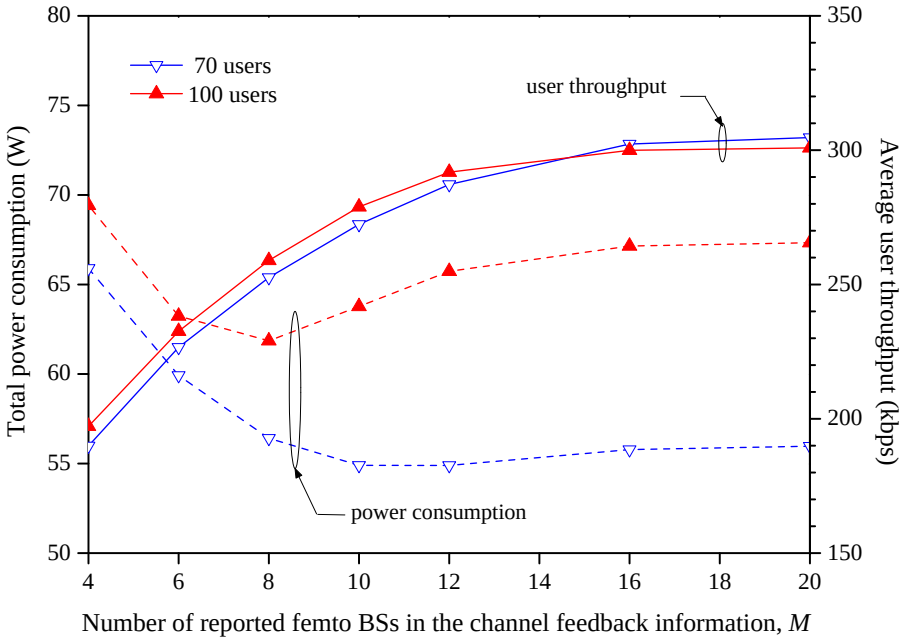

Fig. 4.11: Performance of the proposed scheme according to reporting overhead.

mance of the proposed scheme. As mentioned in Section 3.3.3, each user reports the RSSs from M femto BSs. When any user j reports fewer RSSs (i.e, smaller M), the relative resource requirement of user j at any femtocell i ($\psi_{i,j}$) is underestimated because of the overestimated SIR ($\breve{\gamma}_{i,j}$) and this leads to the throughput decrease of user j. As a result, the total throughput is decreased with smaller M. Furthermore, the underestimated relative resource requirements of each user require the fewer active femto BSs. Thus, the total power consumption also decreases as M gets smaller. However, as shown in Fig. 4.11, when M is excessively small, the power consumption increases greatly rather. This reason is as follows. Since the associated femto BS of a user is selected among the femto BSs whose RSSs are

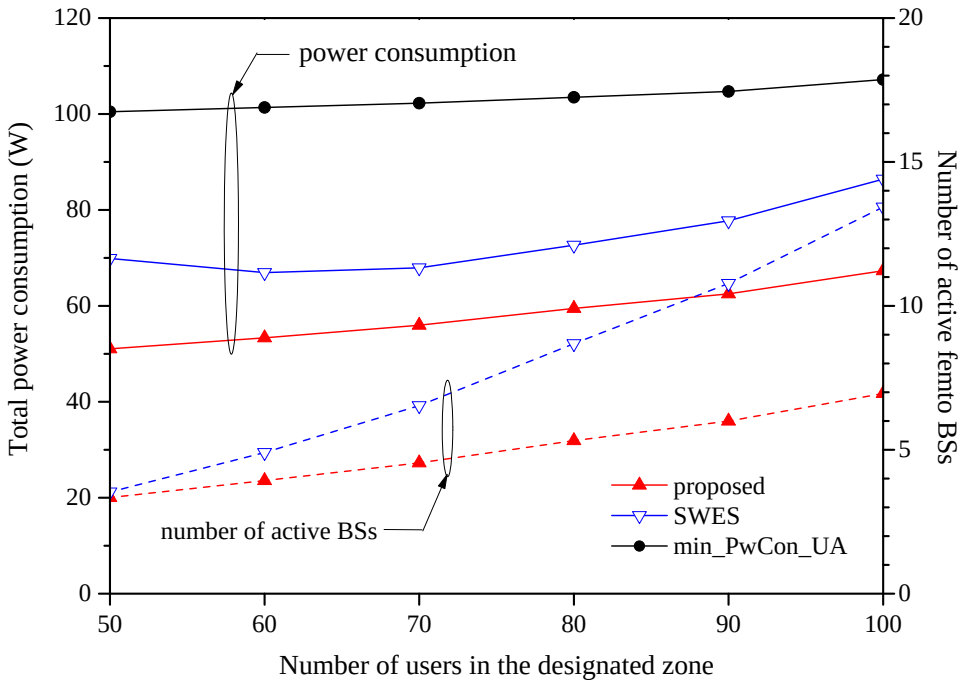

Fig. 4.12: Performance comparison in the total power consumption and the number of active femto BSs.

reported by the user, if M is too small, the number of active femto BSs within the designated zone increases and this results in the increased power consumption.

Finally, we compare in Fig. 4.12 the performances of the proposed scheme and other two schemes, which are respectively called "min_PwCon_UA" and "SWES." With the min_PwCon_UA scheme, all femto BSs are always active and user association is performed by using the UA scheme proposed in this thesis. Thus, we can assess the effect of BS sleeping by comparing the proposed scheme with the min_PwCon_UA scheme. The figure shows that controlling only the user as-

sociation without sleep decision is not effective for energy saving. This is natural because, as already mentioned, the load-dependent power consumption is much lower than the constant power consumption at a femto BS. In the SWES scheme [30], the femto BSs that will increase the loads of neighboring active cells the least when going to sleep are put to sleep one by one. Both the proposed scheme and the SWES scheme select femto BSs to sleep in an iterative manner. However, the proposed scheme performs the user association so that the total power consumption is minimized (global viewpoint), whereas the SWES scheme associates the users with their own best cells which provide the highest RSSs to them (local viewpoint). As a result, the proposed scheme greatly outperforms the SWES scheme in the total power consumption, as shown Fig. 4.12. Furthermore, with the proposed scheme, fewer femto BSs are activated.

Chapter 5. Conclusion

In this thesis, we have designed two resource management schemes for the two-tier femtocell networks, with different purposes: to enhance the spectral efficiency and to enhance the energy efficiency.

First, we have proposed a downlink radio resource partitioning scheme that can enhance the spectral efficiency in the two-tier networks where macrocells adopting FFR are overlaid with femtocells. In the proposed scheme, radio resources in each FP are divided into the macro-dedicated, the shared, and the femto-dedicated groups. We have determined optimally the ratios of each resource group on FPs so that the throughput sum of a macrocell and its underlaid femtocells is maximized while the minimum throughput requirements for both femtocell and macrocell users are satisfied.

Next, we have proposed a femto BS sleep decision and user association (SDUA) scheme to enhance the energy efficiency in the open access femtocell networks. From the statistical analysis on energy efficiency, we have observed that the energy efficiency of the designated femtocell deployment area can be maximized when the total power consumption is minimized while the cells are not overloaded. Based on this, the SDUA problem has been formulated as an optimization problem that aims at minimizing the total power consumption. Since the suggested SDUA problem is too complicated to be solved, we have designed a heuristic but efficient algorithm that jointly determines the operation modes of femto BSs and cell association of users.

The proposed resource partitioning scheme provides good throughput performance to the femtocell users close to the macro BS, by allocating femto-dedicated group on FPs. Furthermore, with the proposed macrocell protection mechanism,

the femto BSs achieves high throughput performance by efficiently reusing the shared resource group without greatly deteriorating transmission quality of macrocell users. In addition, it has been shown by using the simulation that the proposed SDUA scheme can significantly reduce the total energy consumption in the open access femtocell network. We have also discussed the implementation of the proposed schemes.

Bibliography

[1] V. Chandresekhar, J. G. Andrews, and A. Gatherer, "Femtocell networks: A survey," *IEEE Commun. Mag.*, vol. 46, no. 9, pp. 59–67, Sept. 2008.

[2] Small cell forum, "Small cell market status - Informa," [Online]. Available: http://www.smallcellforum.org/resources-reports, Feb. 2013.

[3] 3GPP, "Home Node B (HNB) Radio Frequency (RF) requirements (FDD)," TS 25.967 (release 11), 2012.

[4] A. Fehske, G. Fettweis, J. Malmodin, and G. Biczòk, "The global footprint of mobile communications: the ecological and economic perspective," *IEEE Commun. Mag.*, vol. 49, no. 8, pp. 55–62, Aug. 2011

[5] Y. Li, H. Celebi, M. Daneshmand, C. Wang, and W. Zhao, "Energy–efficient femtocell networks: Challenges and opportunities," *IEEE Wireless Commun.*, vol. 20, no. 6, pp. 99–105, Dec. 2013.

[6] Y. Sun, R. P. Jover, and X. Wang, "Uplink interference mitigation for OFDMA femtocell networks," *IEEE Trans. Wireless Commun.*, vol. 11, no. 2, pp. 614–625, Feb. 2012.

[7] M. Andrews, V. Capdeville, A. Feki, and P. Gupta, "Autonomous spectrum sharing for mixed LTE femto and macro cells deployments," in *Proc. IEEE INFOCOM 2010*, San Diego, USA, Mar. 2010.

[8] IEEE Std 802.16m–2011, "Part 16: Air intrference for broadband wireless access systems amendent 3: Advanced air interface," May 2011.

[9] 3GPP, "UTRAN architecture for 3G Home Node B (HNB); Stage 2." TS 25.467 (release 10), 2011.

[10] A. L. Stolyar and H. Viswanathan, "Self-organizing dynamic fractional frequency reuse in OFDMA systems," in *Proc. IEEE INFOCOM 2008*, Phoenix, USA, Apr. 2008.

[11] T. D. Novlan, R. K. Ganti, A. Ghosh, and J. G. Andrews, "Analytical evaluation of fractional frequency reuse for OFDMA cellular networks," *IEEE Trans. Wireless Commun.*, vol. 10, no. 12, pp. 4294–4305, Dec. 2011.

[12] J. Kim and W. S. Jeon, "Two practical resource allocation techniques for fractional frequency reuse in IEEE 802.16m networks," in *Proc. IEEE IWCMC 2011*, Istanbul, Turkey, July 2011.

[13] M. Qian, W. Hardjawana, Y. Li, B. Vucetic, J. Shi, and X. Yang, "Inter-cell interference coordination through adaptive soft frequency reuse in LTE networks," in *Proc. IEEE WCNC 2012*, Paris, France, Apr. 2012.

[14] J. Y. Lee, S. J. Bae, Y. M. Kwon, and M. Y. Chung, "Interference analysis for femtocell deployment in OFDMA systems based on fractional frequency reuse," *IEEE Commun. Lett.*, vol. 15, no. 4, pp. 425–427, Apr. 2011.

[15] Z. Zhao, F. Zheng, A. Wilzeck, and T. Kaiser, "Femtocell spectrum access underlaid in fractional frequency reused macrocell," in *Proc. IEEE ICC 2011*, Cape Town, South Africa, May 2011.

[16] S. Rangan, "Femto-macro cellular interference control with subband scheduling and interference cancelation," in *Proc. IEEE GLOBECOM 2010*, Miami, USA, Dec. 2010.

[17] W. Cheng, H. Zhang, L. Zhao, and Y. Li, "Energy efficient spectrum allocation for green radio in two-tier cellular networks," in *Proc. IEEE GLOBECOM 2010*, Miami, USA, Dec. 2010.

[18] W. Li, W. Zheng, H. Zhang, T. Su, and X. Wen, "Energy-efficient resource allocation with interference mitigation for two-tier OFDMA femtocell networks," in *Proc. IEEE PIMRC 2012*, Sydney, USA, Sept. 2012.

[19] K. B. S. Manosha, N. Rajatheva, and M. Latva-aho, "Energy effcient power and time allocation in a macrocell/femtocell network," in *Proc. IEEE VTC 2013–Spring*, Dresden, Germany, June 2013.

[20] L. B. Le, D. Niyato, E. Hossain, D. I. Kim, and D. T. Hoang, "QoS-aware and energy-efficient resource management in OFDMA femtocells," *IEEE Trans. Wireless Commun.*, vol. 12, no. 1, pp. 180–194, Jan. 2013.

[21] G. Auer et al., "Cellular energy efficiency evaluation framework," in *Proc. IEEE VTC 2011–Spring*, Yokohama, Japan, May 2011.

[22] I. Ashraf, F. Boccardi, and L. Ho, "SLEEP mode techniques for small cell deployments," *IEEE Commun. Mag.*, vol. 49, no. 8, pp. 72–79, Aug. 2011.

[23] I. Haratcherev, C. Balageas and M. Fiorito, "Low consumption home femto base stations," in *Proc. IEEE PIMRC 2009*, Tokyo, Japan, Sept. 2009.

[24] I. Ashraf, L. T.W. Ho, and H. Claussen, "Improving energy efficiency of femtocell base stations via user activity detection," in *Proc. IEEE WCNC 2010*, Sydney, USA, Apr. 2010.

[25] M. Wildemeersch, T. Q. S. Quek, A. Rabbachin, C. H. Slump, and A. Huang, "Energy efficient design of cognitive small cells," in *Proc. IEEE ICC 2013*, Budapest, Hungary, June 2013.

[26] L. Saker, S. E. Elayoubi, R. Combes, and T. Chahed, "Optimal control of wake up mechanisms of femtocells in heterogeneous networks," *IEEE J. Sel. Areas Commun.*, vol. 30, no. 3, pp. 664–672, Apr. 2012.

[27] E. Oh, B. Krishnamachari, Xin Liu, and Zhisheng Niu, "Toward dynamic energy-efficient operation of cellular network infrastructure," *IEEE Commun. Mag.*, vol. 49, no. 6, pp. 56–61, June 2011.

[28] Z. Niu, Y. Wu, J. Gong, and Z. Yang, "Cell zooming for cost-efficient green cellular networks," *IEEE Commun. Mag.*, vol. 48, no. 11, pp. 74–79, Nov. 2010.

[29] K. Son, S. Nagaraj, M. Sarkar, and S. Dey, "QoS-aware dynamic cell reconfiguration for energy conservation in cellular networks," in *Proc. IEEE WCNC 2013*, Shanghai, China, Apr. 2013.

[30] E. Oh, K. Son, and B. Krishnamachari, "Dynamic base station switching–on/off strategies for green cellular networks," *IEEE Trans. Wireless Commun.*, vol. 12, no. 5, pp. 2126–2136, May 2013.

[31] D. Cao, S. Zhou, and Z. Niu, "Optimal combination of base station densities for energy-efficient two-tier heterogeneous cellular networks," *IEEE Trans. Wireless Commun.*, vol. 12, no. 9, pp. 4350–4362, Sept. 2013.

[32] Y. S. Soh, T. Q. S. Quek, M. Kountouris, and H. Shin "Energy efficient heterogeneous cellular networks," *IEEE J. Sel. Areas Commun.*, vol. 31, no. 5, pp. 840–850, May 2013.

[33] S.-R. Cho and W. Choi, "Energy-efficient repulsive cell activation for heterogeneous cellular networks," *IEEE J. Sel. Areas Commun.*, vol. 31, no. 5, pp. 870–882, May 2013.

[34] W. S. Jeon, J. Kim, and D. G. Jeong, "Downlink radio resource partitioning with fractional frequency reuse in femtocell networks," *IEEE Trans. Veh. Technol.*, vol. 63, no. 1, pp. 308–321, Jan. 2014.

[35] J. Kim and W. S. Jeon, "Fractional frequency reuse-based resource sharing strategy in two-tier femtocell networks," in *Proc. IEEE CCNC 2012-RSW*, Las Vegas, USA, Jan. 2012.

[36] J. Kim, W. S. Jeon, and D. G. Jeong, "Base station sleep management in open access femtocell networks," *submitted to IEEE Trans. Veh. Technol.*, May 2014.

[37] T. D. Novlan, R. K. Ganti, J. G. Andrews, and A. Ghosh, "A new model for coverage with fractional frequency reuse in OFDMA cellular networks," in *Proc. IEEE GLOBECOM 2011*, Houston, USA, Dec. 2011.

[38] V. Chandresekhar and J. G. Andrews, "Spectrum allocation in tiered cellular networks," *IEEE Trans. Commun.*, vol. 55, no. 10, pp. 3059–3068, Oct. 2009.

[39] X. Qiu and K. Chawla, "On the performance of adaptive modulationin cellular systems," *IEEE Trans. Commun.*, vol. 47, no. 6, pp. 884–895, June 1999.

[40] A. M. D. Turkmani, "Probability of error for M-branch macroscopic selection diversity," *IEE Proc. Commun. Speech and Vision*, vol. 139, no. 1, pp. 71–78, Feb. 1992.

[41] Z. Bharucha, H. Haas, G. Auer, and I. Cosovic, "Femto-cell resource partitioning," in *Proc. IEEE GLOBECOM 2009-workshops*, Hawaii, USA, Nov. 2009.

[42] B. Li, Y. Zhang, G. Cui, W. Wang, J. Duan, and W. Chen, "Interference coordination based on hybrid resource allocation for overlaying LTE macrocell and femtocell," in *Proc. IEEE PIMRC 2011*, Toronto, Canada, Sept. 2011.

[43] L. F. Fenton, "The sum of log-normal probability distributions in scatter transmission systems," *IRE Trans. Commun. Syst.*, vol. CS-8, pp. 57–67, Mar. 1960.

[44] N. B. Mehta, J. Wu, A. F. Molisch, and J. Zhang, "Approximating a sum of random variables with a lognormal," *IEEE Trans. Wireless Commun.*, vol. 6, no. 7, pp. 2690–2699, July 2007.

[45] X. Chu, Y. Wu, D. Lopez-Perez, and X. Tao, "On providing downlink services in collocated spectrum-sharing macro and femto networks," *IEEE Trans. Wireless Commun.*, vol. 10, no. 12, pp. 4306–4315, Dec. 2011.

[46] M. Abramowitz and I. Stegun, *Handbook of Mathematical Functions with Formulas, Graphs, and Mathematical Tables*, 10th edition, John Wiley & Sons, 1972, pp. 923–924.

[47] J. Kim, W. S. Jeon, and D. G. Jeong, "Effect of base station-sleeping ratio on energy efficiency in densely deployed femtocell networks," *submitted to IEEE Commun. Lett.* (in revision), Apr. 2014.

[48] S. Boyd and L. Vandenberghe, *Convex Optimization*, Cambridge Univrsity Press, 2004.

[49] *Guideline for Evolution of Radio Transmission Technologies for IMT-2000*, ITU-R M.1225, 1997.

[50] W. C. Jakes, *Microwave Mobile Communications*, IEEE Press, 1994.

[51] H. M. Chaskar and U. Madhow, "Fair scheduling with tunable latency: a Round-Robin approach," *IEEE/ACM Trans. Netw.*, vol. 11, no. 4, pp. 592–601, Aug. 2003.

[52] C.-Y. Oh, M. Y. Chung, H. Choo, and T.-J. Lee, "Resource allocation with partitioning criterion for macro-femto overlay cellular networks with fractional frequency reuse," *Wireless Pers. Commun.*, vol. 68, no. 2, pp. 417–432, Jan. 2013.

초 록

모바일 트래픽 수요가 폭발적으로 증가함에 따라 실내 사용자들에게 낮은 비용으로 고품질의 데이터 서비스를 제공할 수 있는 펨토셀이 주목을 받고 있다. 본 논문에서는 펨토셀이 기존의 매크로셀 위에 구축된 two-tier 펨토셀 네트워크에서 주파수 효율과 에너지 효율 향상을 위한 두 가지 자원 관리 기법을 제안하였다. 먼저, 주파수 효율을 향상시키기 위한 펨토셀들과 중첩 매크로셀 사이의 하향 링크 무선 자원 분할(radio resource partitioning) 기법을 설계하였다. 제안하는 무선 자원 분할 기법에서는 모바일 데이터 폭증 문제에 대한 또 다른 해결 방안인 분할 주파수 재사용(fractional frequency reuse, FFR) 기술이 적용된 매크로셀 네트워크를 고려하였다. FFR 구조에서 매크로셀의 주파수 대역은 다수의 주파수 분할들(frequency partitions, FPs)로 나누어지고, FP마다 다른 전송 전력이 할당된다. 제안한 기법에서 각 FP는 다시 매크로 전용 부분(macro-dedicated portion), 공용 부분(shared portion), 그리고 펨토 전용 부분(femto-dedicated portion)으로 구성되고, 이 세 부분의 비율은 FP마다 다르게 설정된다. 제안하는 기법은 최적화 방식을 이용하여 주파수 효율을 최대화하도록 각 FP 내 자원 분할 비율을 결정한다. 다음으로, 공항 및 쇼핑몰과 같이 사용자들이 밀집된 공공장소에 많은 수의 펨토 기지국들이 설치된 개방형 펨토셀 네트워크에서 에너지 효율을 향상시키기 위한 자원 관리 기법을 제안하였다. 고려하는 펨토셀 네트워크에서는 펨토 기지국들이 최대 트래픽 부하를 지원하기 위해 높은 밀도로 설치되기 때문에 대부분의 동작 시간 동안 펨토셀들은 무선 자원을 충분히 활용하지 않는다. 따라서 사용자들의 셀 접속을 적절히 조정하여 가능한 적은 펨토 기지국들을 활성화시키고 그 이외의 펨토 기지국들을 수면 모드(sleep mode)로 동작시킨다면 해당 펨토셀 설치 지역에서의 네트워크 에너지 효율을 크게 향상시킬 수 있을 것이다. 따라서 본 논문에서는 에너지 효율을 향상시키기 위해 펨토 기지국의 동작 모드(active 또는 sleep)와 사용자들의 셀 접속을 동시에 결정하

는 펨토 기지국 동작 모드 결정 및 사용자 접속 (femto BS sleep decision and user association, SDUA) 기법을 설계하였다. 제안하는 기법에서 SDUA 문제는 사용자들에게 만족할 만한 서비스를 제공하면서 전체 에너지 소모를 최소로 하는 것을 목표로 하는 최적화 문제로 정식화되었다. SDUA 문제는 기지국의 동작 모드와 사용자의 셀 접속이 상호 영향을 주어서 계산 복잡도가 높으므로 본 논문에서는 먼저 활성화 펨토 기지국들의 집합이 주어진 상태에서 최적의 사용자 접속(user association, UA) 문제를 풀고, 각기 다른 집합들에 대해서 최적화 UA를 반복적으로 수행함으로써 최선의 활성화 펨토 기지국 집합을 찾는 휴리스틱 알고리즘을 설계하였다. 제안하는 두 자원 관리 기법들이 각각 주파수 효율과 에너지 효율에 대해서 기존의 기법들보다 우수한 성능을 보임을 시뮬레이션을 통해 확인하였다.

주요어: 펨토셀, 자원 관리, 주파수 효율, 에너지 효율, 이종 셀룰러 네트워크,
학 번: 2009-30913